Characterisation and Process Development Studies on Waxes Derived from Plastic Pyrolysis

By

JOSHUA NICHOLAS ROBINSON

In collaboration with

Kerax Ltd.

JANUARY 2020

A thesis submitted for the degree of Master by Research in Chemistry at Lancaster University, United Kingdom

This project was supported by the Centre for Global Eco-Innovation and is part financed by the European Regional Development Fund.

Abstract

Pyrolysis enables plastic waste to be utilised as a resource to produce useful raw materials for further downstream processing. Light olefin gases, oils and waxes are major products of plastic pyrolysis that have applications in the manufacture of petroleum products (e.g. gasoline, diesel and paraffin wax) and polymers. Pyrolysis-derived waxes possess undesirable colour and odour properties that must be improved to produce a useful raw material.

It has been the aim of this work to remove colour and odour inducing impurities from pyrolysis-derived waxes using suitable refining methods. Liquid chromatography, solvent de-oiling using ethyl acetate and urea clathrate formation were investigated as methods to separate impurities from crude waxes. Crude waxes, refined waxes and extracts/fractions containing impurities were comprehensively analysed to determine: chemical functionality by FTIR and NMR, molecular weight distribution by GPC, heavy metals content by ICP and the identification of volatiles by GC-MS. Headspace GC-MS was used to analyse volatile components to identify possible odour inducing contaminants emitted by crude waxes. UV-vis spectroscopy was introduced in this research as a method to assess the bulk colour characteristics of wax to identify wavelengths in which colour-contaminated wax absorbs and refined wax does not. Two suitable wax refining procedures have been proposed based on methods of separation known to be effective: solvent de-oiling and hydrogenation. Silica adsorption was used as a pre-treatment for both refining procedures to remove polar components which may be harder to remove by solvent de-oiling or hydrogenation alone.

Separation of impurities was most effective using liquid chromatography and afforded a wax with the most desirable colour and odour characteristics at high mass recoveries, while solvent de-oiling and urea clathrate extraction afforded a hard wax and an oil. The hard waxes obtained by solvent de-oiling exhibited the least favourable colour characteristics and had a high oil content. Urea clathrate extraction of waxes was not possible for wax A, however, waxes B and C exhibited desirable colour characteristics after the procedure had been carried out. The main disadvantage of solvent de-oiling and urea clathrate extraction processes is the low recovery of wax due to the high oil content of pyrolysis derived waxes. The combination of solvent de-oiling using ethyl acetate and silica adsorption demonstrated that the removal of polar components by adsorption prior to solvent de-oiling improves the colour properties

significantly compared to solvent de-oiling alone. Similarly, the combination of silica adsorption and hydrogenation was highly effective at decolourising the waxes. Hydrogenation successfully converted the yellow/orange oil extract (obtained by solvent de-oiling of wax B) into colourless soft wax. This is advantageous compared to solvent de-oiling, however, the requirement of hydrogen gas, catalyst and catalyst regeneration/recycling process are bound to lead to increased monetary expenditure.

Acknowledgements

I am extremely grateful to have been given this unique and exciting opportunity to work on this Masters by research project. My experience studying at Lancaster University has been thoroughly enjoyable.

I would like to acknowledge the ERDF for the funding of this program. I would also like to thank the staff and researchers at the Centre for Global Eco-innovation at Lancaster University for the ERDF funding, administration of the project and continued support. I am sincerely thankful to Mr. Chris Bradley and members of Kerax Ltd for their keen interest in the project, positive feedback and trust in my work. I am also extremely grateful to Kerax Ltd for their financial contribution to the project.

I would like to express deep gratitude to my research supervisors, Professor Joe Sweeney and Dr Julien Doulcet for their continued support, encouragement and constructive feedback on my research throughout the year. I also thank Dr Anthony Ball for his continued support throughout the project, who also played a role in the supervision of my project.

I would like to give a special thank you to Peter Wilson for his invaluable guidance and support in some of the key areas of the project. I extend my appreciation to my colleagues in the Sweeney group for their valuable advice, suggestions and watching over me in the lab.

The assistance provided by the technicians of the Department of Chemistry at Lancaster University for offering their expertise and assisting me in developing some of the analytical procedures used in this study is massively appreciated.

Finally, I wish to thank my parents and close family for their support and encouragement throughout my studies.

Table of Contents

Abbreviations

ABS – acrylonitrile butadiene

ASTM – American Standards for Testing Materials

BTX – benzene, toluene and xylene

CSBR – conical spouted bed reactor

DCM – Dichloromethane

EA – ethyl acetate

FCC – fluid catalytic cracking

FID – flame ionisation detector

GC – gas chromatography

GPC – gel permeation chromatography

LC – liquid chromatography

MS – mass spectrometry

NIST – National Institute of Standards and Technology

PAH – polyaromatic hydrocarbons

PC – polycarbonate

PDI – Polydispersity Index

PE – polyethylene

PET – polyethylene terephthalate

PMMA – polymethyl methacrylate

PP – polypropylene

PS – polystyrene

PTFE – polytetraflouroethylene

PUR – polyurethane

PVC – polyvinyl chloride

SD – Solvent de-oiling

THF – Tetrahydrofuran

UCE – Urea clathrate extraction

Glossary of Terms (as they relate to the thesis)

Clathrate – an inclusion compound formed between urea and straight chain hydrocarbons or *n*-paraffins.

Clathrate oil – oil content recovered by urea clathrate extraction.

Clathrate wax – wax separated by urea clathrate extraction.

De-oiled wax – wax recovered by solvent de-oiling experiments.

High polarity fraction – components separated by liquid chromatography by eluting with a polar solvent such as methanol.

Medium polarity fraction – components separated by liquid chromatography by eluting with a slightly more polar solvent than hexane (such as toluene or 15% ethyl acetate/hexane).

Non-polar fraction – wax purified by liquid chromatography.

Oil extract – oil extracted by the solvent de-oiling of wax.

Solvent De-oiling – the extraction of impurities in a solvent in which impurities are soluble and the wax is not.

Urea Clathrate Extraction – the formation of urea inclusion compounds (clathrates) with *n*-paraffins and their decomposition to extract *n*-paraffins.

List of Figures

List of Tables

List of Appendices

A. Appendix A: Sample Masses and Mass Recoveries

B. Appendix B: GPC and GC-MS Chromatograms

C. Appendix C: GC-MS and ICP Raw and Processed Data Tables

The appendices are physically bound separately to this thesis as a single document.

1. Introduction

Packaging plastic accounts for the largest contribution of plastic waste sent to landfill sites in the European Union. In 2016 the European Union sent 20.4% of packaging plastic was sent to landfill sites, while 40.8% was recycled and 38.8% was used for energy recovery. Since 2006 the amount of packaging plastic sent to landfill has decreased by 53% and may continue to decrease due to an increasing demand in the modern climate for the valorisation of plastic waste.[1] The European demand of plastics by type is illustrated in Figure 1.

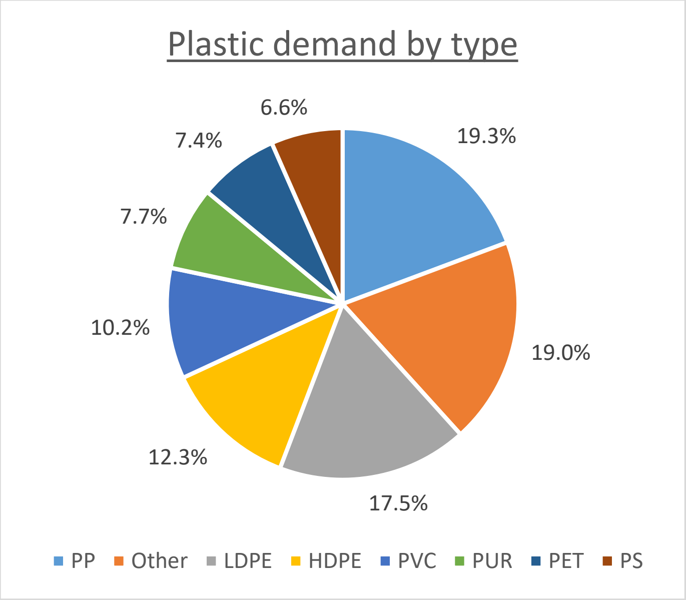

Figure 1. European plastic demand by type (other: ABS, PBT, PC, PMMA and PTFE)[1]

Commercial interest is ever growing for producing valuable petrochemicals from the pyrolysis of plastic waste. The production of diesel, gasoline, wax and light olefins from plastic waste pyrolysis has been the subject of various studies aiming to improve the efficiency and product recovery for their processes.[2–6] Wax production during pyrolysis has high potential as a feedstock in steam cracking and fluid catalytic cracking applications to produce re-useable olefins and gasoline.[6,7] However, waxes have a more direct use as an alternative raw material in the wax manufacturing industry.

Paraffin waxes consist of straight chain hydrocarbons with a typical carbon number between C_{20} and C_{60} and are solid at room temperature. Currently, paraffin waxes are produced by solvent refining crude oil distillates to produce refined lubricating oil and slack wax as a by-product as illustrated in Figure 2. Slack wax is a type of crude paraffin wax with a relatively high content of sulphur, aromatic and nitrogen compounds. Slack wax is further refined by solvent de-oiling to remove soluble impurities to acceptable levels.[8] Waxes may act as solid matrices capable of retaining liquid components through Van der Waals interactions. Oils may contain impurities such as aromatics and sulphur and nitrogen containing compounds. A solvent such as 2-butanone or butyl acetate is used to dissolve the wax, which is then cooled to a low temperature (below -20 °C) to allow the wax to precipitate.[9] Oily components and impurities are removed by filtration which affords a wax with low oil content. High grade paraffin waxes typically have an oil content of less than 0.5 wt %.[10,11]

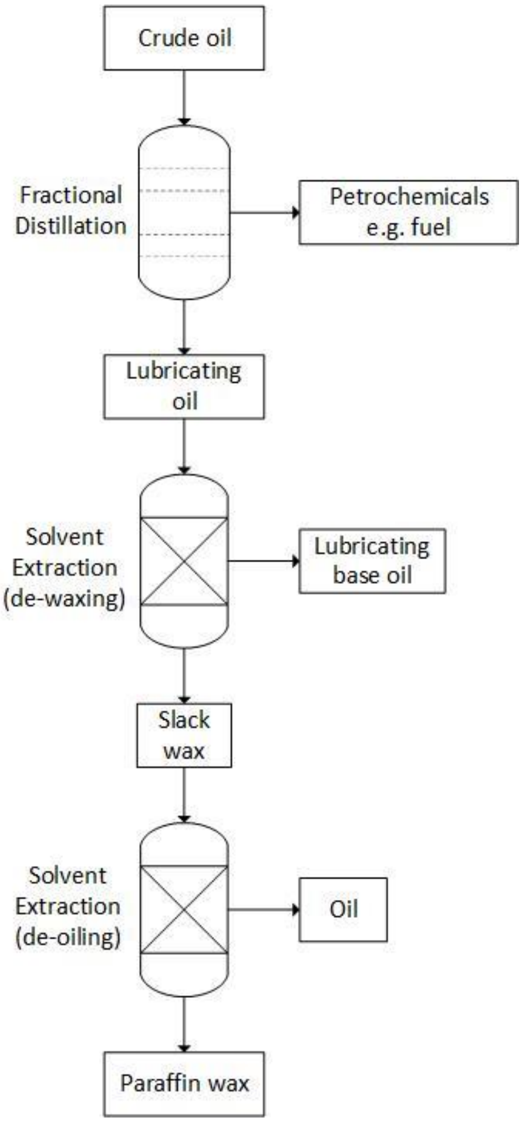

Figure 2. Generalised process scheme for the manufacture of paraffin wax

Although simple in design, the solvent refining of wax suffers from poor environmental credentials, the handling of large volumes of solvent and high operating and maintenance costs. It is, therefore, a necessity to identify a more sustainable and environmentally friendly feedstock for the manufacture of wax. Plastic waste is a well-known environmental issue with no clear route to a practical solution. The pyrolysis of plastic waste breaks the polymers down into crude wax for their potential use as a wax manufacturing feedstock. The crude waxes provided for the research project by Kerax Ltd (industry partner) exhibit undesirable colour and odour properties, which are challenging to improve by conventional wax refining procedures. Reducing the odour and improving the colour of pyrolysis-derived wax is critical to the success of this novel supply chain. Therefore, this research project aims to address what the contaminant components are using suitable analytical techniques and investigate processes to decolourise and deodorise these crude waxes. This will enable the development of a large-scale process to for the successful recycling of large quantities of waste into useful raw material.

2. Literature Review

The aim of this review chapter is to provide a background on how waxes are formed by plastic pyrolysis and what suitable analytical techniques can be used to determine their characteristics.

2.1. Plastic Pyrolysis

The pyrolysis of plastic waste affords a wide product distribution owing to the complexity of plastic waste composition. Plastic waste pyrolysis-feedstock may vary in composition, resulting in uneven product distributions between batches. Therefore, it is crucial to assimilate how changes in plastic feedstock and process parameters influence the composition of the product. Furthermore, the characterisation of pyrolysis-derived wax provides vital feedback on how processes can be developed to afford the desired product distribution.

2.1.1. Thermal Degradation of Polyethylene and Polypropylene

The type of plastic used as pyrolysis feedstock is a major influencer of product distribution. High density polyethylene (HDPE) is a linear polymer known for its high strength and is widely used for manufacturing disposable containers such as milk bottles, fuel tanks, piping and more. Low density polyethylene (LDPE) is less dense owing to the increased branching of the polymeric chain and is more suited to uses where flexibility is favoured over robustness e.g.

carrier bags, wrapping foil, squeeze-bottles and more. Polypropylene (PP), like HDPE, is also known for its high tensile strength and is often found use in applications such as container caps, living hinges, piping, plastic furniture and more.

Figure 3. Repeating units for polyethylene (left) and polypropylene (right)

It is well known that the thermal degradation of polyethylene and polypropylene proceeds via random chain scission of the polymeric chain and results in a wide distribution of products.[12–16] The thermal decomposition mechanism that takes place during the pyrolysis of polyethylene is represented in Figure 4. Initiation of the radical mechanism proceeds by random scission of the polymer chain to produce primary radicals. Propagation of the mechanism occurs by intramolecular and intermolecular hydrogen transfer and β-scission. Primary radicals are stabilised by radical hydrogen transfer, resulting in the formation of a secondary radical. B-scission may occur on the primary radical to form another primary radical and ethylene, as shown in Figure 5, while mid-chain β-scission on secondary radicals produces larger olefins.[17] It is noteworthy that ethylene formation during pyrolysis plays a role in the formation of aromatic compounds, which is later illustrated in Figure 9. Termination reactions proceed by radical re-combination, resulting in the formation of long chain paraffins; or by radical disproportionation, which results in the formation of a paraffin and an olefin.

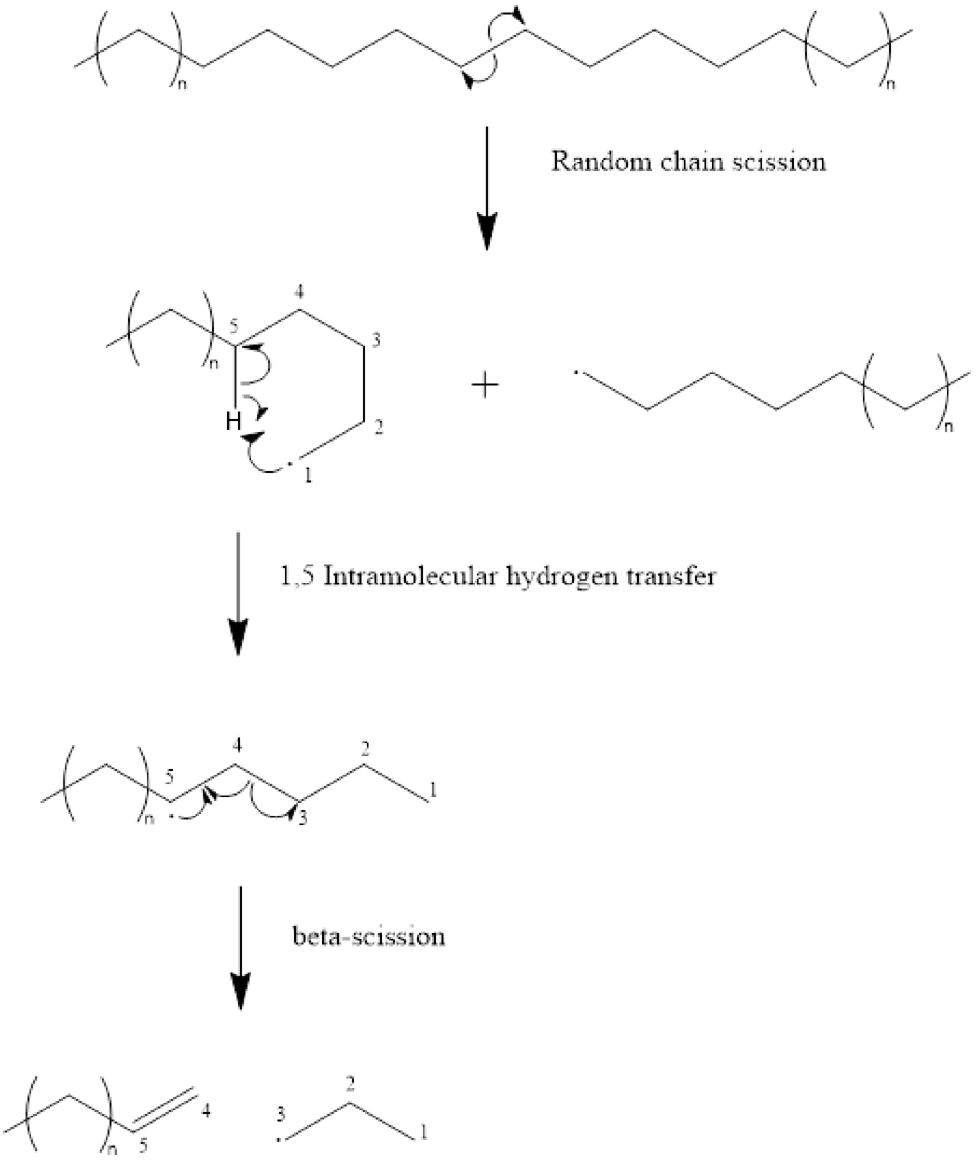

Figure 4. Overview of the thermal degradation of polyethylene[17]

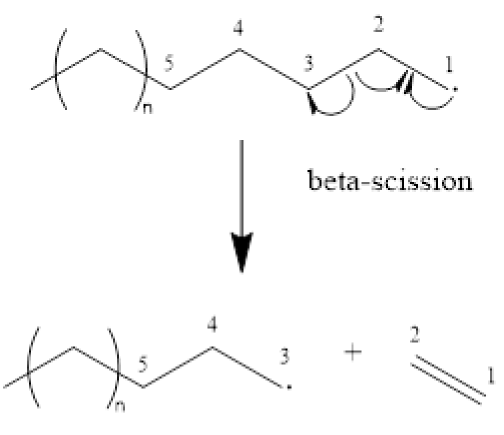

Figure 5. Beta-scission of a primary radical to form ethylene[17]

The formation of lower molecular weight hydrocarbons is promoted at higher temperatures resulting by an increase in intramolecular hydrogen transfer reactions, which propagate β-scission reactions.[17] An increase in mid-chain and end-chain β-scission, therefore, increases the formation of low molecular weight hydrocarbons and light gaseous olefins. It would make sense that lower residence times of pyrolysis volatiles in the reactor reduces the extent of these propagating reactions resulting in the formation of higher molecular weight hydrocarbons. This conclusion summarises the formation of waxes during pyrolysis and that wax production is favoured at lower temperatures. Arabiourrutia et al. confirm this to be the case from their study on the pyrolysis of PE and PP in a conical spouted bed reactor (CSBR) operating at 450-500 °C.[7]

Thermal degradation of PP proceeds in the same manner as PE, as shown in Figure 6. A higher proportion of branched products can be expected, owing to the higher branching of the PP chain. Predel and Kaminsky carried out an experiment to compare the product distribution of PE, PP and PS pyrolysis using different mixtures of the plastics in varying proportions.[18] They found that the trimer of propene (2,4-dimethylheptene) is formed in very high amounts when PP is present in the feedstock. Increasing the amount of PP in the feedstock was found to increase the oil content (b.pt < 300 °C) as a result of the formation of higher branched compounds such as 2,4-dimethylheptene. Compounds such as 2,4-dimethylheptene possess a high cetane number owing to their higher degree of branching, which increases the energy density and, therefore, would be of commercial interest to fuel companies seeking to convert plastic waste into useful raw materials.

Yan et al. observed a similar trend in their results, in which an exceptionally high yield of 2,4-dimethylheptene (18.3 wt %) was obtained.[13] The formation of this compound can be attributed to the thermal degradation of polypropylene, resulting in the formation of a 1 alkene (2,4-dimethyl-1-heptene) and a primary radical. The increased stability of the tertiary radical would seem to be the driving force for the formation of this compound. An increased yield of branched C_6, C_9 and C_{12} iso-alkenes and iso-alkanes was also observed.[13] Evidently, these results demonstrate that these branched compounds are a result of successive losses of repeating units from the polymeric chain.

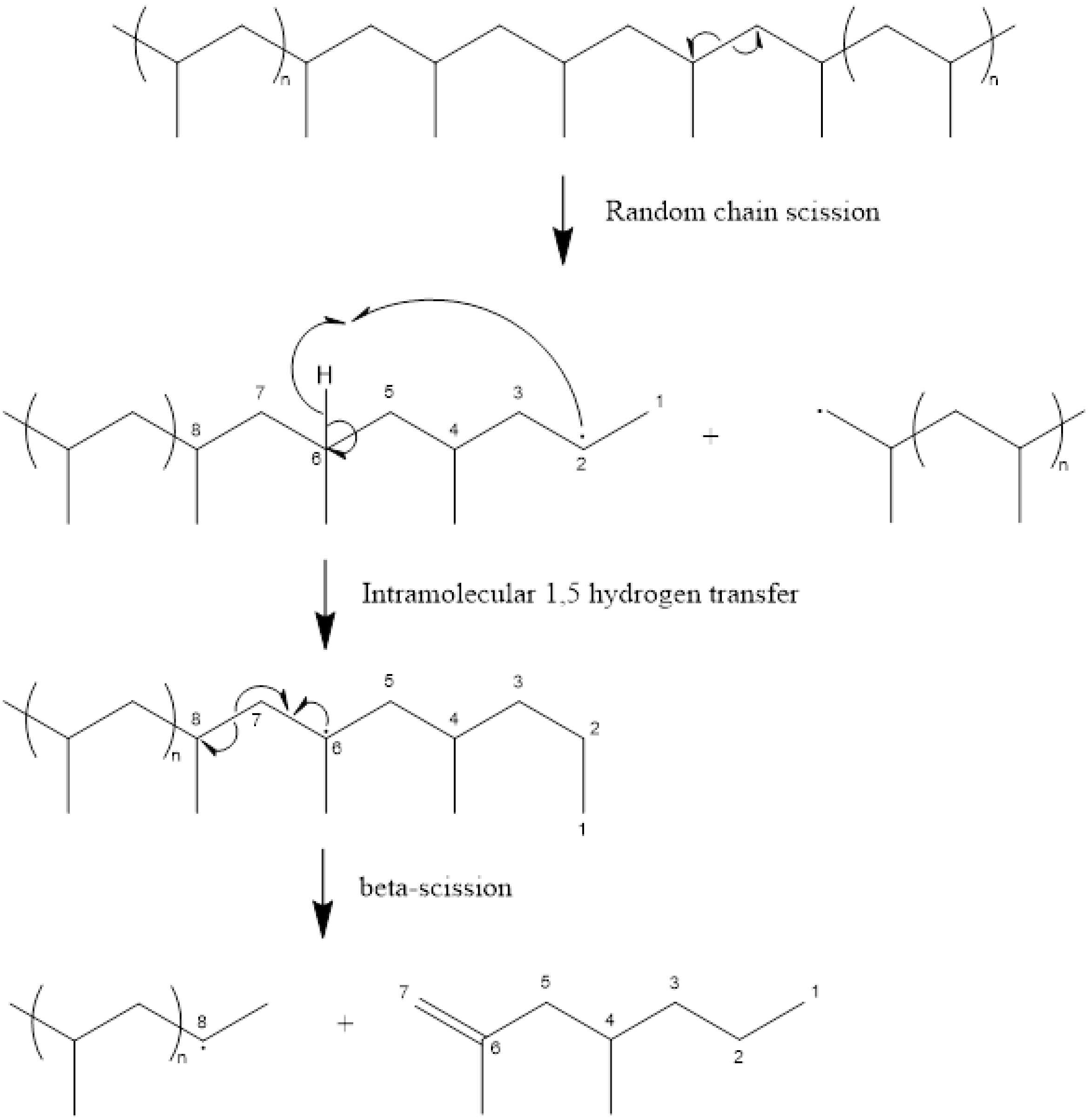

Figure 6. Thermal degradation of polypropylene[19]

The review by Pilusa et al. adequately summarises aromatisation of cyclic compounds formed by Diels-Alder reactions arising from high temperature pyrolysis of scrap tyres.[20] This mechanism is also described in detail by Williams and Williams in their study on the pyrolysis of LDPE.[12] The general mechanism of the formation of dienes, leading to the formation of benzene is illustrated in Figure 7 and Figure 8.

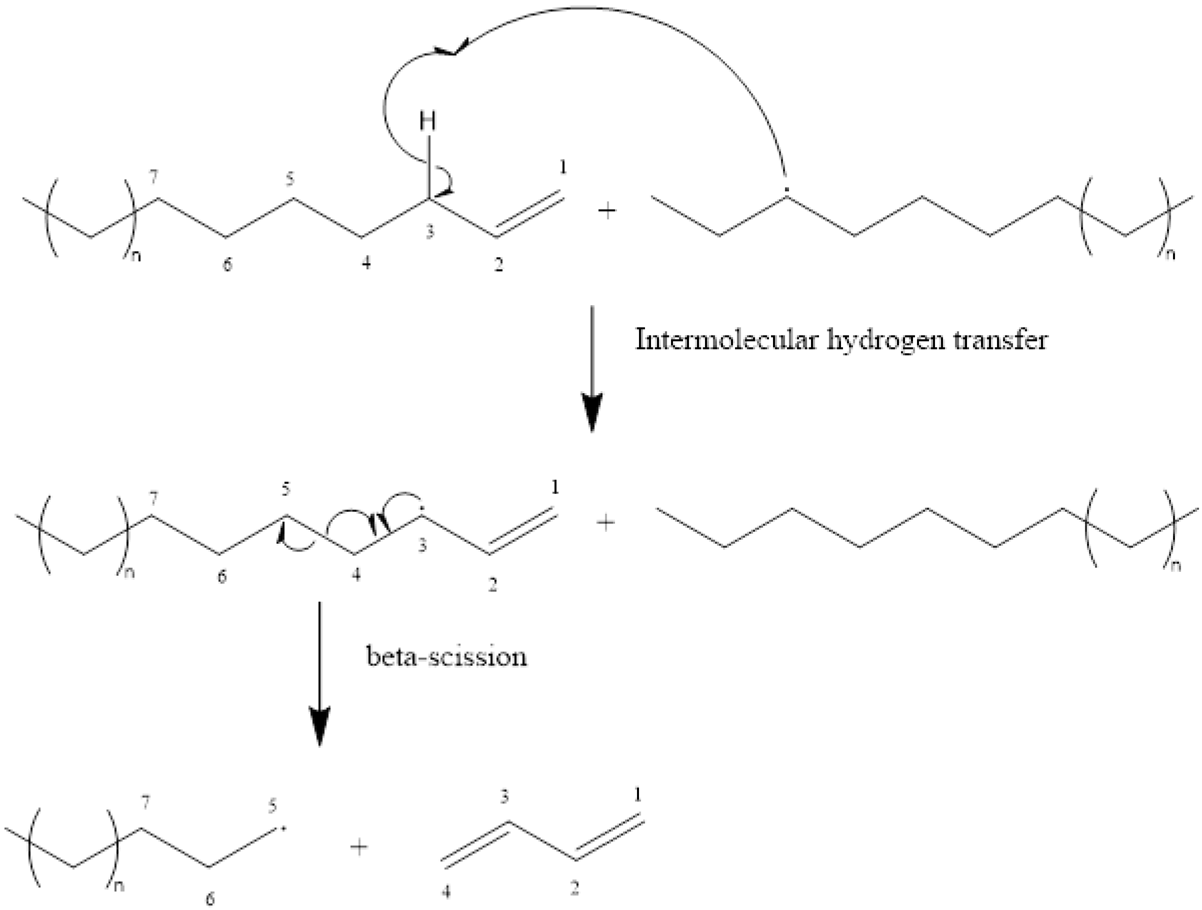

Figure 7. A mechanism for the formation of dienes[20]

Diels-Alder type reactions between ethylene and 1,4-butadiene produces cyclohexene, which undergoes aromatisation at high temperatures (above 700 °C).[12] Furthermore, polyaromatic hydrocarbon (PAH) formation during polyolefin pyrolysis is thought to be a result of multiple cyclisation reactions, followed by aromatisation.[20] PAH compounds may be present in the solid residue (char) formed during pyrolysis and can be attributed to long residence times.

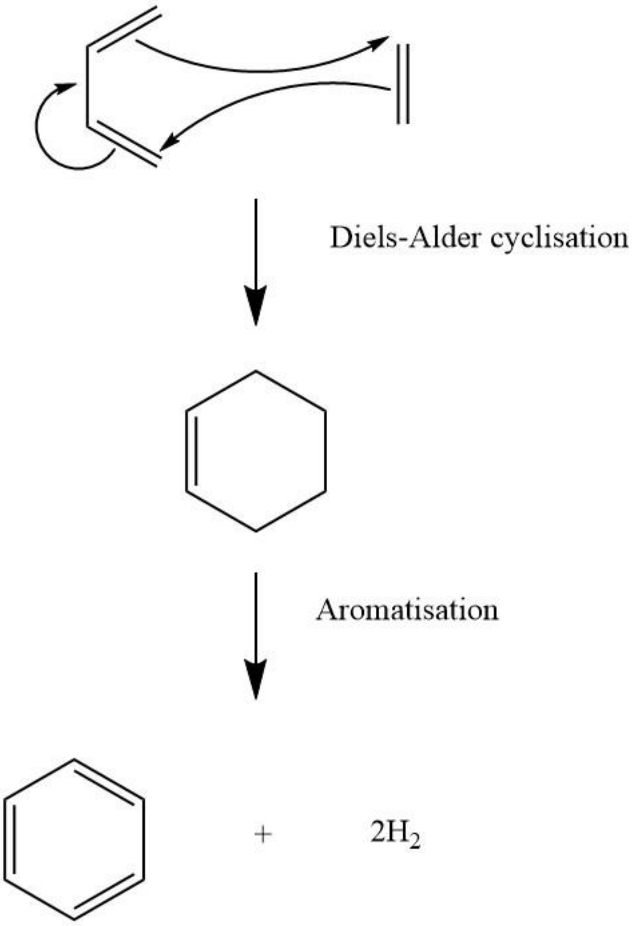

Figure 8. Diels-Alder mechanism for the formation of aromatic compounds during pyrolysis[20]

2.1.2. Pyrolysis Processes

The temperature, type of reactor and catalysts are very important factors that can determine the product distribution. Pyrolysis catalysts can be used to selectively produce more of the desired product e.g. the production of light olefins, gasoline and diesel using a suitable acid catalyst. Acid catalysts decrease the activation energy of higher cracking reactions, favouring the production of lower molecular weight hydrocarbons (liquids and gases) at lower temperatures. In their review, Lopez et al. provide a more in-depth evaluation of catalytic plastic pyrolysis.[21] In contrast, the production of wax by pyrolysis can be achieved without the use of catalysts and is optimisable by varying instrument parameters such as temperature and residence time.[6,7,12,13,22]

Fixed bed reactors are the simplest in design and are usually operated in batch mode, incorporating a suitable temperature program. Fixed bed processes are easily scalable due to their simplicity in design; however, the processing of larger quantities of material generally suffers from poor heat and mass transfer and therefore, is less energy efficient than other processes.

Fluidised bed pyrolysis has advantages over fixed bed pyrolysis, such as increased heat and mass transfer and lower residence time of volatiles in the gas phase. However, this process is not without problems and can be affected by bed de-fluidisation and the segregation of particles that are difficult to fluidise.[5] These limitations are a result of the irregular, sticky nature of plastics under pyrolysis conditions, making them difficult to handle.

The conical spouted bed reactor (CSBR) is a type of fluidised bed reactor that has advantages over the more traditional fluidised bed reactors used in pyrolysis. This technology has seen a lot of development in plastic pyrolysis processes due to its enhanced capability of handling sticky solids with wide size distributions.[4,5,7,23] High yields of wax have been reported in the literature (see Table 1) and can be attributed to the low residence time of volatiles in the gas phase, which minimises higher cracking reactions and produces lower molecular weight products such as aromatics and light olefins.[7] Despite the more complex design, the up-scaling of pyrolysis in a CSBR was successfully implemented by Elordi et al. in the pyrolysis of HDPE; carried out at 500-700 ˚C in continuous mode at a production rate of 25 kg h^{-1}.[4]

The recovery of pyrolysis-derived wax obtained by various authors is represented in Table 1.[4,6,7,12,18] Their results are in good accordance and demonstrate that increasing the temperature decreases the recovery of wax and that the content of liquid (oils) and gases increases. The short residence times and low temperatures produce higher molecular weight hydrocarbons, owing to the reduced severity of radical propagation reactions such as radical hydrogen transfer and β-scission.

Table 1. Mass Recovery of Wax from Plastic Pyrolysis

Plastic	**Reactor**	**Temperature (°C)**	**Mass recovery of wax (%)**	**Reference**
HDPE	CSBR	500	67	Elordi et al.[4]
HDPE	CSBR	700	12	Elordi et al.[4]
HDPE	CSBR	450	80	Arabiourrutia et al.[7]
HDPE	CSBR	500	68	Arabiourrutia et al.[7]
HDPE	CSBR	600	49	Arabiourrutia et al.[7]
LDPE	CSBR	450	80	Arabiourrutia et al.[7]
LDPE	CSBR	500	69	Arabiourrutia et al.[7]
LDPE	CSBR	600	51	Arabiourrutia et al.[7]
PP	CSBR	450	92	Arabiourrutia et al.[7]
PP	CSBR	500	75	Arabiourrutia et al.[7]
PP	CSBR	600	50	Arabiourrutia et al.[7]
LDPE	Fluidised bed	450	75	Hájeková and Bajus.[6]
PP	Fluidised bed	450	88	Hájeková and Bajus.[6]
PE/PP/PS	Fluidised bed	510	85-88	Predel and Kaminsky.[18]
LDPE	Fluidised bed	500	89	Williams and Williams.[12]
LDPE	Fluidised bed	700	29	Williams and Williams.[12]

It can be expected that as the temperature is lowered the recovery of wax increases. This trend confirms that thermal cracking is less severe at lower temperatures, affording higher molecular weight products that can be classified as waxes.

2.2. Methods of Characterisation

Bulk characterisation by infrared and NMR spectroscopy enables the rapid identification of major constituents based on functionality. Molecular weight distribution can be determined by GPC and works well as a comparative tool to draw trends from different processes. ICP-AES is a highly sensitive method for the determination of heavy metal concentrations. GC-MS is a highly sensitive for the separation and identification of volatile and semi-volatile compounds. The characterisation of contaminants is of high importance to the wax manufacturing industries to ensure that levels of harmful chemicals such as PAHs and heavy metals are below required specifications. The analytical procedure will incorporate a combination of methods to produce a chemical profile of pyrolysis-derived waxes and is illustrated in Figure 9.

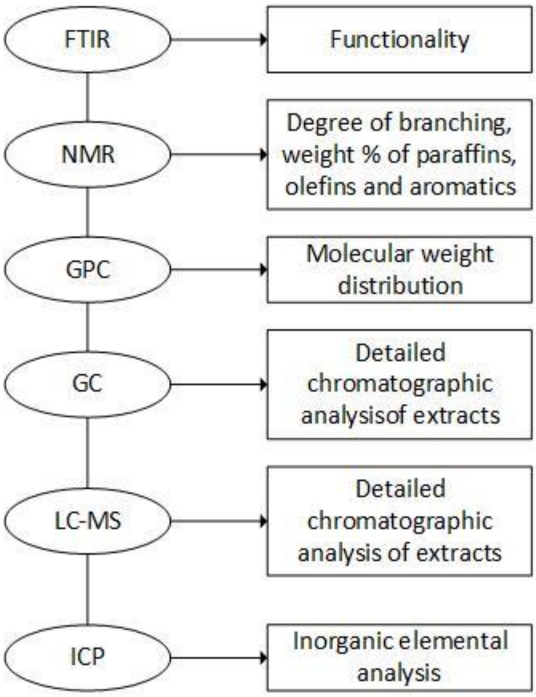

Figure 9. Analytical procedure for the research project

2.2.1. Infrared Spectroscopy

Infrared spectroscopy is a versatile and rapid technique that requires little to no sample preparation. The sorting plastics of plastic waste based on their chemical functionality is an example of how infrared spectroscopy is used in industry.[24,25] In a similar manner, infrared can be used to determine the chemical functionality of waxes derived from pyrolysis to identify major constituents and indicate what plastic/s may have been used in the pyrolysis process to produce the wax. Peak assignments for waxes are based on the correlations provided by Williams and Fleming and have been provided in Table 2.[26]

Table 2. Characteristic infrared absorbances expected for waxes derived from plastic pyrolysis[26]

Functionality	**Band**	**Peak assignment**
Methyl, Methylene	2960-2850(s)	C-H Symmetric and Asymmetric Stretch
Methine	2890-2880(w)	C-H Symmetric and Asymmetric Stretch
Alkene (conjugated and unconjugated)	1680-1620(v)	C=C stretch
Methyl, Methylene	1470-1430(m)	C-H Asymmetric and Symmetric deformations (rocking and scissoring)
Allyl	995-985(s) and 940-900(s)	C-H Out of plane deformation
Allyl (trans)	970-960(s)	C-H Out of plane deformation
Allyl (terminal)	895-885(s)	C-H Out of plane deformation
Allyl (tri-substituted)	840-790(m)	C-H Out of plane deformation
Allyl (cis)	730-675(m)	C-H Out of plane deformation
Long chain alkanes	720(w)	Long chain $-CH_2-$ rocking

The infrared results obtained from studies that carried out pyrolysis on individual and mixed plastics in waste are in good accordance with the correlations in Table 2.[7,12–14,22,27] Williams and Williams reported the presence of the aromatic groups (3100-3000 cm^{-1}, 1500 cm^{-1} and 900-675 cm^{-1}).[12] The band at 3100-3000 cm^{-1} was reported to be generally weak and may be obscured by methyl and methylene peaks; while the bands around 1500 cm^{-1} can be variable, therefore, making it difficult to analyse aromatics. The intensity of aromatic peaks were reported to increase for samples in which pyrolysis was carried out at increasingly higher temperatures (600 – 700 °C). Their results are in good accordance with the mechanism for aromatic formation at higher temperatures.[28]

The results obtained by Cit et al. on the pyrolysis of LDPE at 700 °C demonstrated less clarity with respect to aromatic formation.[14] The trends from other studies in the literature were generally in good agreement with each other and report high olefin content low aromaticity.[7,13,22]

2.2.2. Nuclear Magnetic Resonance Spectroscopy

Solution state NMR has an array of useful experiments that can be set up in automation for the analysis of various sample types. ^{1}H NMR is the most routinely used experiment for the rapid determination of chemical functionality. Peak integrals are proportional to the number of protons and sample concentration and can be used to measure the concentration of analytes using internal standards. Waxes have a wide distribution of hydrocarbons with the same or very similar functionality and generate peaks with very similar chemical shifts that overlap, therefore, individual concentrations cannot be determined in the same way. Relative proportions of functional groups can be determined by the integrating peak regions corresponding to known functional groups based on their known chemical shift ranges.

Correlations tables produced by Myers et al. have been deployed in several studies to characterise pyrolysis-derived materials by ^{1}H NMR and have been summarised in Table 3.[13,22,27,29,30] By using their equations (see Equation 1, Equation 2, Equation 3 and Equation 4 below), other information such as the iso-paraffin index (ratio between CH_3 and CH_2 peaks) can be determined. More highly branched compounds such as iso-paraffins contain more CH_3 groups than CH_2 groups; therefore, the index value is an indicator of the degree of branching between samples. To ensure the error is minimised, inversion recovery experiments enable the measurement of the T_1 relaxation. The relaxation delay is a delay in the pulse sequence to allow ^{1}H nuclei to fully relax. Therefore, setting the relaxation delay on the NMR instrument to 5 times the longest T_1 is recommended for optimal results.

Although the correlations provided above generate some useful data for a comparison, the correction factors were determined for gasoline samples; therefore, it should not be assumed that the same values can be determined for waxes, owing to differences in their physical properties. For this reason, the correction factors were not used in this study in the analysis of any of the wax samples.

Table 3 ^{1}H NMR Chemical shift assignments in literature[30]

Assignment	**Proton type**	**Chemical shift range (ppm)**
A	Aromatic	6.6 - 8.0
B	Olefin	4.5 - 6.0
C	α-methyl	2.0 - 3.0
D	Methine (paraffins)	1.5 - 2.0
E	Methylene (paraffins)	1.0 - 1.5
F	Methyl (paraffins)	0.6 - 1.0

Equation 1. Paraffins % = $\frac{\left(D-2B+\frac{E}{2}+\frac{F}{3}\right)0.97\times 100}{\left(A+\frac{C}{3}\right)0.97+\left(D-2B+\frac{E}{2}+\frac{F}{3}\right)1.02+3.33B}$

Equation 2. Olefins % = $\frac{3.33\mathrm{B}\times 100}{\left(\mathrm{A}+\frac{\mathrm{C}}{3}\right)0.97+\left(\mathrm{D}-2\mathrm{B}+\frac{\mathrm{E}}{2}+\frac{\mathrm{F}}{3}\right)1.02+3.33\mathrm{B}}$

Equation 3. Aromatics % = $\frac{\left(\mathrm{A}+\frac{\mathrm{C}}{3}\right)0.97\times 100}{\left(\mathrm{A}+\frac{\mathrm{C}}{3}\right)0.97+\left(\mathrm{D}-2\mathrm{B}+\frac{\mathrm{E}}{2}+\frac{\mathrm{F}}{3}\right)1.02+3.33\mathrm{B}}$

Equation 4. Isoparaffin index = $\mathrm{CH}_3 : \mathrm{CH}_2 = \frac{\mathrm{F}}{3} : \frac{\mathrm{E}}{2}$

The results from two different studies have been tabulated for comparison in Table 4. The overall trend demonstrates that differences in the product distribution can be mostly attributed to the feedstock and temperature. This would suggest that a higher content of PP was used as feedstock. Higher iso-paraffin index values can be observed for the pyrolysis of PP compared to that of HDPE and LDPE. These values are indicative of the higher branched products which are derived from PP pyrolysis. Furthermore, the higher aromatic content of mixed plastic waste indicates the presence of other plastics in the feedstock with aromatic functionality such as polystyrene and PET.

Table 4. ^{1}H NMR % composition

Feedstock	Paraffin %	Olefin %	Aromatic %	CH_3/CH_2	Reference
LDPE	65.6	30.1	3.7	0.16	Das and Tiwari [22]
HDPE	72.1	25	2.8	0.19	Das and Tiwari [22]
PP	62.1	35.9	2	1.34	Das and Tiwari [22]
Waste (mix)	65.6	28.9	7.4	0.19	Das and Tiwari [22]
LDPE	93.15	5.71	1.14	0.14	Yan et al. [13]
PP	92.21	5.33	2.46	0.53	Yan et al. [13]
Waste LDPE	93.18	6.14	0.68	0.22	Yan et al. [13]
Waste PP	90.8	7.66	1.53	0.49	Yan et al. [13]

Yan et al. reported a lower content of olefins from the pyrolysis of PE and PP, which contrasts with the results from Das and Tiwari who reported a much higher olefin content for the pyrolysis of the same plastics.[13,22] Das and Tiwari reported that the maximum paraffin content was achieved by increasing the pyrolysis reaction time, indicating that the reaction times used in their experiment must have been shorter.[14,22]

2.2.3. Gel Permeation Chromatography

Gel permeation chromatography (GPC) separates molecular components in a sample based on their size. Samples are dissolved in an appropriate solvent such as chloroform or tetrahydrofuran and then eluted through a column packed with microporous gel. Molecules that flow through the column can enter the pores at varying degrees of ease based on their size; whereby larger molecules elute first and smaller molecules elute later. Refractive index detectors are most commonly used for GPC, since peaks are directly proportional to the sample concentration owing to the relatively constant refractive index that polymers above 1000 g mol^{-1} possess.

Molecular weight average can be defined as: 1) the number-average molecular weight (M_n), which is the total weight of a polymer divided by the number of molecules and 2) the weight-average molecular weight (M_w), which is the total weight divided by number of molecules times by molecular weight. Since M_w takes into account the molecular weight, it gives more of an indication of the contribution of each molecule has on the average i.e. the larger the molecule, the more it contributes to M_w. These values can be determined by GPC and used to calculate the polydispersity index (PDI), which is defined as the ratio M_w/M_n. A PDI value equal to one would indicate that all the molecules within a sample have the same molecular weight, with larger values indicating an increasingly broader distribution of molecular weights. The equations to determine the molecular weight average and the polydispersity index values are given below (see equations 5 – 7).

Equation 5. $Mn = \frac{\sum NiMi}{\sum Ni}$

Equation 6. $Mw = \frac{\sum NiMi}{\sum NiMi}$

Equation 7. $Polydispersity\ Index\ (PDI) = \frac{Mw}{Mn}$

The table below enables a comparison between two studies on how the molecular weight of wax is affected by pyrolysis temperature. See Table 5 .[7,12]

Table 5. Molecular weight distribution of waxes produced from LDPE

Feedstock	**Pyrolysis temperature (°C)**	**M_n (Da)**	**M_w (Da)**	**PDI**	**Reference**
LDPE	450	1118	1734	1.55	Arabiourrutia et al.[7]
LDPE	500	1045	1577	1.51	Arabiourrutia et al.[7]
LDPE	600	1000	1460	1.46	Arabiourrutia et al.[7]
LDPE	500	494	968	1.96	Williams and Williams[12]
LDPE	550	556	959	1.72	Williams and Williams[12]
LDPE	600	498	893	1.79	Williams and Williams[12]
LDPE	650	388	736	1.90	Williams and Williams[12]
LDPE	700	341	842	2.47	Williams and Williams[12]

The results from Arabiorrutia et al. on waxes derived from the pyrolysis of LDPE between 400 and 600 °C demonstrate that the PDI decreases as the temperature increases as a result of the formation of smaller, more uniformly sized products at higher pyrolysis temperatures.[7] Although Williams and Williams obtained higher PDI values for their waxes, the same trend can be observed for waxes produced from LDPE between 500 – 600 °C.[12] A further increase in the PDI may be expected as the temperature is increased beyond 600 °C. However, the observed increase in the PDI could be explained by the formation of aromatic and polyaromatic hydrocarbons at higher pyrolysis temperatures.

2.2.4. Gas Chromatography-Mass Spectrometry

Gas chromatography is a highly sensitive routine method for the separation and characterisation and volatile and semi-volatile compounds that are present in complex mixtures. The two most commonly used types of detectors are: Flame ionization detection (FID) and mass spectrometry (MS). GC-MS is routinely used for the identification of compounds used in conjunction with the NIST (National Institute of Standards and Technology) library of compounds to match known retention times and mass spectral fragmentation patterns. GC-FID is routinely used to determine the concentration of analytes using internal and calibration standards owing to the more constant proportionality of signal intensity relative to the concentration of analytes. Another use of GC-MS is simulated distillation, which is an industry standard method of testing (ASTM) to determine the boiling point range, which can be correlated to the carbon number distribution using calibration standards.[7,22]

The gas chromatographic analysis of pyrolysis waxes conducted by Williams and Williams as well as Predel and Kaminsky both demonstrate that a series of triplet peaks corresponding to hydrocarbons with the same carbon number, in the order of: alkadiene, alkene and alkane can be observed.[12,18] Similarly, Yan et al. reported a series of double peaks that correspond to 1-olefins and *n*-paraffins.[13]

Williams and Williams report no detection of aromatic compounds after being separated by sequential elution on a column.[12] Their preparative separation step is particularly important for analysing contaminants so that interference from intensely overlapping peaks such as those from paraffins can be minimised. A different method of preparative separation was employed by Nyiri et al. to separate fatty acid methyl esters (FAME) from infant formula.[31] They used urea to form inclusion compounds with the straight chain FAMEs to make them easier to separate from the analyte mixture. Their results validated the method for the detection of trace PAH using a triple quadrupole GC-MS operating in multiple reaction monitoring (MRM) mode.[31] Both methods of separation are examples of efficient baseline separation, which enables the trace analysis of impurities.

2.2.5. Inductively Coupled Plasma-Atomic Emission Spectroscopy

ICP-AES is a highly sensitive technique for determining concentrations of inorganic ions at levels of 10 ppb or lower in most cases. The ionisation source produces a highly stable plasma using argon gas at extreme temperatures which produces a characteristic emission spectrum for each element. This enables the simultaneous analysis of multiple elements in a complex matrix with low spectral interferences. Concentrations are determined by the standard addition calibration method using an internal standard which reduces the error introduced by matrix effects and spectral interferences.[32]

For complex samples that do not dissolve well in aqueous solution, samples must be digested in a concentrated acid or mixture of acids such as nitric acid, hydrochloric acid or sulphuric acid. Some elements are unstable in certain matrixes such as titanium dioxide (TiO_2) which forms a white precipitate in nitric acid. Titanium dioxide is commonly used to increase opacity in plastics and as a white pigment; therefore, it is highly likely to be present in plastic-derived samples. This was confirmed to be the case by Sakurai et al. for the determination of toxic metals in household PE and PVC.[33] Although the formation of a white precipitate may prove to be a hindrance to analytical results, it can be separated by filtration or centrifuging and analysed separately to determine its elemental identity. A solution to eliminate the white precipitate is to use hydrofluoric acid in a mixture with nitric acid, since titanium dioxide is known to be more soluble in hydrofluoric acid.

2.3. Separations and Refining Processes

Traditional wax refining methods exploit differences in physical characteristics between waxes and impurities, enabling the selective removal of impurities by methods like solvent de-oiling (summarised in Section 1, Introduction) or adsorption. Furthermore, waxes are less reactive than certain compounds such as olefins, halogenated alkanes and aromatics, which can be converted by hydrogenation, sulphonation and oxidation into compounds that are easier to separate.

2.3.1. Adsorption and Liquid Chromatography

Hydrocarbons by type can be determined by silica column chromatography and eluting with increasingly polar solvents.[34] In this way, saturates can be eluted using a non-polar solvent (e.g. heptane) and aromatics can be eluted using an aromatic solvent (e.g. xylene, toluene and benzene). Polar compounds are either determined by difference or by eluting with a polar solvent.

Fixed bed adsorption is typically used as a wax finishing process that removes colour-inducing contaminants using fixed beds of alumina/bauxite/silica/clay. The fixed bed is typically part of a swing system whereby the spent bed is replaced with a fresh one and then regenerated by steam treating or roasting in air.[35–37]

2.3.2. Urea and Thiourea Clathrate Extraction

In the presence of methanol at the correct temperature, urea can form stable inclusion compounds (clathrates) with long chain *n*-paraffins by adopting a hexagonal crystalline structure with an internal diameter of 5 Å, which corresponds to the diameter of hydrocarbons with a straight chain.[38] The driving force behind urea clathrate formation is the stabilisation of hydrogen bonds between urea molecules through Van der Waals interactions between the channel walls and the adducted paraffin chain.[39] Similarly, thiourea may also form clathrates with branched and polychlorinated alkanes, owing to the slightly larger internal diameter (7 Å) of the adduct crystals.[38] The general procedure for the extraction of straight-chain compounds by UCE is provided in Figure 10 below.

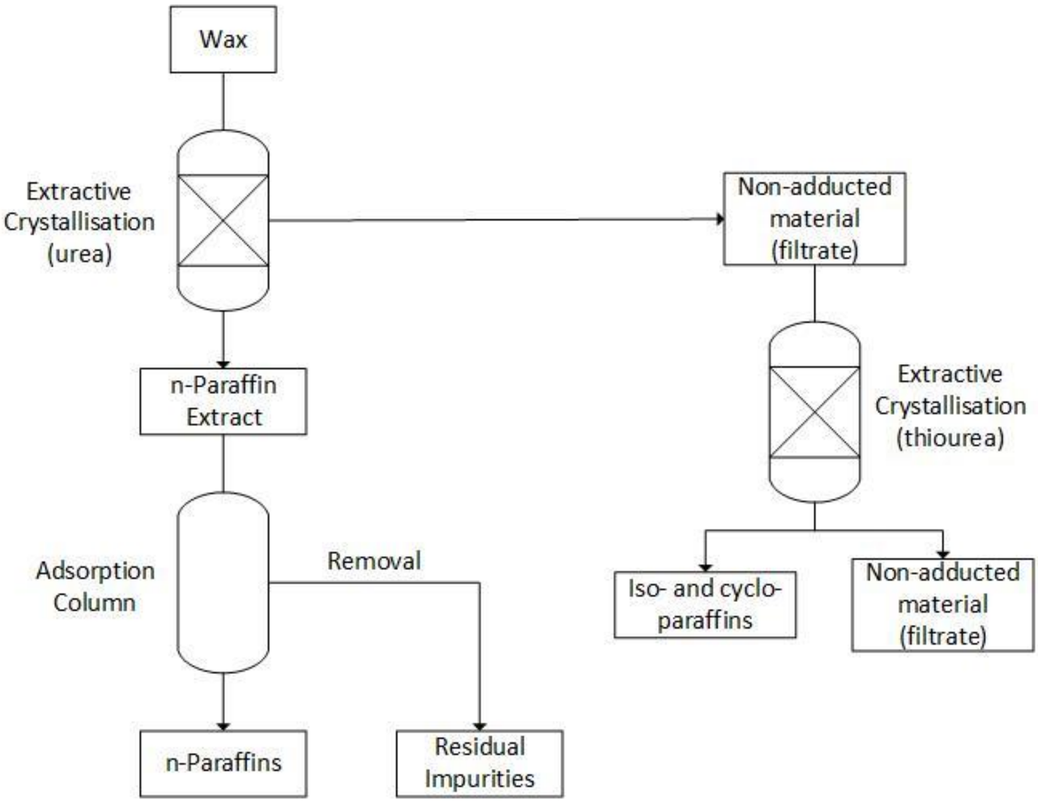

Figure 10. General scheme for urea and thiourea clathrate extraction[40]

Further investigation and optimisation of urea clathrate extraction has seen a re-emergence in recent years.[31,41,42] Yamazaki et al. studied the role of methanol on clathrate formation and concluded that methanol is not always required, however, it plays a role in decreasing the equilibrium temperature of clathrate formation.[41] However, the solubility of urea in methanol destabilises the clathrate at ambient temperatures and as a result may lead to a lower mass recovery of lower molecular weight straight-chain hydrocarbons.

The procedure could be made scalable due to the cheap reagents required and may be able to be carried out without the use of a solvent by adding crystalline urea directly to a wax melt maintained at a suitable temperature (e.g. 50°C). However, the lack of a requirement to develop scalable processes based on this method can be rationalised by the already popular method of solvent de-oiling; which produces a similar result with respect to the separation of impurities from crude wax.

2.3.3. Hydrogenation

Hydrogenation is a widely used industrial process for the conversion of unsaturated oil into saturated fats or wax in the presence of a heterogeneous solid-supported catalyst such as palladium on carbon or nickel on alumina.[43] With regard to highly olefinic waxes, it's possible to saturate olefins with a melting point below that of the corresponding paraffin i.e. olefins that are liquids at room temperature can be converted into saturated solids by hydrogenation. In addition to this, hydrogenation is used as a 'wax finishing' process in the manufacturing industry, whereby components such as fatty ketones and aldehydes bestow undesirable colour properties on crude wax and are subsequently converted into their corresponding paraffins by hydrogenation.[8]

2.3.4. Oxidation

Pyrolysis-derived waxes are suspected of having a high olefin content; therefore, the oxidising reagent must not be reactive with double bonds. Oxone® is a commercially available oxidant with high stability, selectivity and has a low cost. Although Oxone® is used in epoxidation reactions, catalysts are usually required to generate dioxiranes in situ, which are highly reactive with alkenes.[44]

Oxone® is also used in many oxidation reactions to convert thiols, sulphides and disulphides into sulphoxides and sulphones.[45] The oxidation of sulphur containing compounds enables them to be more easily separated by liquid-liquid extraction or by adsorption onto silica. In this way, oxidation may be used to oxidise impurities present in crude wax such as sulphur and nitrogen-containing, which may then be subsequently removed by adsorption/chromatography or liquid-liquid extraction.

Kropp et al. demonstrated the adsorption-mediated oxidation of sulphides and sulphoxides using silica-supported Oxone® as a reagent.[46] Furthermore, Silva et al. describe a highly versatile flow oxidation system using a fixed bed of Oxone®.[47] Fixed bed processes are desirable for commercially scalable processes owing to their simplicity in design and can be operated continuously. Furthermore, fixed bed packing materials are usually cheap, commercially available and can easily be regenerated by washing with solvents e.g. DCM.[47]

3. Results and Discussion

Pyrolysis-derived waxes often smell and are coloured which is not desirable for direct use. Three different waxes: wax A, wax B and wax C were provided for the project with the objective of developing a process to decolourise and deodorise these waxes. In the first instance, characterisation of crude waxes was carried out to provide the following information on chemical properties: functionality, molecular weight distribution and heavy metal content. Separation methods were carried out to recover purified wax and extract or fractionate the waxes to determine the properties of contaminant components using the following methods: liquid chromatography, solvent de-oiling and urea clathrate extraction in combination with the analytical procedure. The final aim was to develop a process to decolourise and deodorise crude waxes using simple and effective wax refining techniques such as: adsorption, solvent de-oiling and hydrogenation.

Please refer to the appendices, bound as a separate document to this thesis, to refer to sample masses (appendix A), GCMS chromatograms (appendix B), GPC chromatograms (appendix B), GCMS data tables (appendix C) and ICP data tables (appendix C).

3.1. Methods of Separation and Characterisation

Each fraction and extract obtained from the procedures outlined in this section was analysed by ATR-FTIR, NMR and GPC. ICP analysis was carried out only on wax samples to assess the removal of heavy metals by each separation method. Liquid injection GC-MS was carried out only on fractions and extracts containing impurities since the high abundance of long chain hydrocarbons may interfere with the identification of impurities. Wax A was filtered through celite prior to the solvent extraction procedure being carried out to remove insoluble residue.

3.1.1. Characterisation of Crude Waxes

The appearance of each wax is shown in Figure 11. Wax A exhibits a black colour, an undesirable odour and has a tar-like texture. Wax B is a brown wax with a softer texture and is not associated with a strong odour. Wax C is an orange wax with a softer texture than wax B and also does not have a strong odour.

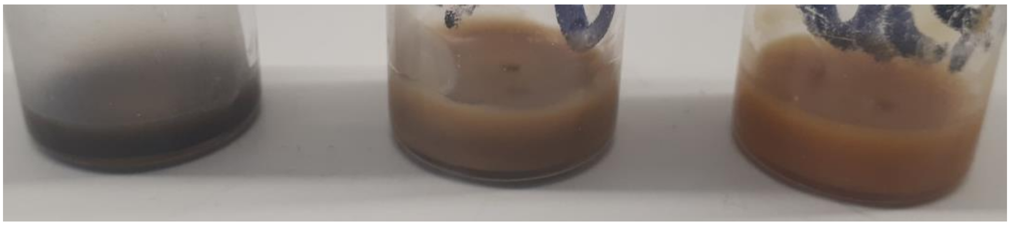

Figure 11. Crude wax A (left), wax B (middle) and wax C (right)

3.1.1.1. Solubility

The solubility of wax A, B and C was tested in a range of solvents to determine the most effective solvent to use for analytical methods and separations. The solvents used were: benzene, toluene, chloroform, hexane, cyclohexane, dichloromethane, ethyl acetate, THF, acetone, acetonitrile and methanol.

Wax A was partially insoluble in the tested solvents due to the presence of insoluble residue and elevating the temperature appeared to have no effect. The mass of insoluble residue from filtering waxes in toluene is given in Table 6. There was very little insoluble content present in wax B and C (see entries 2 and 3). Wax B appeared to be slightly cloudy in toluene, chloroform and benzene; an indication of immiscibility. Immiscibility may arise due to the presence of polar compounds in a non-polar medium and vice versa, in the case of waxes it’s the former. When the temperature was elevated, wax B dissolved in all of the tested solvents except methanol, acetone and acetonitrile. Wax C was soluble in chloroform, toluene and benzene at room temperature and dissolved in all other solvents when the temperature was elevated, with the exception of acetone, methanol and acetonitrile.

Table 6. Determination of insoluble residue

Entry	**Wax**	**Solvent**	**Wax to solvent ratio (wt %)**	**% Mass of insoluble residue**
1	A	Toluene	10	34.3
2	B	Toluene	10	0.2
3	C	Toluene	10	0.4

Increasing the temperature increases the solubility of waxes in non-polar solvents, even with more polar solvents such as ethyl acetate and THF. This fits with the conclusions by Provost et al. on the solubility of long-chain alkanes in non-polar solvents: 1) solubility increases as temperature is increased and 2) solubility decreases as chain-length increases.[48]

It is noteworthy that a white precipitate formed when wax B and C were dissolved in ethyl acetate and cooled to room temperature. The procedure was ineffective for wax A due to the high content of insoluble material that remained in the solid phase. The mass recovery of white precipitate (entries 1 and 2) for waxes B and C are provided in Table 7. The white precipitate was sequestered by filtration, however, the colour deteriorated when the solvent was removed under reduced pressure. When the filtrate (entries 3 and 4) was evaporated under reduced pressure a brown and orange coloured soft wax was afforded for waxes B and C, both possessing an unpleasant smell. This discovery was the basis of carrying out the solvent de-oiling experiments in ethyl acetate (see section 3.1.3).

Table 7. Mass recovery of precipitate and filtrate obtained by precipitating wax in ethyl acetate

Entry	**Wax**	**Solubility in ethyl acetate**	**% Mass recovery**
1	B	Precipitate	21.5
2	C	Precipitate	11.9
3	B	Filtrate	70.5
4	C	Filtrate	78.3

Chloroform was the solvent of choice for GPC and GC-MS experiments. For NMR experiments, the solubility of wax A, B and C was tested in tetrachloroethane-d2, owing to the positioning of the solvent peak away from the aromatic region. However, the solubility of wax was improved in chloroform, therefore, tetrachloroethane-d2 was not used for any further experiments.

3.1.1.2. Acid-Base Extraction

Acid-base extraction of crude waxes was carried out to determine the mass percentages of acidic and basic components in crude waxes. The mass recovery of acidic and basic components is shown in Table 8. The colour of waxes did not appear to improve following the extraction procedure and neither did the odour.

Table 8. Acid-base extraction of waxes.

Entry	**Wax**	**Sample**	**% Mass recovery**
1	A	Recovered wax	56.5
2	A	Basic components	0.4
3	A	Acidic components	0.1
4	B	Recovered wax	92.4
5	B	Basic components	0.7
6	B	Acidic components	1.0
7	C	Recovered wax	77.8
8	C	Basic components	0.5
9	C	Acidic components	0.0

3.1.1.3. GPC

The GPC results indicate the differences in sample composition by their molecular weight distribution. This enables the differentiation of heavy and light waxes, which is beneficial to know since heavy and light waxes have different uses in the wax industry e.g. paraffin wax and microcrystalline wax are examples of light and heavy waxes, respectively. PDI values are a good indication of how complex (or contaminated) a given sample is, considering that a PDI of 1.0 corresponds to the molecular weight distribution of a single compound. For example, samples with a high PDI could indicate how contaminated a sample is. The number average and weighted average molecular weight values (relative to the molecular weight of the polystyrene calibration standards) for each sample and their PDI values are displayed in

Table *9* and the chromatograms are displayed in the Appendix B section 1.1.

Table 9. Molecular weight distribution of crude waxes determined by GPC

Entry	**Sample**	**Number average molecular weight M_n (Da)**	**Weight average molecular weight M_w (Da)**	**PDI**
1	Crude wax A	1106	2212	2.00
2	Crude wax B	494	596	1.21
3	Crude wax C	299	456	1.53

It has been alluded to in the literature that lower molecular weight averages can be expected to decrease the PDI owing to the formation of smaller and more uniformly sized compounds as a result of higher pyrolysis temperatures.[6,7,12] However, the trend observed for waxes A, B and C in this study possibly indicates different levels of contamination. Contaminants include any components that contribute to colour and odour. The crude waxes used in this project are derived from real plastic waste and can be expected to possess a polydisperse nature owing to the different types of plastic and plastic additives present in mixed plastic waste. Therefore, one might expect a highly contaminated wax sample to have a higher PDI value than a less contaminated one.

Based on the GPC data presented above, wax A (entry 1) appears to be the densest wax and the PDI obtained for this wax also indicates that it is the most complex sample. Wax B (entry 2) is the least polydisperse sample and possesses a considerably lower average molecular weight than wax A. Wax C (entry 3) is the lightest wax and possesses a PDI value that is higher than wax B, possibly indicating that wax C is more highly contaminated than wax B.

GPC has demonstrated good applicability for comparing waxes derived from plastic pyrolysis, enabling the differentiation between heavy and light waxes and the degree of contamination between samples. Furthermore, the data afforded by GPC is good feedback on how pyrolysis processes might be optimised in the future to produce the desired product specification. Waxes derived from the pyrolysis of mixed plastic waste can be expected to be more contaminated, therefore, possessing higher PDI values than waxes derived from sorted plastic.

3.1.1.4. FTIR

In the first instance, the chemical functionality of major constituents was carried out by FTIR. A summary of all of the peaks characterised for all three waxes is provided in Table 10. The peak assignments are based on known infrared absorbances in the literature.[26]

Table 10. FTIR peak assignments

Wavenumber (cm^{-1})	**Assignment**
2952 (m)	Asymmetric methyl C-H
2917 (s)	Asymmetric methylene C-H
2849 (s)	Symmetric methylene C-H
1640 (w)	C=C stretch
1461 (m)	Asymmetric C-H deformation
1375 (m)	Symmetric C-H deformaion
997 (w)	Out of plane deformation 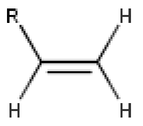
970 (w)	Out of plane deformation 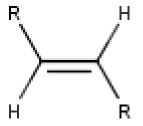
909 (w)	Out of plane deformation 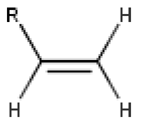
887 (w)	Out of plane deformation 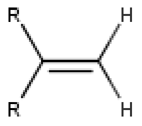
720 (m)	Long chain C-H rocking

The spectra for wax A, B and C are given in Figure 12. The peaks between 2960 – 2840 cm^{-1} correspond to the C-H vibrations of $-CH_2-$ and $-CH_3$ groups. Asymmetric and symmetric deformations of methyl and methylene groups are observed in the regions; 1470 – 1430 cm^{-}

^{1} and 1390 – 1370 cm^{-1} respectively. The peak at 720 cm^{-1} is characteristic of the rocking of -CH$_2$- groups present in long chain hydrocarbons. Vinyl and aryl C-H stretching vibrations in the general region of 3095 – 3010 cm^{-1} cannot be observed on the spectrum. The vinyl C=C stretch may be observed at 1640 cm^{-1} for all three waxes; however, it has a very weak intensity. There are three variable aromatic C=C stretching vibrations which are usually absent at ~1500, ~1580 and ~1600 cm^{-1}. The most likely explanation for the lack of aromatic stretching vibrations is the low abundance of these compounds in the crude waxes. Although the vinyl stretching vibrations cannot be observed, they can be characterised by their out of plane deformations between 1000 – 880 cm^{-1}.

Figure 12. Infrared spectra of crude waxes

The infrared spectrum obtained for waxes A, B and C do not greatly differ and confirm that paraffins are the major constituents. The C=C stretch at 1640 cm^{-1} and the out of plane deformations between 887 – 997 cm^{-1} confirm olefins to be present, which is consistent with the thermal degradation mechanism, in which the beta-scission of secondary radicals leads to their formation during pyrolysis.[17] The infrared spectrum provides little clarity regarding the presence of aromatic compounds, which is consistent with the observations from other studies.[13,22,27] Cit et al. and Williams and Williams both confirm the presence of the aromatic

Ar-H stretch in their study on the pyrolysis of LDPE at 700 °C, which is consistent with the formation of aromatic and PAH compounds by Diels-Alder reactions that occur at higher pyrolysis temperatures.[12,14,28] The absence of this peak indicates that the aromatic content of waxes is very small. The infrared data obtained for waxes A, B and C appears to be most consistent with the results obtained by Arabiourrutia et al. for wax derived from LDPE pyrolysis at 450 ˚C.[7] All things considered, it may be speculated that waxes A, B and C were obtained by low temperature pyrolysis (below 600 ˚C) of plastic waste containing a high composition of polyethylene and polypropylene in the pyrolysis feedstock.

3.1.1.5. NMR

The NMR spectrum of wax A, B and C can be characterised by the peak regions given in Table 11 below. The assignment of peaks was carried out based on known literature values.[26,30] The equations provided by Myers et al. were not used to generate any data for this study, since their correction factors apply to oils (such as diesel and gasoline) and could introduce error.

Table 11. NMR peak assignments

Proton type	**Chemical shift range (ppm)**
Aromatic Ar-**H**	6.70 - 8.00
Vinyl $\mathbf{H}_2$C=C**H**-, $\mathbf{H}_2$C=CR- -**H**C=C**H**-	4.50 – 6.00
Allyl H$_2$C=CH-C$\mathbf{H}_2$-, -HC=CH-C$\mathbf{H}_2$-, Ar-C$\mathbf{H}_3$, Ar-C$\mathbf{H}_2$-R,	1.62 – 3.00
Methine R$_3$C**H**	1.49 – 1.90
Methylene -C$\mathbf{H}_2$-	1.03 - 1.49
Methyl –C$\mathbf{H}_3$	0.60 - 1.03

The spectra for wax A, B and C are illustrated below in Figure 17. As expected, methylene and methyl groups produce the most intense signals, while olefinic signals are relatively weak and aromatic peaks are very weak on the NMR spectrum. This peak at 5.84 ppm is highly resolved and enables a first order approximation of the splitting pattern, where the observed doublet of doublet of triplets (ddt) is characteristic of terminal allyl groups. A tertiary substituted allyl proton (-CH=CH-C**H**R-) would appear as a doublet of doublet of doublets (ddd) and would be shifted slightly further downfield of where the ddt multiplet appears. Since this cannot be observed on the spectrum, it may be concluded that tertiary substituted allyl groups are not present.

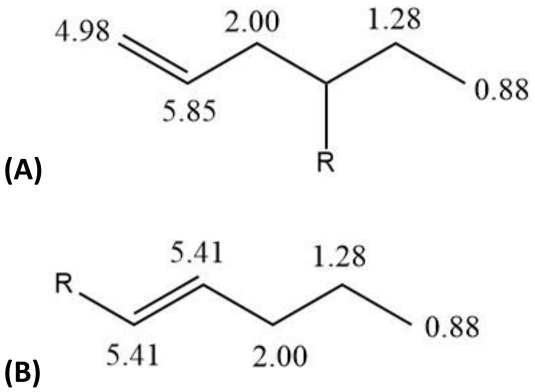

Figure 13. General overview of peaks identified by NMR. Values correspond to chemical shift (ppm). (A) aliphatic and terminal alkene. (B) aliphatic and mid-chain alkene.

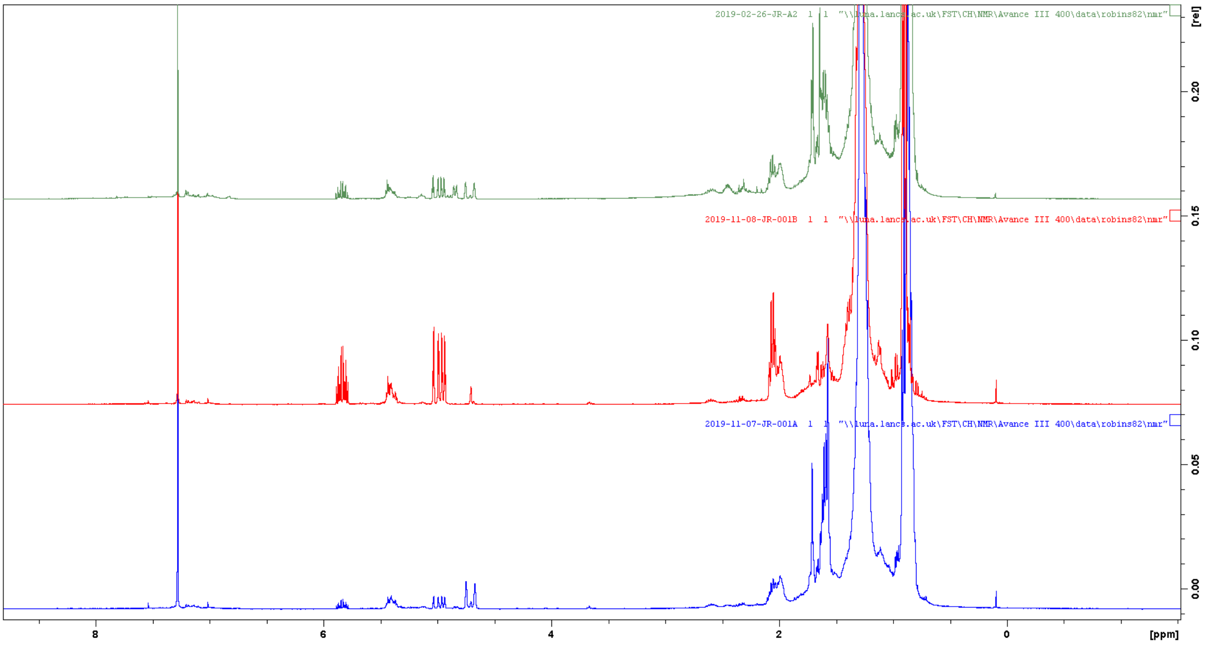

Figure 14. Wax A (bottom, blue), wax B (middle, red) and wax C (top, green) NMR spectra

There are overlapping signals in the 1.5 – 1.9 ppm region which correspond to allyl and methine protons. This does not seem to be accounted for in the literature and this peak region has usually been assigned to correspond to only methine carbons.[13,22,27] The correlation tables developed by Myers et al. do not include allyl protons since their correlations are based around characterising gasoline samples, which contain far smaller quantities of olefinic compounds.[30] The values in Table 10 for allyl and methine protons were determined by the COSY experiment and the proton couplings can be seen in the example below in Figure 15.

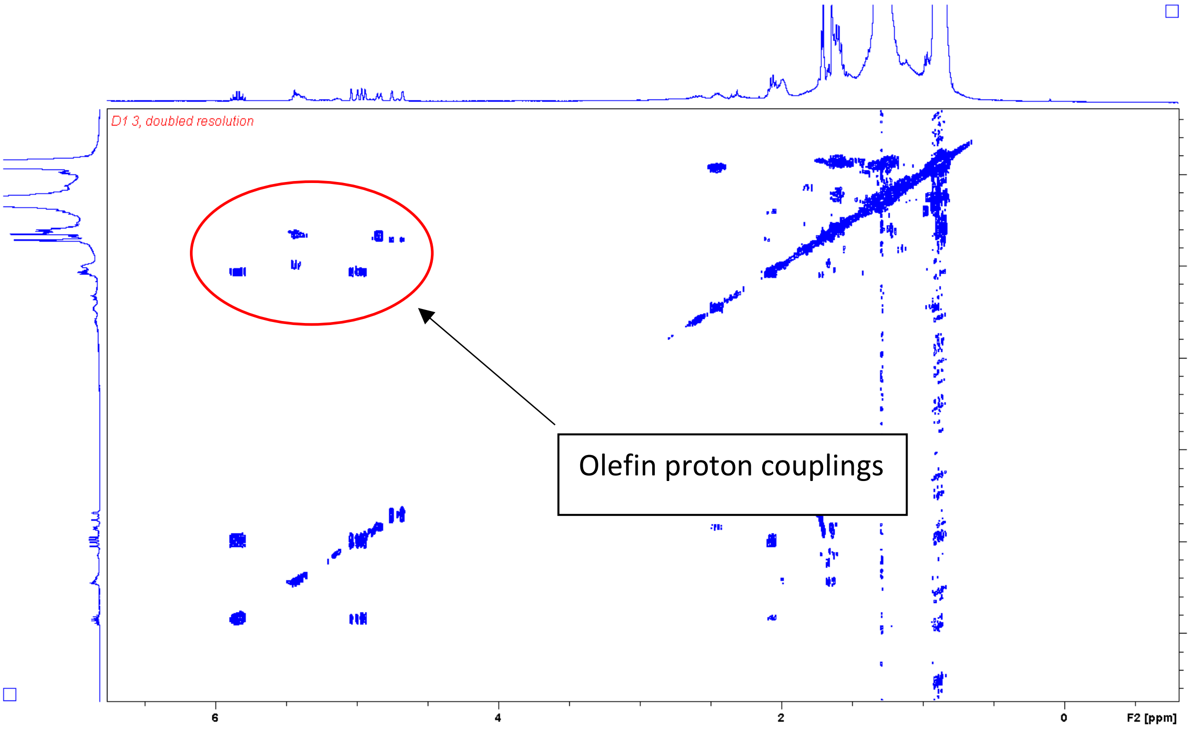

Figure 15. COSY spectrum of wax C – identifying allyl peaks in the aliphatic region between 1.62 – 1.90 ppm

3.1.1.6. ICP

The possible origins of heavy metals detected in waxes A, B and C have been summarised in

Table *12*. The presence of heavy metals in plastic-derived wax can be attributed to the inorganic additives in plastic waste, catalysts used in the pyrolysis process and metals leached from the reactor (iron, nickel, chromium and manganese from steel alloys). Although inorganic plastic additives make up a small concentration of plastics, the concentration of heavy metals present in the wax is likely a result of build-up over time of residual heavy metals during the pyrolysis process.

Table 12. Possible sources of heavy metals present in plastic-derived wax[49]

Function	**Substances**	**w/w in plastic (range)**
Flame Retardant	Zinc borate, aluminium oxide trihydrate	0.70 – 3.00 %
Antioxidants and UV stabilisers	Cadmium and lead compounds	0.05 – 3.00 %
Heat Stabilisers	Cadmium and lead compounds, barium and calcium salts of nonylphenol	0.50 – 3.00 %
Slip additives	Zinc Stearate	0.10 – 3 %
Inorganic pigments	Zinc sulphide, iron oxide, cadmium-based, manganese-based, chromium-based, titanium dioxide	0.01 – 10.00 %
Filler	Calcium carbonate, clay, zinc oxide, magnesium sulphate, barium sulphate	Up to 50.00 %

The concentration of heavy metals present in waxes A, B and C was determined by by ICP and the values are provided below in Figure 17, Figure 18 and Figure 19. Waxes have widespread commercial applications, therefore, it is important to monitor the content of potentially toxic metals. The detection of heavy metals is particularly important since Cadmium, chromium, lead and nickel are known to be toxic at low concentrations.[50] The ICP experiment carried out in this research was for the purpose of determining the major heavy metal components present.

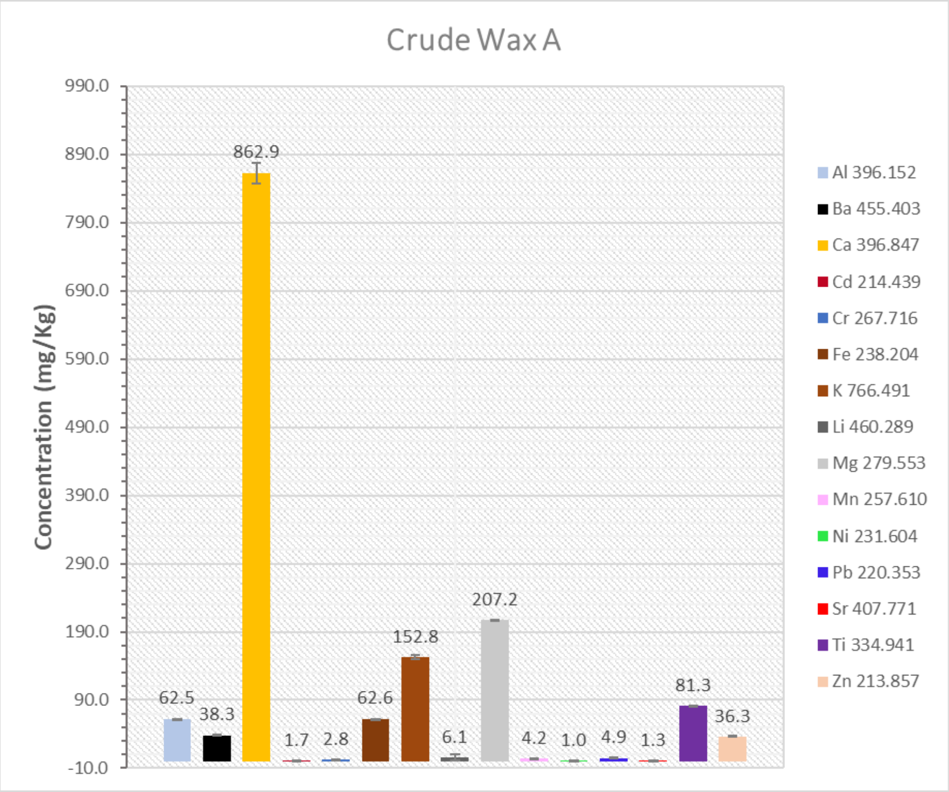

Figure 16. Wax A heavy metal concentrations determined by ICP

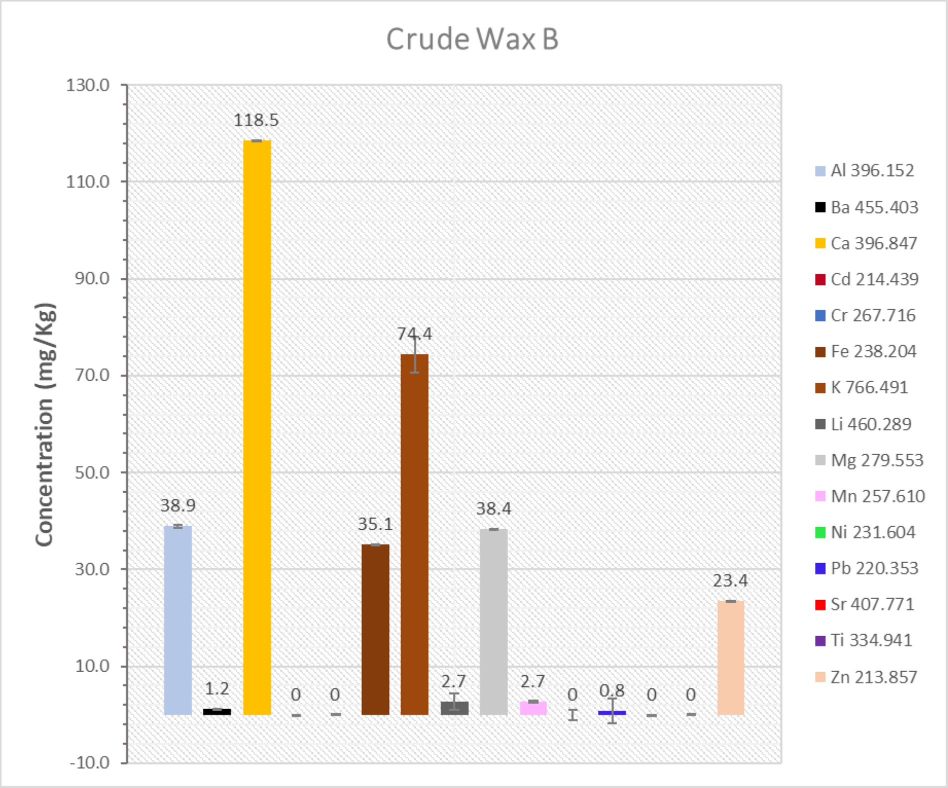

Figure 17. Wax B heavy metal concentrations determined by ICP

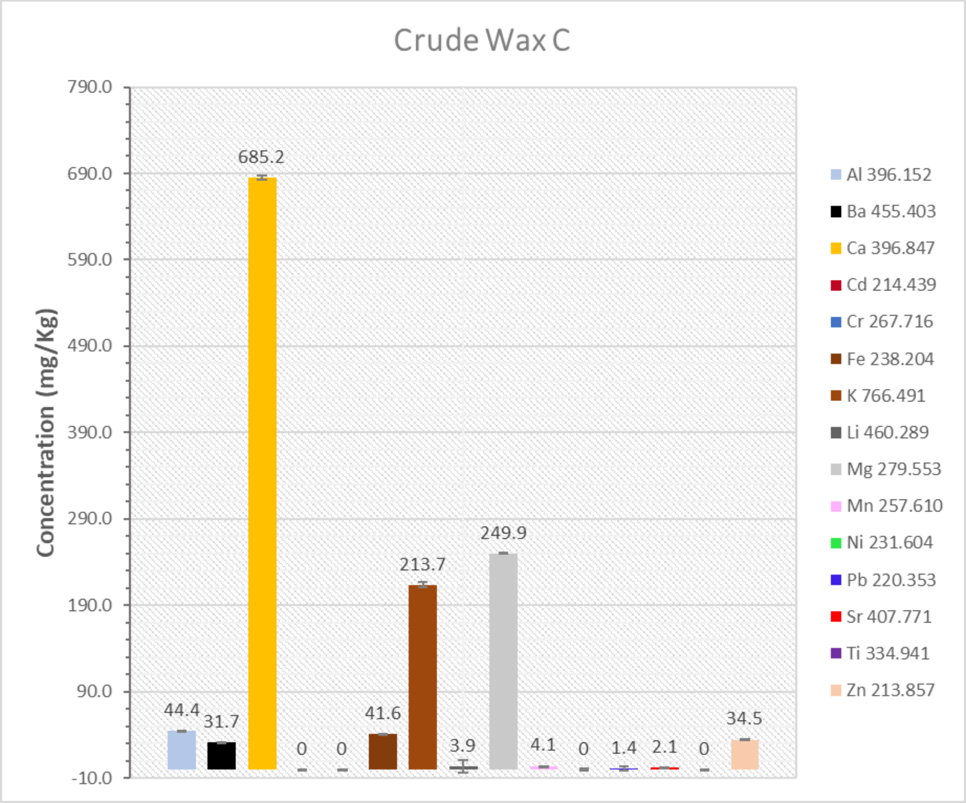

Figure 18. Wax C heavy metal concentrations determined by ICP

3.1.1.7. Headspace GC-MS

The identification of volatiles was carried out by headspace GC-MS. The odour of waxes B and C are far less intense than wax A’s odour. This was reflected by the GC-MS chromatograms obtained for each wax in which the split ratio had to be decreased from 100 to 10 for waxes B and C. The detected volatile components are predominantly hydrocarbons; however, none of the components detected are known to have particularly unpleasant odours. Most odour-inducing compounds don’t require high concentrations to produce a noticeable odour. Sulphur, nitrogen and oxygenated compounds can produce noticeable odours at sub ppm (mg/kg) levels.[51] However, the detection of sulphur and oxygen compounds is hindered due to the co-elution of these compounds with hydrocarbon peaks. Usually specialised detectors are required to enable the detection of sulphur and oxygen containing compounds.[52]

3.1.2. Liquid Chromatography

Crude waxes were separated into fractions on a silica column based on their affinity for the stationary phase (silica) by sequentially eluting the sample with increasingly polar solvents (100% hexane to 81:15 hexane to 100% methanol).

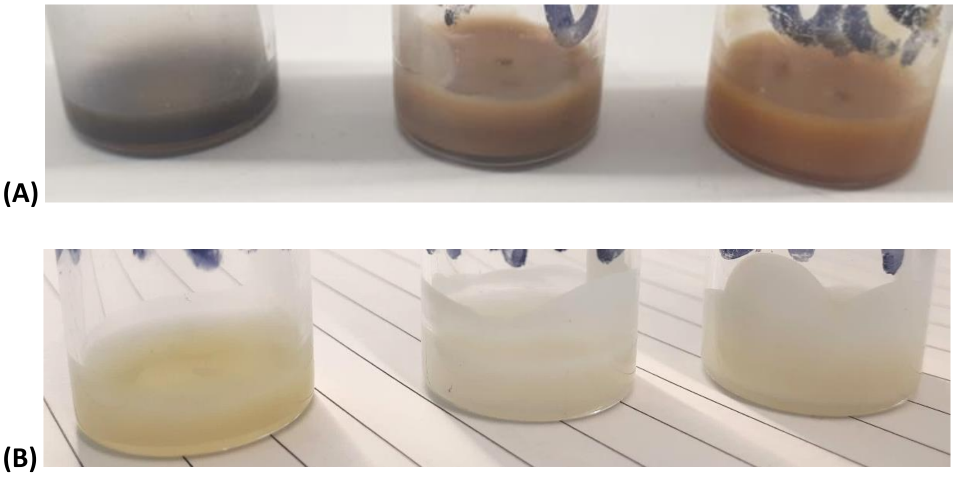

Figure 19. **(A)** Crude wax A (left), crude wax B (middle), crude wax C (right). **(B)** Non polar fractions of wax A (left), wax B (middle) and wax C (right)

Three distinct fractions can be defined: a colourless non-polar fraction comprised of wax, a yellow/orange medium polarity fraction, and a high polarity fraction with the appearance of a brown residue. The brown residue adsorbs strongly onto silica and elutes rapidly using high polarity solvents such as methanol or isopropyl alcohol (IPA). The yellow-coloured fraction appeared as a broad yellow band on the column and rapidly eluted when 15% ethyl acetate/hexane was used as an eluent. The non-polar fractions recovered from waxes B and C did not have any noticeable odour and exhibit favourable colour properties, as illustrated in Figure 19. There was a slight odour noticeable in the case of wax A, however, it was far less intense than the crude wax A. The downside to this method is the poor solubility of wax in hexane, which can result in practical issues such as; high volumes of solvent required and blockage of the column and sinter funnel. This method proved to be the most effective method of separation for acquiring a quality set of data from the analytical procedures.

Masses of fractions recovered by liquid chromatography are provided in Table 13. The mass of wax recovered was high for waxes B (entry 4) and C (entry 7) and was lowest for wax A (entry 1) owing to the high content of insoluble residue. This procedure has demonstrated that the impurities that produce unpleasant odours and undesirable colours in crude waxes can be separated by their increased affinity of the stationary phase (in this case silica) and are present in small quantities.

Table 13. Mass recovery of fractions separated by liquid chromatography

Entry	Wax	Fraction	% Mass Recovery
1	A	Non-polar	75.7
2	A	Medium polarity	3.5
3	A	High polarity	0.6
4	B	Non-polar	95.2
5	B	Medium polarity	2.7
6	B	High polarity	0.7
7	C	Non-polar	93.1
8	C	Medium polarity	6.5
9	C	High polarity	1.0

3.1.2.1. GPC analysis of fractions

GPC data for fractions separated by liquid chromatography are displayed below in Table 14. Medium and high polarity fractions obtained from liquid chromatography exhibit relatively high PDI values and lower number average molecular weight values compared to waxes. This supports the conclusion from the previous section, regarding the GPC data of crude waxes (section 3.1.1.3): that as the complexity of a sample increases the PDI value increases. Entries 5 and 6 possess higher molecular weight averages and PDI values compared to entries 8, 9, 11 and 12, confirming that wax A is the most contaminated sample. Entries 5 and 6 possess higher PDI values than the recovered wax (entry 4), confirming the removal of impurities. The impurities (entries 5 and 6) possess high molecular weight averages, which confirm the impurities to consist of high molecular weight components, in contrast to impurities fractionated from waxes B and C (entries 8, 9, 11 and 12), which confirms them the impurities to consist of low molecular weight impurities.

Table 14. Molecular weight distribution of liquid chromatography fractions determined by GPC.

Entry	**Wax**	**Fraction**	**Number average molecular weight M_n (Da)**	**Weight average molecular weight M_w (Da)**	**PDI**
1	Crude wax A	n/a	1106	2212	2.00
2	Crude wax B	n/a	494	596	1.21
3	Crude wax C	n/a	299	456	1.53
4	A	Non-polar	1235	2224	1.80
5	A	Medium polarity	1124	2836	2.52
6	A	High polarity	558	1475	2.64
7	B	Non-polar	487	602	1.24
8	B	Medium polarity	168	391	2.32
9	B	High polarity	246	458	1.86
10	C	Non-polar	429	530	1.23
11	C	Medium polarity	142	236	1.67
12	C	High polarity	176	322	1.82

3.1.2.2. FTIR

The FTIR spectra obtained for wax A, B and C non-polar fractions exhibited the same properties to that of the crude wax and no further elucidation of structures could be provided. FTIR spectra for wax A, B and C non-polar fractions are provided in Figure 20.

Figure 20. Non-polar fraction FTIR spectra

Figure 21 shows the infrared spectra obtained for the medium polarity fractions. The sharp peak at 730 cm^{-1} (s) is most intense in the case of wax A and is less intense for waxes B and C. GPC data confirms the molecular weight average of this fraction to be relatively high, therefore, it is possible that this peak corresponds to long-chain hydrocarbon rocking. The peak at 905 cm^{-1} (s) for wax A is found in the region that corresponds to terminal olefins. The high intensity of this peak along with the long-chain rocking peak may be an indication that terminal olefins are long-chain compounds present in the sample. The two sharp peaks identified at 1185 (m) and 1080 cm^{-1} (m) for wax B are present in the region in which the ester C-O stretch is usually found (1300 – 1050 cm^{-1}). Furthermore, the peak at 1718 cm^{-1} (w) may correspond to the C=O stretch, which would confirm the presence of an ester. There are few identifiable characteristics in the fingerprint region for wax C. The two broad peaks present at 1597 cm^{-1} (w) and 1701 cm^{-1} (w) are in the region in which aldehydes and ketones are present; these peaks are also present for wax A. There are no broad O-H peaks above 3000, which confirms that the C-O and C=O peaks identified do not correspond to carboxylic acids or alcohols but compounds containing an O-R group. It has been reported that the thermal degradation of polyesters affords carbon monoxide, carbon dioxide, water and hydrogen gas at higher temperatures via a six membered ring rearrangement at 770 °C.[53,54] The presence of polyesters in wax B would indicate the incomplete thermal degradation of polyesters. The possible presence of polyesters is supported by GC-MS data obtained from liquid chromatography fractions (section 3.1.2.4).

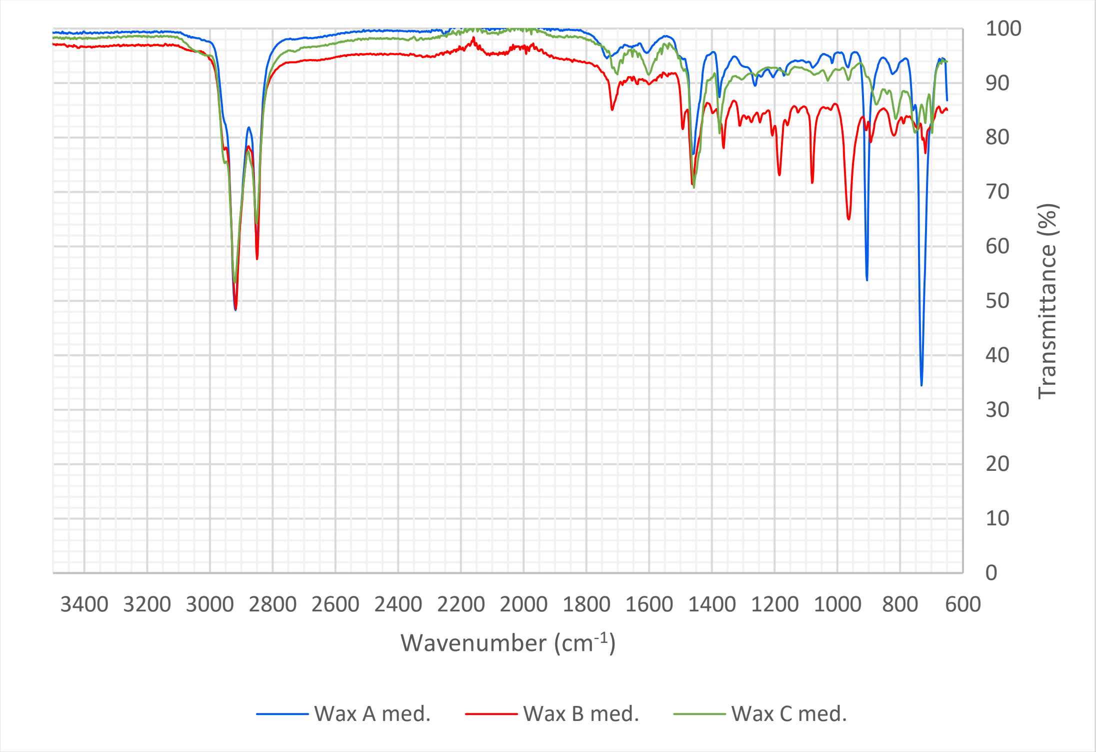

Figure 21. Medium polarity fraction FTIR spectra

Figure 22 shows the infrared spectrum obtained for the high polarity fraction. The O-H stretch at 3600 – 3100 cm $^{-1}$ could correspond to residual methanol and/or water. Methanol was used as the eluent to afford the high polarity fraction; therefore, inefficient removal of methanol/water under reduced pressure is the likely source of this peak. The tailing of the O-H peak in wax C between 3600 – 2300 cm^{-1} could correspond to a carboxylate O-H peak, with the C-O peaks appearing as a broad peaks around 1200 – 900 cm^{-1}. The broadness of this peak suggests that it possibly corresponds to multiple chemical species: carboxylates, esters, phenols and alcohols. The broad peak at 1750 – 1500 cm^{-1} likely corresponds to multiple species: alkenes (C=C), aromatics (C=C), esters (C=O), aldehydes and ketones (C=O) owing to the perceived high complexity of contaminant fractions. The overlapping of weak signals prevented any further elucidation of molecular species present in the high polarity fraction.

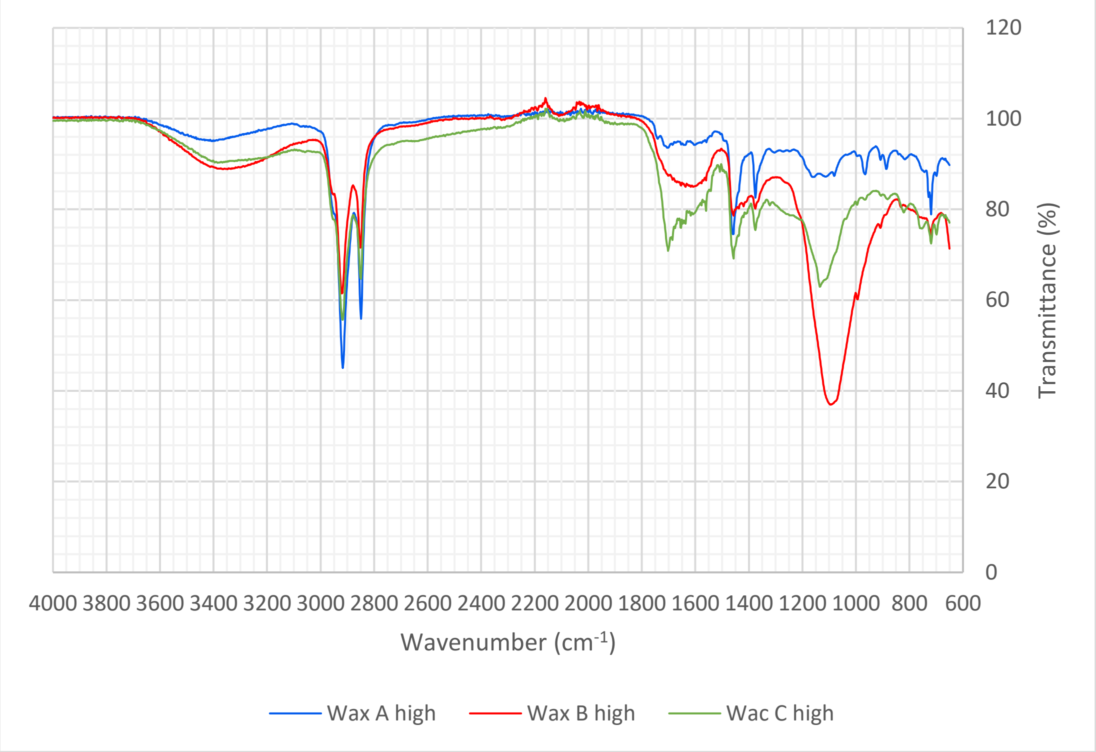

Figure 22. High polarity fraction FTIR spectra

3.1.2.3. NMR

NMR spectra of non-polar fractions exhibit much of the same characteristics as that of the crude waxes. The NMR spectra for non-polar fractions is illustrated in Figure 23. Aromatics give rise to weak and broad signals between 6.7 – 8.5 ppm for all three waxes. The same is true for most of the aliphatic peaks between 0.6 – 3.00 ppm for all three waxes. Inhomogeneity in the magnetic field caused by the presence of particulate matter in the samples is the most likely reason for the broad peaks on the NMR spectrum. For this reason, it made it very difficult to elucidate any further information from the NMR spectra of medium and high polarity fractions. The NMR spectra for these fractions are illustrated below in Figure 24 and Figure 25.

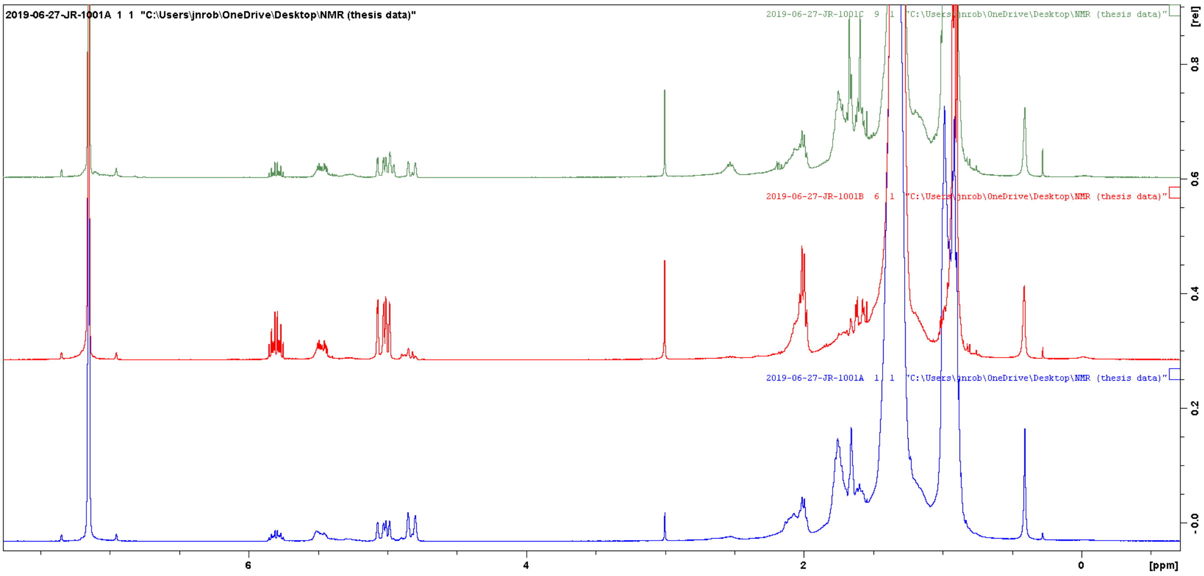

Figure 23. NMR spectra of non-polar fractions. Wax A (bottom, blue), wax B (middle, red) and wax C (top, green)

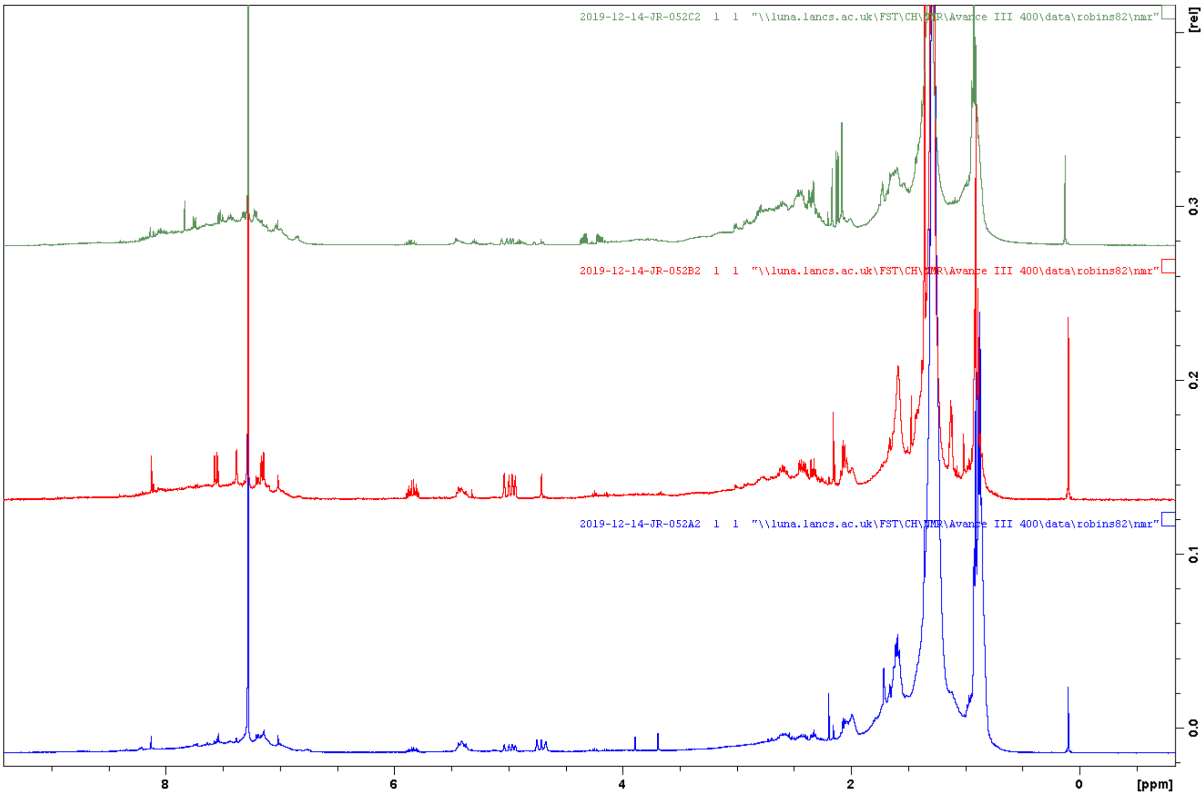

Figure 24. NMR spectra of medium polarity fractions. Wax A (bottom, blue), wax B (middle, red) and wax C (top, green)

Elucidation of peaks in the aliphatic region (0.6 – 3.00 ppm) is difficult owing to the complexity of spectra and the overlapping of peaks. Aromatic and olefinic peaks are weaker in comparison to the NMR spectra of crude waxes. The presence of peaks between 3.50 – 4.50 ppm suggests the presence esters, which is supported by the FTIR data, however, the further elucidation of structures by NMR was hindered by the overlapping of peaks. There are no peaks between 9.00 and 12.00 ppm, indicating that no carboxylic acids or aldehydes are present.

The FTIR and NMR data obtained for the medium and high polarity fractions of waxes A, B and C is too unclear to make any clear trends owing to the complexity of spectra and the overlapping signals..

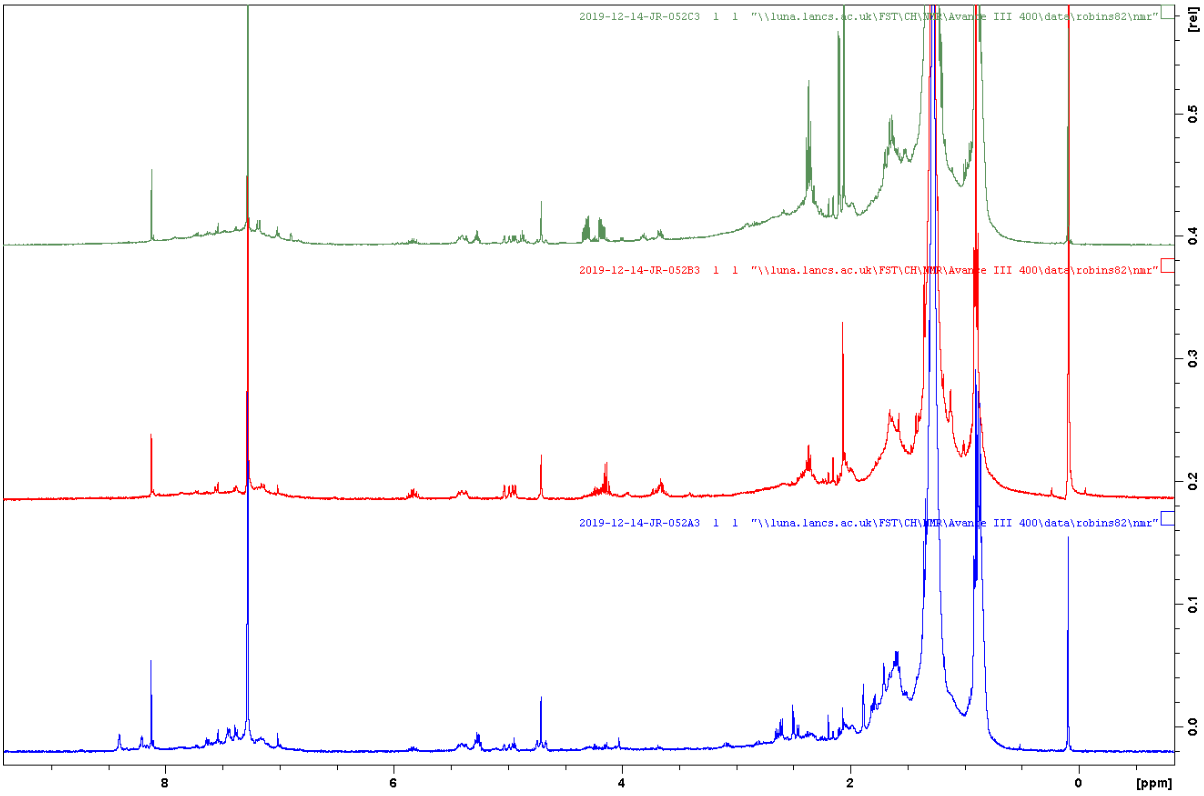

Figure 25. NMR spectra of high polarity fractions. Wax A (bottom, blue), wax B (middle, red) and wax C (top, green)

3.1.2.4. GC-MS

GC-MS was carried out on wax A, B and C medium and high polarity fractions to identify the major contaminant components. Chromatographic peaks were referenced to mass fragmentation patterns and retention indices of known compounds in the NIST library. Only matches ≥ 90% were selected to identify analytes. Some analytes can be attributed to plastics and plastic additives commonly found in plastic waste and are displayed in Table 15 and Table

16. The full set of data and the chromatograms for each sample can be found in the appendix. Good peak separation of non-hydrocarbon analytes from dominating hydrocarbon peaks was achieved by liquid chromatography. Various types of compounds were identified including: PAHs, plasticisers, nitrogen and oxygen containing compounds and elude to plastic types and additives that may be present. There were some peaks corresponding to residual paraffins and olefins, however, their presence did not greatly affect the identification of other peaks.

Table 15. Possible thermal degradation products and their possible plastic waste origins

Detected compounds and compound types	**Waste origin (type of polymer or additive)**	**Wax detected in**
Benzaldehyde	PET	A, B, C
Benzyl alcohol	PET	A, B, C
Di-tert-butylphenol	Polycarbonate	A, B, C
Isopropylphenol	Polycarbonate	A
Diisopropylnaphthalene	Polycarbonate	A
Methyl- and dimethylnapthelene	Polystyrene	A
Pentamethylbenzene	Polystyrene	A
Triphenylbenzene	Polystyrene	C
Tetradecanamide	Polyamide (e.g. nylon)	A, B, C
Hexadecanamide	Polyamide (e.g. nylon)	A, B, C
Methyl Stearate	Plastic additive (slip additive)	A, C
Esters	Polyester	A
Alcohols	Polyester, amides	A, B, C
Aldehydes	Polyester, amides	B
Phthalates	Plastic additives (plasticiser)	A, B, C
Polychlorinated hydrocarbons	PVC	B, C
Polyflourinated hydrocarbons	PTFE (Teflon)	A, B,

The presence of aromatic compounds and their alkylated derivatives may arise from variations in plastic feedstock (e.g. PS, PET, PC) and from secondary Diels Alder reactions occurring at higher temperatures.[14,28,55] No PAH compounds were detected for wax A, however, it is also possible that the sample preparation procedure (filtration through celite) removed PAH compounds. Unfortunately, this could not be avoided due to the presence of insoluble residue that had to be removed to prepare samples of wax A. The polyaromatic compounds detected in medium fractions of waxes B and C are given below in Table 16. Peaks corresponding to PAH had very low intensity on the chromatogram, suggesting that the concentration of these components is very small.

Table 16. Possible Trace PAH detected by GC-MS

Compound detected	Wax detected in
Fluoranthene	B, C
Perylene	B, C
Indenopyrene	B, C
Bis(bromomethyl)anthracene	C
Dihydro-4H-benz[de]anthracene	C
Methylpyrene	B, C
Dimethylpyrene	C

Several compounds were identified that could be derived from polycarbonate: 2,4-di-tert-butylphenol, 3-isopropylphenol and 2,6-diisopropylnaphthalene. In their review, Antonakou and Achilias have stated that the pyrolysis of polycarbonate results in the formation of isopropyl-substituted aromatic compounds.[56] Furthermore, 2,4-ditertbutylphenol is used in the production of polycarbonate. Therefore, the detection of these compounds by GC-MS indicates that polycarbonate could be present in the feedstock. Moreover, the detection of amides and carboxylates are likely to be derived from the thermal degradation of polyamides and polyesters.

3.1.2.5. Silica Column Regeneration and Elution Volume

The elution volume can be defined as the volume of wax solution (in hexane) that can be eluted before the elution of yellow coloured compounds occurs and begins to contaminate the purified wax. Initially, the column regeneration procedure involved flushing with 15 % ethyl acetate/hexane and then neat methanol to remove impurities, followed by reconditioning by flushing again with 15 % ethyl acetate/hexane and then neat hexane (entry 1 and 2). The elution volume of wax and number of column regenerations is illustrated in Table 17.

Table 17. Determination of elution volume, experiment 1

Entry	**Number of column regenerations**	**Mass of silica (g)**	**Concentration of wax solution in hexane (g/L)**	**Elution Volume (mL)**
1	1	20	35.7	175
2	2	20	35.7	0

From experiment 1, yellow-coloured contaminants eluted straight away after the column was regenerated for the first time (entry 2). This result could indicate that methanol was not efficiently removed by reconditioning the column. The presence of methanol on the column increases the mobility of polar compounds on the silica, which could explain this observation. It is also possible that eluting with methanol moves polar compounds further down the column without fully removing them, resulting in the contamination of any further fractions collected after reconditioning the column.

For experiment 2, methanol was substituted for IPA as the polar regeneration solvent, however, this also proved to be unsuitable for regenerating the column owing to the retention of polar solvents onto silica. IPA is fully miscible with hexane; therefore, it was thought that reconditioning the column would be more effective using this solvent. However, the same problem persisted (contamination of non-polar fraction after reconditioning) and it can be concluded that other methods such as thermal treatment in an oven or vacuum oven should be tried.

Table 18. Determination of elution volume, experiment 2

Entry	Number of column regenerations	Mass of silica (g)	Concentration of wax solution in hexane (g/L)	Elution Volume (mL)
1	1	20.07	21.28	250
2	2	20.07	21.28	0

Experiment 2 demonstrated that high polarity solvents (methanol and IPA) increase the mobility of colour-inducing impurities on silica, causing early contamination of the purified wax.

The quality of wax produced by removing the high polarity solvent from the regeneration step for experiment 3 and using only a medium polarity solvent: 15 % ethyl acetate/hexane (entry 1, 2 and 3). This proved to be effective; however, due to blockage of the column, it was not possible to continue the experiment past entry 3. If the column is not dried fully before re-use, then the residual solvent present on the column will result in contamination of purified wax. The poor solubility of wax in the eluting solvent (hexane) is a hindrance which cannot easily be overcome in the laboratory. A temperature-maintained process would be ideal and solve issues of solubility and blockage of the column, however, this cannot easily be done in the lab. Furthermore, increasing the volume of solvent used to dissolve the wax does not aid in dissolution. Long experiment times and large volume of solvent are disadvantages that hinder the scalability of the process.

Table 19. Determination of elution volume, experiment 3

Entry	Number of column regenerations	Mass of silica (g)	Mass of wax in hexane (g)	Elution volume (mL)
1	1	20.08	20.3	150 mL
2	2	20.08	20.3	150 mL
3	3	20.08	20.3	150 mL

3.1.3. Solvent de-oiling

Usually, 2-butanone and butyl acetate are used in industrial processes for the de-oiling of wax owing to the increased solubility of impurities and the decreased solubility of wax in these solvents and other solvents with similar properties.[9,57] The observations from the solubility test (section 3.1.1.1) experiment are the basis of why the solvent de-oiling process was developed using ethyl acetate (section 3.3.1). Solvent de-oiling is a method used to extract oil (liquid) and solvent-soluble impurities such as colour-inducing compounds and aromatics. The purpose of this procedure was to decolourise and deodorise wax and separate impurities. Wax A was filtered through celite to remove insoluble content prior to the experiment being carried out.

The appearance of de-oiled waxes is shown below in Figure 26. The appearance of oil extracts is illustrated in Figure 27. The oil extracts were viscous and possessed an unpleasant odour and undesirable colour properties, indicating the successful removal of contaminants.

Cooling from an elevated temperature to room temperature produced a white precipitate and further cooling to -32 °C increased the mass of recovered white precipitate (wax). De-oiled wax A possessed the least favourable colour properties, demonstrating that the impurities present have poor solubility in ethyl acetate. Wax B’s colour properties were improved slightly, however, the wax still exhibited undesirable colour, demonstrating that wax B too contains impurities that are hard to remove by extraction with ethyl acetate. The colour properties were significantly improved for wax C, which exhibited only a slight trace of colour after the procedure. Overall, the separation method proved that there are hard to remove impurities still present after solvent de-oiling, therefore, by combining the procedure with another method such as fixed-bed adsorption, the colour properties of wax can be improved further, as with the solvent de-oiling procedure (section 3.3.1).

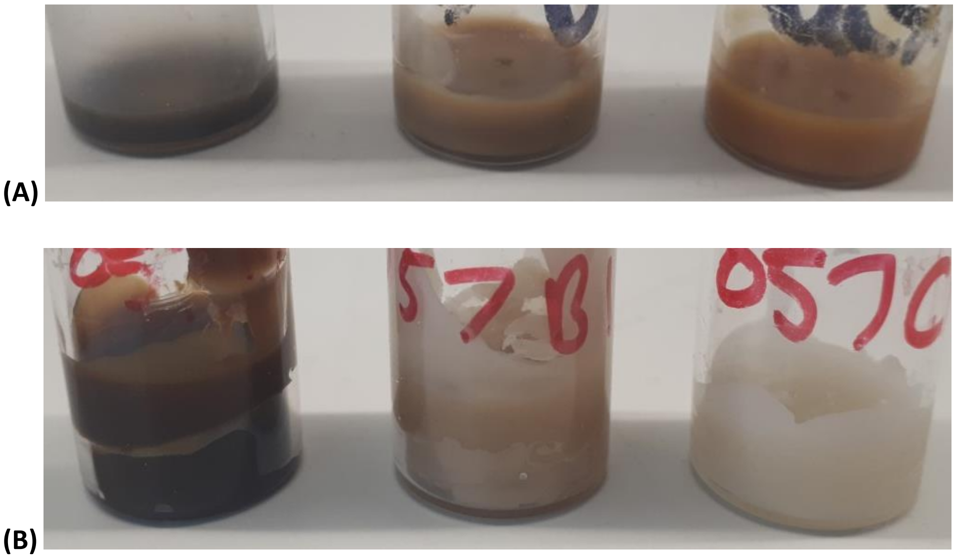

Figure 26. Comparison between crude wax and wax after solvent de-oiling. **(A)** Crude wax A (left), crude wax B (middle), crude wax C (right). **(B)** Recovered wax A (left), recovered wax B (middle) and recovered wax C (right) from solvent de-oiling

Figure 27. Wax A oil extract (left), wax B oil extract (middle) and wax C oil extract (right)

The mass recovery for oil extracts exhibits the same trend: as the average molecular weight of the crude wax decreases (wax A > wax B > wax C) the oil content increases, which can be attributed to the lower melting points of lower molecular weight hydrocarbons. These values are provided in

Table *20*. The waxes recovered from solvent de-oiling (entries 1, 3 and 5) are harder than the crude waxes, however, mass loss due to the removal of oil content is detrimental to the recovery of wax. The mass loss from wax A was determined to be 41.3 wt % after filtering through celite.

Table 20. Mass recovery of de-oiled wax and oil extracts

Entry	Wax	Extract	Mass recovery (%)
1	A	De-oiled wax	39.4
2	A	Oil Extract	10.8
3	B	De-oiled wax	52.4
4	B	Oil Extract	37.7
5	C	De-oiled wax	34.2
6	C	Oil Extract	57.8

3.1.3.1. GPC

GPC data for de-oiled waxes and oil extracts are given below in

Table 21. Oils (entries 5, 7 and 9) possess a higher PDI, indicating the removal of a complex mixture comprised of lower molecular weight impurities. The average molecular weight values obtained for oil extracts (entries 5, 7 and 9) coupled with FTIR data (Figure 28 and Figure 29) indicate that the major components could be long-chain unsaturated and branched hydrocarbons. The de-oiled waxes (entries 4, 6 and 8) possess higher average molecular weights than crude waxes (entries 1-3) and confirm the removal of low molecular weight impurities. PDI values for oils (entries 5, 7 and 9) are higher than for recovered waxes (entries 4, 6 and 8). Overall, these results indicate the removal of lower molecular weight hydrocarbons, affording a hard wax with a narrow molecular weight distribution and a low oil content. It is also clear that oil extracts (entries 5, 7 and 9) must consist of a mixture of long chain and short chain hydrocarbons most likely arising from the presence of branched and unsaturated compounds.

Table 21. Molecular weight distribution of de-oiled waxes and oil extracts determined by GPC.

Wax	**Extract**	**Number average molecular weight M_n (Da)**	**Weight average molecular weight M_w (Da)**	**PDI**
Crude wax A	n/a	1106	2212	2.00
Crude wax B	n/a	494	596	1.21
Crude wax C	n/a	299	456	1.53
A	De-oiled wax	1688	2411	1.42
A	Oil extract	663	953	1.44
B	De-oiled wax	677	722	1.07
B	Oil extract	323	436	1.35
C	De-oiled wax	649	761	1.17
C	Oil extract	213	359	1.69

3.1.3.2. FTIR

Infrared spectra for de-oiled waxes and oil extracts exhibit similar characteristics to the crude wax with respect to the major constituents present. De-oiled waxes possess a more pronounced long-chain rocking band at 720 cm^{-1} than that of the oil extracts (Figure 28). The peak at 720 cm^{-1} is still present for oil extracts, suggesting that some long-chain compounds are still present (Figure 29). The presence of the peak at 1750 cm^{-1} in the oil extract of wax A could suggest the presence of C=O functionality relating to ketones or aldehydes. No broad peaks present indicates that carboxylates are not present, however, these peaks could be obscured by the more intense C-H peaks since they would be much lower intensity if they were present. Unsaturation is confirmed by the presence of the peak at 1650 cm^{-1} along with peaks in the 1000 – 880 cm^{-1} region. As with the wax product, the olefinic character of the oil is confirmed by the presence of peaks in the 1000 – 880 cm^{-1} region. No further elucidation was possible and there were no other major differences in the spectra in comparison to that of crude wax.

Figure 28. Infrared spectra of solvent de-oiled waxes

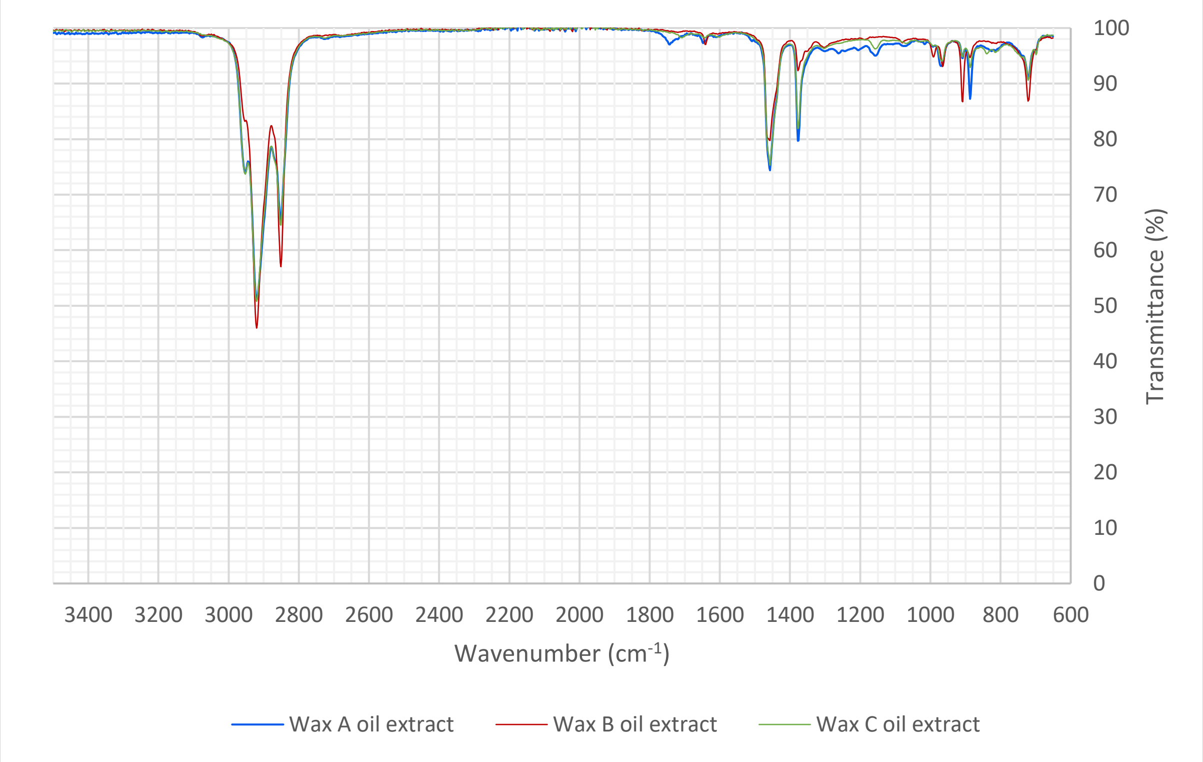

Figure 29. Infrared spectra of solvent extracted oil

3.1.3.3. GC-MS

The GC-MS chromatogram obtained for oil extracts suffers from overlapping of peaks of interest such as PAHs by interference with hydrocarbon peaks. Therefore, the identification of individual compounds was unsuccessful using this method of separation.

3.1.4. Investigation of Urea and Thiourea Clathrate Extraction for Wax Characterisation

The shape selective nature of UCE enables the extraction of compounds containing straight long straight-chain alkyl groups. Branched, unsaturated, polyhalogenated and aromatic compounds do not form clathrates owing to their incompatibility with the hexagonal structure of urea clathrates.[38] During the procedure, it was important to enhance phase-transfer conditions by a high rate of stirring to enable the efficient contact between the urea-methanol phase and the wax-toluene phase to maximise the formation of clathrates. However, mass recoveries of wax were low, owing to the high oil content of both waxes. The oil that was left after the extraction of straight-chain compounds by UCE (clathrate oil) appeared to have similar properties to those obtained by solvent de-oiling; a dark-coloured viscous oil with unfavourable colour and odour properties (Figure 30). Wax B had improved colour properties following UCE extraction, in contrast to wax B recovered after solvent de-oiling (Figure 26), which was less effective at removing colour. Wax A did not form clathrates with urea which was indicated by unrecovered wax in the reaction flask after the procedure had been carried out. The procedure was still carried out for waxes B and C to assess the effectiveness of the separation method with respect to colour and odour removal.

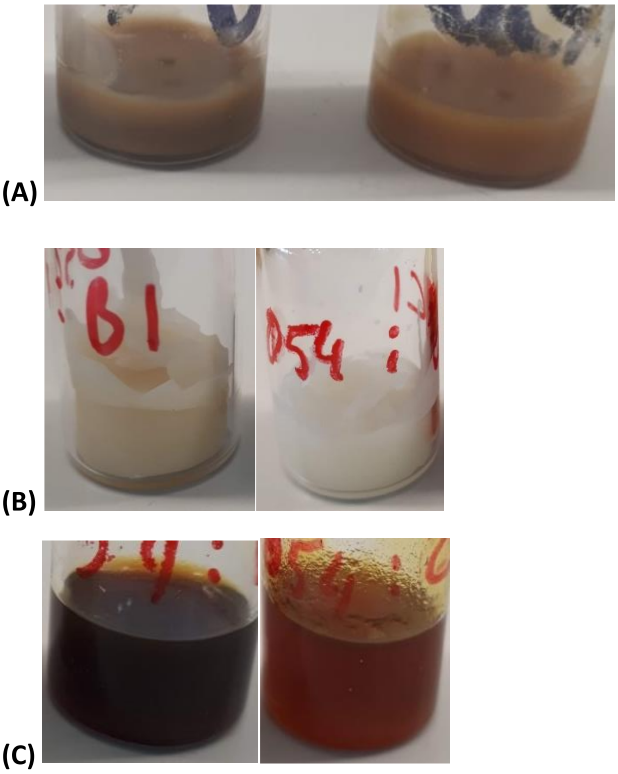

Figure 30. Comparison between crude waxes and oils obtained by UCE. **(A)** Crude wax A (left), crude wax B (middle), crude wax C (right). **(B)** Recovered wax B (left), recovered wax C (right). **(C)** Wax B clathrate oil (left), wax C clathrate oil (right)

Mass recoveries are given in Table 22 for recovered waxes and clathrate oils. The colour properties were most improved in the case of wax C; however, the oil content was higher. Soft wax was also observable in the oil extract from wax C, which may be a result of thermodynamic instability of lower molecular weight urea clathrates at low temperatures.[42,58] Extraction of iso-paraffins by thiourea clathrate formation was ineffective, indicated by the low mass recovery of extracted material. Although thiourea clathrate formation is well understood in the literature, the process has not been evaluated or optimised in the way that urea clathrate formation has.[31,38,40,42,58] The low mass recovery of iso-paraffins may be a result of poor optimisation of parameters such as temperature and solvents, therefore, may require further optimisation to improve the recovery of iso-paraffins. However, it remains unclear as to whether this is the case, or that there is, in fact, a very small quantity of iso-paraffins present. The presence of iso-paraffins would make sense, since plastic feedstocks usually include polypropylene, which breaks down into lower molecular weight iso-paraffins owing to the presence of the branched methyl group. The mass recoveries of clathrate wax are comparable to those from solvent de-oiling and is poor in both cases owing to the high oil content in the starting material. Although methanol plays a role in decreasing the clathrate formation temperature, it thermodynamically destabilises clathrate formation, owing to the high solubility of urea in methanol.[58] Therefore, it can be concluded that the destabilisation of low molecular weight hydrocarbon-clathrates is a result of the destabilising effect of methanol.[42] The scalability of urea extraction is hindered by the handling of large amounts of solvents and high mass losses arising from the high oil content of waxes.

Table 22. Mass recovery of wax extracts and clathrate oils

Entry	Wax	Fraction	Mass recovery (%)
1	B	Clathrate wax	47.3
2	B	Thiourea extract	0.01
3	B	Clathrate oil	43.6
4	C	Clathrate wax	25.2
5	C	Thiourea extract	0.29
6	C	Clathrate oil	57.0

3.1.4.1. GPC

The GPC results are provided in Table 23. Waxes (entries 3 and 5) possess narrow PDI values in comparison to crude waxes (entries 1 and 2) and oils (entries 4 and 6), which is an indication of the removal of impurities. It is thought that impurities (such as compounds that exhibit colour and odour) possess a smaller molecular size relative to long-chain hydrocarbons (waxes) and therefore, when impurities are present in waxes they contribute to decreasing the number average molecular weight (M_n). Since the weight average molecular weight (M_w) is more sensitive to high molecular weight compounds, this results in an increase in PDI values for waxes containing impurities.

Oils (entries 4 and 6) possess lower average molecular weights and higher PDI values than waxes (entries 3 and 5), indicating that lower molecular weight hydrocarbons are removed. Entries 3 and 5 possess very similar average molecular weight values, suggesting that UCE extraction is effective at extracting the same molecular weight fraction of hydrocarbons.

Table 23. Molecular weight distribution of wax extracts and clathrate oils determined by GPC.

Entry	**Sample**	**Fraction**	**Number average molecular weight M_n (Da)**	**Weight average molecular weight M_w (Da)**	**PDI**
1	Crude wax B	n/a	494	596	1.21
2	Crude wax C	n/a	299	456	1.53
3	B	Clathrate wax	624	715	1.15
4	B	Clathrate oil	401	521	1.30
5	C	Clathrate wax	607	677	1.11
6	C	Clathrate oil	308	443	1.44

3.1.4.2. FTIR

The infrared spectra for clathrate waxes and oils possess similar characteristics as those obtained from solvent de-oiling. Clathrate waxes derived from wax B and C were characterised by a more pronounced peak at 720 cm^{-1} compared to the clathrate oils, indicating that the urea clathrate extraction procedure was effective at separating the long-chain hydrocarbons, as per it’s shape selective nature.[42] These results confirm that the two extraction processes; solvent de-oiling and urea clathrate extraction are comparable and afford extracts that are similar in terms of their composition. It was not possible to elucidate any further characteristics by ^{1}H NMR for clathrate-waxes and clathrate oils.

Figure 31. FTIR spectra of wax extracts

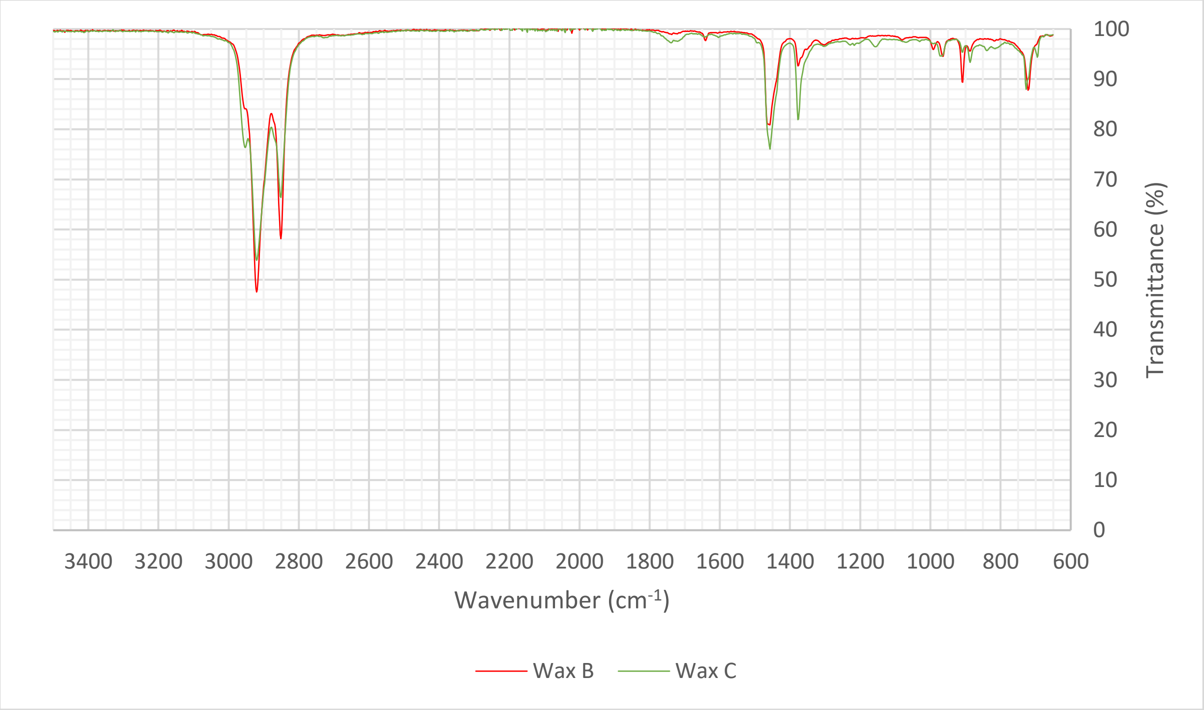

Figure 32. FTIR spectra of clathrate oils

3.1.4.3. GC-MS

The GC-MS results were comparable to that of the solvent de-oiling procedure. Poor separation of peaks resulting from high intensity hydrocarbon peaks that obscure smaller peaks that belong to possible contaminants. The relatively high content of residual hydrocarbons produces a complex chromatogram and the identification of contaminants due to the poor separation of hydrocarbon peaks and peaks of interest.

3.1.5. UV-vis Spectroscopy

The total absorbance spectrum was obtained by UV-vis spectroscopy as a method to assess the colour characteristics of contaminated and refined waxes. A coloured sample should absorb at wavelengths in which a refined wax should not, enabling the differentiation of waxes based on their colour characteristics.

A wax with desirable colour characteristics (obtained from liquid chromatography) was used as a reference standard to compare against a contaminated wax sample (also obtained from liquid chromatography), as shown in Figure 33.

Figure 33. Comparison between contaminated wax (left) and refined wax (right) treated by liquid chromatography/silica adsorption (refer to section 3.1.2.5).

The contaminated wax sample absorbed more strongly than the refined wax at the same wavelengths and also absorbed between wavelengths of 300 – 450 nm. The bands were selected based on the wavelengths of visible light that correspond to colour. The total absorbance spectra for refined and contaminated wax is illustrated below in Figure 34.

Further analysis was carried out to determine the concentration of colour-inducing impurities in refined and contaminated wax. Calibration was carried out by plotting the absorbances at 350 nm against the concentration values of colour-inducing impurities (calibration standards, section 5.4.6). The ‘bulk concentration’ can be defined as the mass of medium polarity fraction (in milligrams) per litre (section 5.4.6) and should be thought of as an index value that indicates how contaminated a sample is with respect to colour. The calibration curve used to determine the bulk concentration of colour-inducing contaminants is shown in Figure 35.

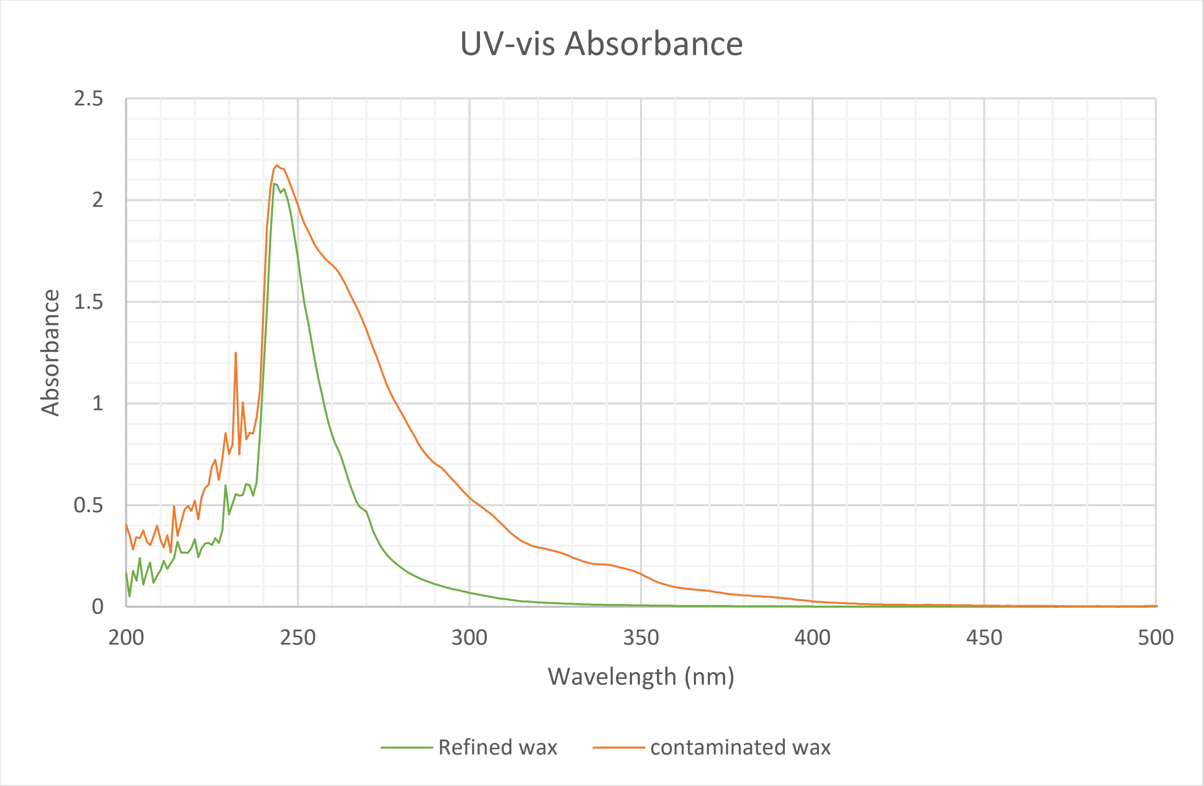

Figure 34. UV-vis absorbance spectrum of refined wax vs contaminated wax

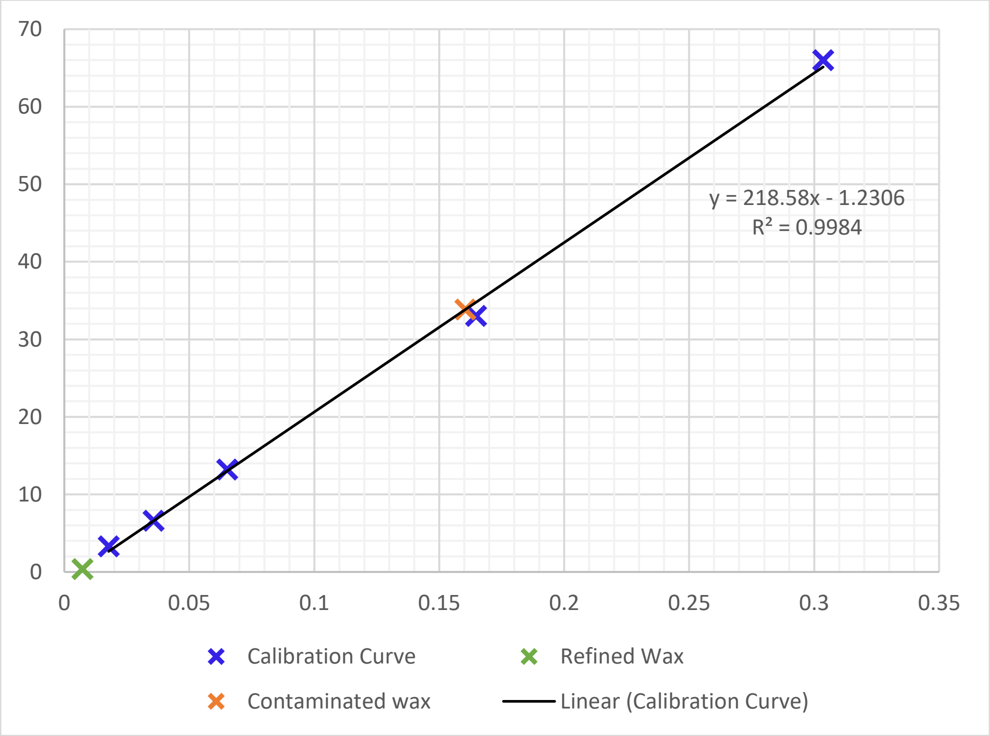

Figure 35. Concentration of colour inducing impurities using standard addition calibration

The UV-vis spectroscopy method for determining colour contamination has demonstrated that the colour of waxes is a property that can be indexed; enabling the differentiation of waxes based on their colour characteristics. The further optimisation of this method could enable UV-vis to be used as a quality control procedure to ensure that the desired colour specifications of refined waxes are met. Ideally this would be implemented as an on-line analytical method to determine the quality of refined wax; however, UV-vis analysis is generally carried out by dissolving the sample to an acceptable concentration prior to analysis. The analysis of wax samples without diluting in a solvent may be unsuitable owing to high detector responses. Further investigation of on-line methods of UV-vis detection using suitable light filters and neutral density attenuation filters is a possible area of further work.[59] Another simpler approach is to subtract the spectrum of a suitable reference standard from that of a refined wax to differentiate between refined wax and contaminated wax by their UV-vis spectral characteristics.

3.2. Decolourisation and Deodorisation Process Development

3.2.1. Catalytic Hydrogenation of Wax Pre-Treated by Silica Adsorption

Hydrogenation is a common industrial process that is used to convert unsaturated oils into saturated fats/waxes in the presence of a catalyst such as palladium or nickel. For wax processing, this can be beneficial for decreasing oil content, since long-chain saturated hydrocarbons are solids (wax) at room temperature.[8] In addition to this, compounds such as fatty ketones and aldehydes are known to exhibit undesirable colour properties in some types of crude. Hydrogenation of these compounds can improve the colour properties by converting them into their corresponding alcohols and paraffins. It is currently not known which types of compound are present in the crude wax that are responsible for their undesirable colour. It is most likely the case that the undesirable colour of pyrolysis-derived wax is caused by multiple chemical species. Nevertheless, this experiment aims to investigate mass recovery and decolourisation effectiveness by carrying out a hydrogenation on wax pre-treated by silica adsorption.

3.2.1.1. Hydrogenation Using Palladium on Carbon

Hydrogenation is a widely used industrial process for the conversion of unsaturated oils into saturated fats, in the presence of a catalyst such as palladium or nickel.[43] For wax processing, this can be beneficial for decreasing oil content, since saturated hydrocarbons above C_{20} are solid (wax) at room temperature. In addition to this, compounds such as fatty ketones and aldehydes may exhibit undesirable colour properties and may be present in some types of crude wax. The hydrogenation of these compounds can improve the colour properties of crude or pre-treated waxes by converting them into their corresponding paraffins.[8]

Initially, a hydrogenation experiment was carried out as a test to determine if the oil content of crude wax can be converted into saturates and therefore, increase the recovery of wax. The orange oil obtained from the solvent de-oiling of wax B (section 3.3.1) was hydrogenated using palladium on carbon at an elevated temperature (70 °C), converting the oil into a colourless, oily soft wax (see Figure 36). The functionalities likely to be present that react to hydrogenation include: olefins and heteroatom-containing hydrocarbons e.g. haloalkanes, ketones, aldehydes, carboxylates, alcohols, sulphides, disulphides, thiols, amines. However, some of these compounds may require harsher conditions i.e. elevated pressure and higher temperatures than what was carried out.

Figure 36. Orange oil sequestered from solvent de-oiling in section 3.3.1 (left). Soft wax (right) produced from hydrogenating the oil fraction of wax B.

The mass recovery of soft wax after hydrogenation of oil obtained by solvent de-oiling is provided in Table 24. Mass recovery of soft wax. Strong retention of wax onto the carbon support may result in higher transfer losses.

Table 24. Mass recovery of soft wax

Entry	**Sample**	**Mass recovery of soft wax (%)**

1	Wax B oil extract (see Figure *46*)	81.0

Another hydrogenation experiment was carried out on crude wax C without being pre-treated by silica adsorption. The hydrogenation of crude wax C improved the colour, however, eluting through silica after the hydrogenation did not improve the colour significantly. These samples are shown below in Figure 37. It is also worth noting that there was no noticeable odour after the procedure had been carried out.

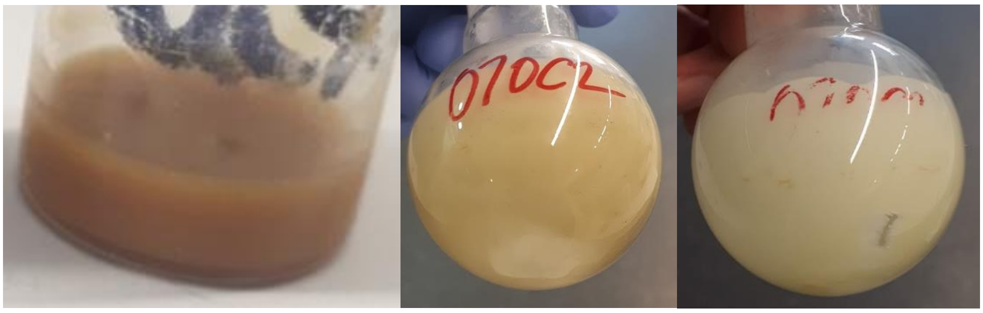

Figure 37. Crude wax C (left), wax C after hydrogenation without adsorptive pre-treatment (middle) and wax C after hydrogenation followed by silica adsorption (right).

Wax A, B and C were filtered through silica to remove polar contaminants prior to adding the wax (as an organic solution in toluene) to the palladium on carbon catalyst. The hydrogenation of waxes was carried out overnight. Carrying out the adsorption as a pre-treatment step followed by hydrogenation afforded colourless waxes (Figure 38). It is plausible that the polar components removed by silica adsorption are responsible for poisoning the catalyst and decreasing the effectiveness of colour removal. Therefore, silica adsorption is necessary as a pre-treatment step to remove impurities that may poison the catalyst.

It is worth noting that the yellow colour of the wax solution rapidly disappeared when hydrogenated. The rapid decolourisation of wax by hydrogenation may suggest that the persisting yellow colour of waxes after silica adsorption is due to the presence of conjugated alkenes. However, there are many possibilities for what components are responsible for inducing an unfavourable colour owing to the complexity of product streams afforded by plastic pyrolysis. The pyrolysis products afforded by plastic pyrolysis are rather unpredictable, owing to the uncertainty in what plastic additives and plastic types may be present in the pyrolysis feedstock.

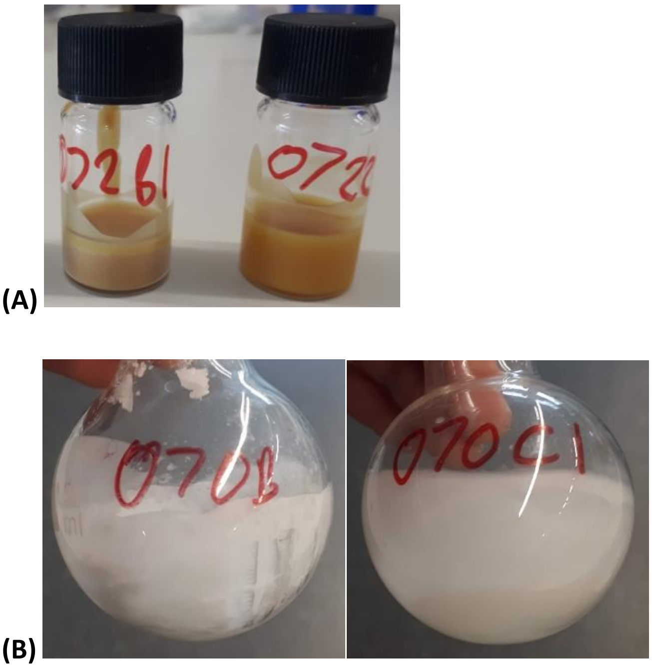

Figure 38. (A) Wax B (left) and wax C (right) pre-treated by silica adsorption. (B) Wax B (left) and wax C (right) after hydrogenation with Pd/C.

Mass recoveries of hydrogenated waxes are given in Table 25 below. Transfer losses are the most likely source of mass loss.

Table 25. Mass recovery of hydrogenated wax using a palladium on carbon catalyst

Entry	Wax	Adsorptive pre-treatment (yes/no)	Mass recovery (%)
1	B	Yes	80.4
2	C	Yes	77.2
3	C	No	89.5

Overall, hydrogenation increased the mass recovery of wax by converting oil content into soft wax as evidenced in section 3.2.1.1, by hydrogenating an oil extract obtained by solvent de-oiling (Figure 46). Furthermore, colour properties were improved significantly and there was no noticeable odour after the procedure had been carried out.

3.2.1.2. Hydrogenation Using Raney Nickel

Raney nickel is a highly active nickel-aluminium alloy with many industrial and synthetic applications such as the reduction of benzene to cyclohexane and the hydrogenation of vegetable oils.[43,60] Wax A, B and C were filtered through silica to remove polar contaminants prior to adding the wax (as an organic solution in toluene) to the Raney nickel catalyst. The hydrogenation of waxes was carried out overnight.

(A)

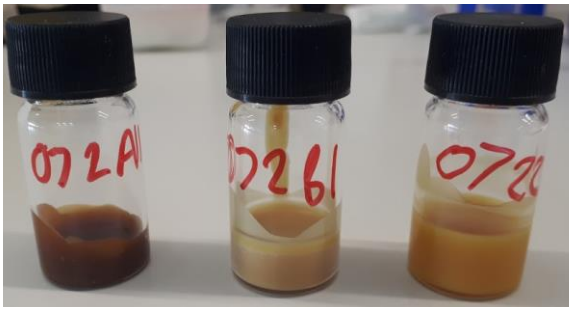

(B)

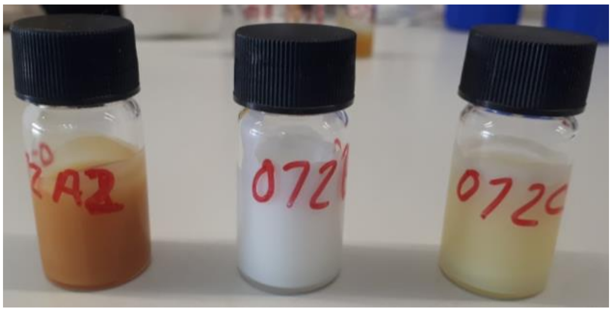

Figure 39. (A) Wax A, B and C pre-treated by silica adsorption (left to right). (B) Wax A, B and C after hydrogenation (left to right)

The hydrogenation process was most effective at decolourising wax B, less effective at decolourising wax C and least effective at decolourising wax A. Although the process was less effective for waxes A and C, the colour properties were still significantly improved over that of the crude waxes as illustrated in Figure 39. Mass recoveries for the hydrogenation of waxes using Raney nickel are provided below in Table 26. One of the sources of mass loss is that when the supernatant (organic wax solution, in toluene) was decanted after the hydrogenation, residual wax left in the flask that was not recovered. Another possible source of mass loss is the loss of volatile matter as a result of the removal of heteroatoms. For example, the hydrogenation of thiol results in the formation of hydrogen sulphide which is expelled as gas.

Table 26. Mass recovery of hydrogenated wax using a Raney nickel catalyst

Entry	**Wax**	**Mass recovery (%)**
1	A	64.5
2	B	83.7
3	C	85.7

The NMR spectra for wax A, B and C are provided below in Figure 40 and confirms the conversion of unsaturated compounds into saturated compounds. The main peaks that confirm the presence of olefins (4.5 – 6.0 ppm) are not present on the spectra for hydrogenated waxes, indicating that the hydrogenation of olefins was a success. Furthermore, peaks that correspond to allylic protons can also be seen to disappear (1.62 – 3.00 ppm), however, this is made less clear by the overlapping of signals corresponding to methine protons in the same region. There are still some low intensity peaks present in this region for waxes A and C, however, possible structures that correspond to these components have not yet been identified. It could be speculated that these peaks correspond to unsaturated compounds that are harder to saturate under the temperature and pressure used in this experiment.

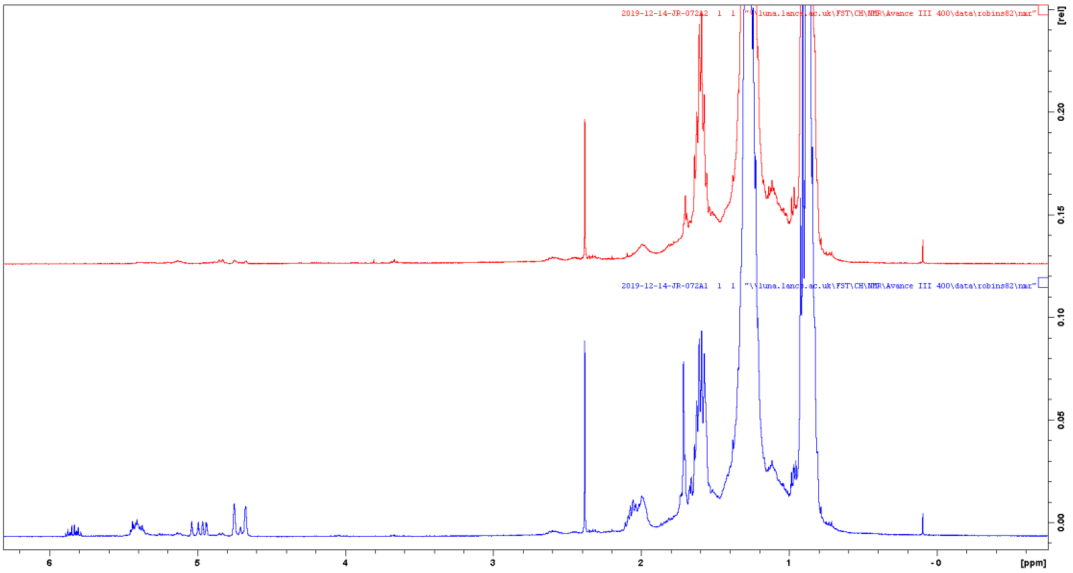
2019-12-14-JR-072A2 1 1 "\\luna.lancs.ac.uk\FST\CH\NMR\Avance III 400\data\robins82\nmr"
2019-12-14-JR-072A1 1 1 "\\luna.lancs.ac.uk\FST\CH\NMR\Avance III 400\data\robins82\nmr"
[rel]
0.20
0.15
0.10
0.05
0.00
6
5
4
3
2
1
0
[ppm]

(A)

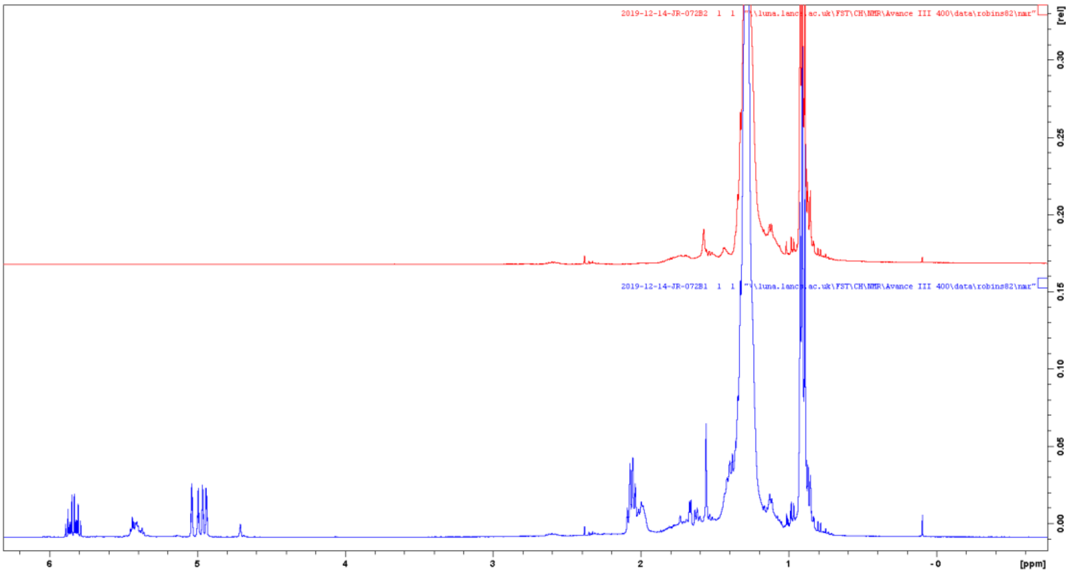
2019-12-14-JR-072B2 1 1 "\\luna.lancs.ac.uk\FST\CH\NMR\Avance III 400\data\robins82\nmr"
2019-12-14-JR-072B1 1 1 "\\luna.lancs.ac.uk\FST\CH\NMR\Avance III 400\data\robins82\nmr"
[rel]
0.30
0.25
0.20
0.15
0.10
0.05
0.00
6
5
4
3
2
1
0
[ppm]

(B)

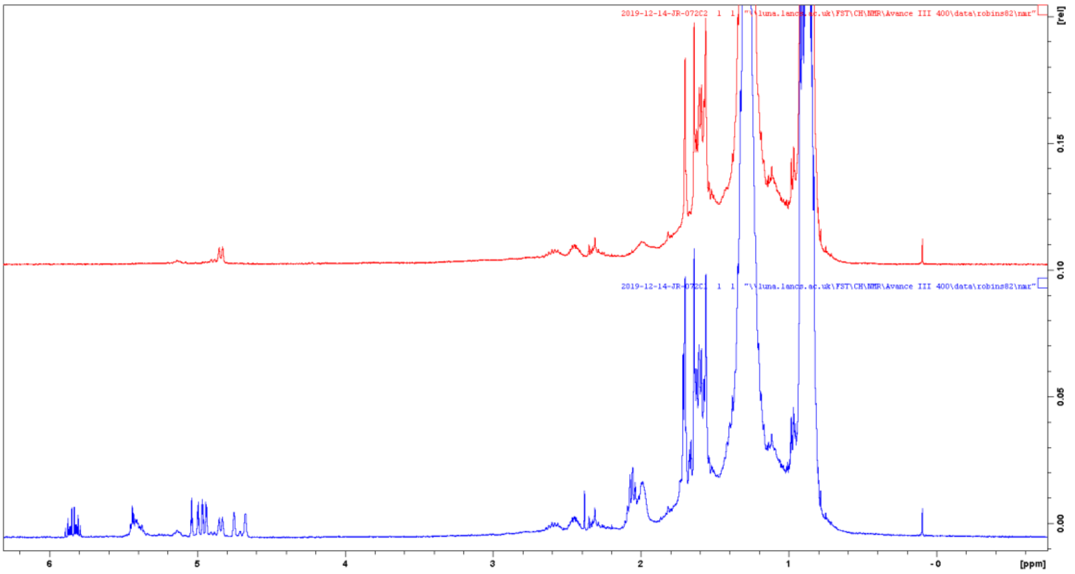
2019-12-14-JR-072C2 1 1 "\\luna.lancs.ac.uk\FST\CH\NMR\Avance III 400\data\robins82\nmr"
2019-12-14-JR-072C1 1 1 "\\luna.lancs.ac.uk\FST\CH\NMR\Avance III 400\data\robins82\nmr"
[rel]
0.15
0.10
0.05
0.00
6
5
4
3
2
1
0
[ppm]

(C)

Figure 40. NMR comparison between waxes before and after hydrogenation. **(A)** Wax A. **(B)** Wax B. **(C)** Wax C. (legend: blue – adsorption pre-treated wax, red – hydrogenated wax)

An overview of the proposed hydrogenation process for the decolourisation and deodorisation of pyrolysis-derived wax is illustrated in Figure 41. Wax may be fed as a melt to avoid the use of large volumes of solvent. Moreover, Fixed bed adsorbent regeneration and catalyst regeneration processes are important to improve the industrial viability of the operation. Fixed bed adsorption is a wax refining process which removes colour-inducing impurities by the percolation of wax through a bed of alumina/silica/clay. The fixed bed can be one of multiple beds operating in a swing system to regenerate the spent beds while continuing the process with a fresh one.[35] Fixed bed processes are susceptible to pressure drop during operation resulting in high recycling rates, which can have a large impact on the operational costs of the process. An alternative type of reactor is the slurry bed reactor, based on the design of a conventional fluidised bed it is much cheaper and easier to operate than fixed bed processes.[61] Slurry beds enable more efficient heat transfer to take place due to the continuous mixing of the two phases (catalyst/adsorbent and feedstock). In contrast, fixed beds are associated with poor heat transfer characteristics. However, a major drawback to slurry beds is that the separation of wax and adsorbent/catalyst can be difficult and that the adsorbent/catalyst is more susceptible to attrition due to the continuous circulation in the reactor.[62]

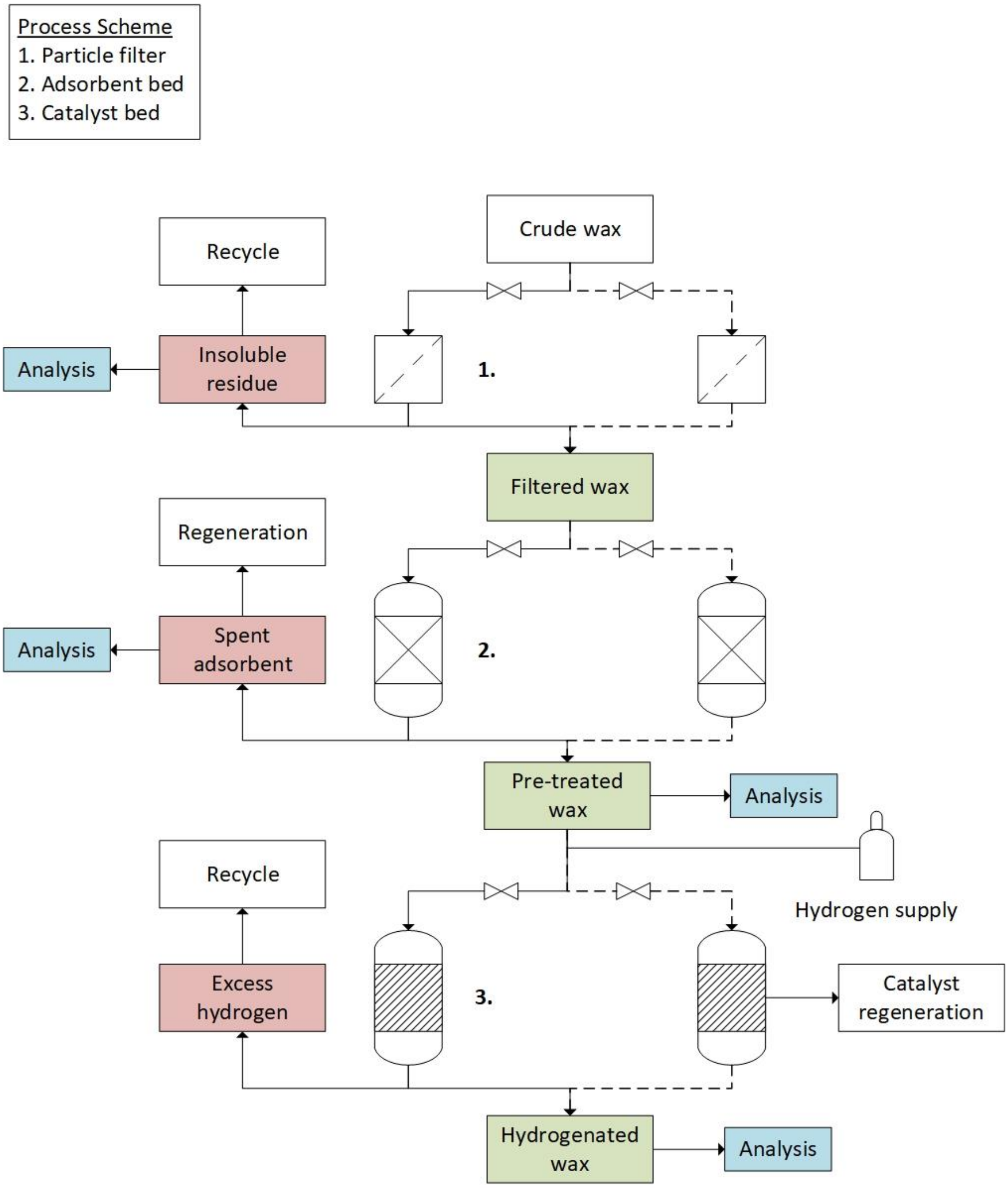

Figure 41. Proposed process scheme for the decolourisation of crude waxes by hydrogenation and adsorptive pre-treatment

Adsorption onto silica is effective at removing polar compounds that are responsible for undesirable colour and odour and can be incorporated as a fixed bed process with a swing-system type regeneration process.[35] Hydrogenation was effective for the decolourisation of wax after pre-treatment by adsorption onto silica. Furthermore, the optimisation of the temperature, catalyst type, catalyst regeneration process, reaction time and amount of catalyst required are areas of further work.

3.2.2. Oxidation

For the oxidation, cyclohexane and toluene were used as solvents due to their higher boiling points to enable higher oxidation temperatures to be used, without evaporating the solvent. Stirring speed was maintained high (1000 rpm) for the efficient mixing between the solid Oxone® phase and the wax solution (in toluene/cyclohexane) phase. The appearances of waxes B and C after oxidative treatment are shown in Figure 42 and Figure 43, respectively. The initial procedure was not carried out for wax A, since the oxidation was a test to determine the effeciveness of oxidation for decolourising waxes. A later experiment was carried out in which wax A was used, however, the proces was inneffective and is described later in this chapter.

Figure 42. Oxidation of crude wax B using Oxone®. Crude wax B (left), wax B after oxidation using toluene as a solvent (middle) and wax B after oxidation using cyclohexane as a solvent (right)

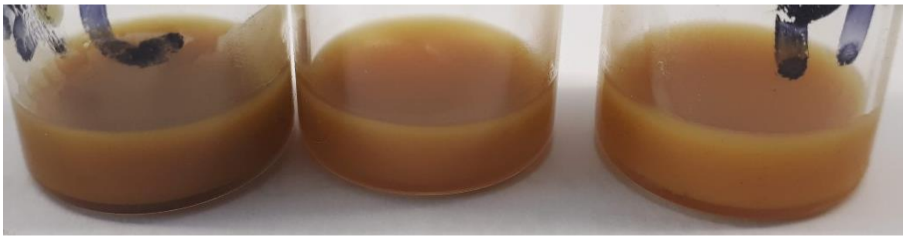

Figure 43. Oxidation of crude wax C using Oxone®. Crude wax C (left), wax C after oxidation using toluene as a solvent (middle) and wax C after oxidation using cyclohexane as a solvent (right)

The procedure improved the colour characteristics more using cyclohexane as solvent for the oxidation. After oxidation, wax B and C possessed no noticeable odour, suggesting that these components are removed by the procedure. The colour of waxes B and C were not significantly improved. Therefore, it is likely that impurities are removed by filtration owing to their differences in solubility in the organic solvents.

The procedure was carried out up to 9 times to determine repeatability regarding the mass recovery. The mass recoveries were relatively inconsistent for each wax: 72-89% for wax B and 78-98% for wax C. Mass recoveries are shown below in Table 27 and Table 28. If the wax solution is left to cool, the solubility of wax in the solvent will decrease, resulting in a mass loss by filtration. For this reason, wax solutions must be filtered while still hot.

Table 27. Mass recoveries from 1st oxidation experiment using cyclohexane

Wax	**Repetition**	**% Mass recovery**	**Wax**	**Repetition**	**% Mass recovery**
B	1	58.3	C	1	89.0
B	2	43.9	C	2	86.5
B	3	72.9	C	3	82.0
B	4	78.4	C	4	79.2
B	5	73.8	C	5	83.3
B	6	78.4	C	6	97.9
B	7	81.8	C	7	78.4
B	8	89.2	C	8	84.0

Table 28. Mass recoveries from 2nd oxidation experiment using toluene

Wax	**Repetition**	**% Mass recovery**	**Wax**	**Repetition**	**% Mass recovery**
B	1	74.4	C	1	86.8
B	2	70.1	C	2	83.4
B	3	79.6	C	3	64.3
B	4	75.5	C	4	91.2

B	5	78.2	C	5	84.2
B	6	78.3	C	6	95.3
B	7	76.3	C	7	37.6
B8	8	85.9	C	8	84.6
B9	-	-	C	9	81.4

Oxidation of wax A, B and C was carried out using 10 % v/v hydrogen peroxide at an elevated temperature (80 °C) to ensure the wax was fully melted and behaved as a liquid. High stirring (1000 rpm) ensured that efficient mixing between phases was maintained. The wax was extracted by adding hexane to the reaction flask and transferring the biphasic mixture into a separation funnel. The colour properties of wax B and C were improved, however, not significantly (Figure 44 and Figure 45). Excessive foaming meant that the procedure was discontinued for wax A, which could indicate that the peroxide is decomposed resulting from an incompatibility with some impurities known to be present like metals or metal oxides such as iron (identified by ICP). As previously mentioned in this chapter, the decolourisation of waxes is most likely to be a result of poor solubility of impurities in the solvent, which are then removed by filtration or during liquid-liquid extraction.

Figure 44. Wax B after oxidation using hydrogen peroxide

Figure 45. Wax C after oxidation using hydrogen peroxide

Mass recoveries of wax following the oxidation of wax melt using 10 v/v % hydrogen peroxide are provided below in Table 29.

Table 29. Mass recovery of wax after oxidation using hydrogen peroxide

Sample	% Mass recovery
Wax A	-
Wax B	91.2
Wax C	88.8

Colour properties were not significantly improved in comparison to other methods of treatment carried out in this research. Furthermore, a simple test was carried out to determine if any possible oxidised impurities could be removed more effectively by filtration through a silica plug. No further improvements to colour were observed, suggesting that oxidation of impurities was ineffective. It is likely that there are small quantities present that are oxidised, however, this is not observable. Oxidised impurities should have an increased retention to silica, enabling their separation; since no further improvements to colour were observed it could confirm that the impurities present are not easily oxidised using the conditions of this procedure.

3.3. Combined Methods

3.3.1. Solvent De-Oiling of Wax Pre-Treated by Silica Adsorption

Colour-inducing impurities are difficult to remove by solvent de-oiling alone, therefore, by combining two processes: adsorption and solvent de-oiling, hard to remove polar compounds are removed by adsorption while solvent de-oiling removes residual impurities.[63]

Wax B was heated in ethyl acetate until dissolved and then cooled to -32 °C and a light yellow precipitate formed. The precipitate was filtered and washed three times with acetone to remove residual impurities. Solvent was removed from the precipitate under reduced pressure and afforded a wax with good colour and odour properties. The filtrate was evaporated under reduced pressure and afforded an orange oil which had no noticeable odour. The silica was desorbed to remove the brown residue by heating to 60 °C in 15 % chloroform/methanol.

Figure 46. Decolourised wax from solvent de-oiling (left), orange oil (middle) and residue sequestered from the desorption of silica (right)

The colour-inducing impurities present in the oil extract presumably consist of slightly polar compounds, owing to their poor retention to silica and high affinity for ethyl acetate. Such compounds could include: ketones, aldehydes, esters and amides derived from plastic feedstock materials, which is supported by GC-MS data in section 3.1.2.4. Although present in small quantities, some of these molecular species are known to induce unfavourable colours and can converted into their corresponding *n*-paraffins by hydrogenation or removed by solvent de-oiling, or a combination of both.[8,51] Mass recoveries of wax, oil and brown residue are provided below in Table 30.

Table 30. Mass recovery of adsorption and solvent refined wax

Wax	**Extract**	**Mass recovery (%)**
B	De-oiled wax	33.3
B	Oil extract	26.1
B	Brown residue	26.4

The wax content present in the residue is most likely a result of inefficient mass transfer of wax from the batch adsorption flask. In an operating process plant, this could be avoided by maintaining a constant heat source on the wax feed, allowing the wax to behave as a liquid and flow through the bed of adsorbent more efficiently. For this reason, the mass recovery of wax was low. Higher solvent-feed ratios and increasing the number of washing/solvent de-oiling cycles must be minimised to prevent mass loss. Mass loss can further be minimised by ensuring that the wash solvent is maintained at low temperatures (e.g. -32°C).

A process scheme for the solvent de-oiling procedure is illustrated below in Figure 47. The first step of the process removes polar contaminants which are otherwise difficult to remove. The wax may be fed into the process as a melt to reduce the use of solvents. Fixed bed adsorbent regeneration processes can proceed via chemical or thermal treatment and operate in a swing system, enabling continuous processing.[63] The wax melt may then be fed into a crystalliser in which the oil content is removed using a selective solvent such as 2-butanone. The solvent may be recycled by distillation and fed back into the crystalliser. One or more solvent de-oiling cycles may be required to achieve the desired colour specification of wax. The refined wax may then be separated by filtration and the oil content removed.

The main disadvantage to this procedure is the high oil content of wax, resulting in the low mass recovery of wax. Another disadvantage to the process is the solvent de-oiling step; which may pose a challenge since solvent de-oiling is generally carried out in batch processes and may require the use of more expensive equipment to enable continuous processing. Solvent percolation is usually carried out at room temperature, therefore, may result in the loss of lower molecular weight paraffins that are more soluble at room temperature.[57]

Although continuous processes such as solvent percolation could be implemented, refrigerating conditions are usually required to maximise wax recovery.

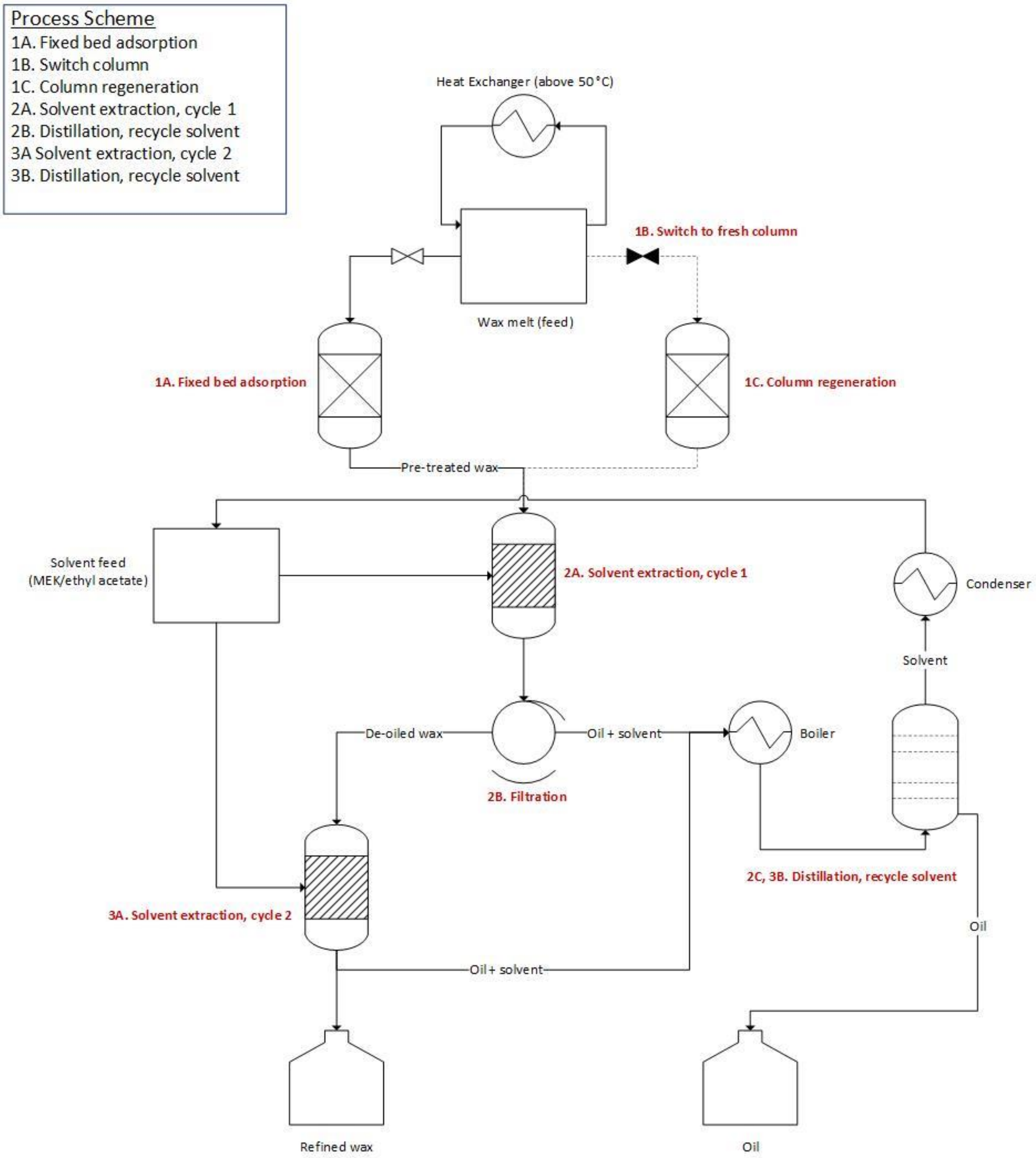

Figure 47. Proposed process scheme for the decolourisation of wax by solvent de-oiling and adsorptive pre-treatment

4. Conclusions and Further Work

The methods of characterisation carried out in this work provided some constructive information on the major components present in pyrolysis-derived wax and the composition of impurities. The attempt to analyse odour inducing compounds directly by headspace GC-MS proved to be ineffective owing to the low sensitivity of the method, resulting in no identification of known odour-inducing compounds. Analysis by UV-vis enabled the determination of bulk colour characteristics by measuring the total absorbance of a contaminated wax against the spectrum of a refined colourless wax. This may be useful for future applications where a stringent colour requirement is needed. In the first instance, FTIR analysis was useful for rapidly determining the major constituents of waxes. Low sensitivity and limited structural information hinder the further characterisation of materials by FTIR alone. Some further structural elucidation was made possible by NMR analysis such as: the identification of tertiary carbons, allyl groups, aromatics and olefins. However, peak overlapping, especially in the 1.5 – 2.0 ppm region, preventing the accurate integration of peaks. GPC proved to be a powerful comparative tool for comparing the effectiveness of separation methods by their differences in molecular weight distribution. Lower PDI values for waxes after removing impurities by liquid chromatography, solvent de-oiling and UCE indicated the successful removal of lower molecular weight, more polydisperse fractions of impurities. ICP enabled the determination of trace heavy metals in the waxes, however, a white precipitate formed for crude wax A and C. Titanium dioxide is known to be unstable in nitric acid and is a white solid that is used as a pigment for opacity or white pigmentation in plastic materials.[33] Therefore, it is plausible that the white precipitate formed in waxes A and C is composed of titanium dioxide. GC-MS made it possible to identify impurities derived from plastic additives and mixed plastic waste as well as PAH compounds, however, the intensity of peaks that were identified as PAHs were very low. Baseline separation was poor for oil samples obtained from solvent de-oiling and UCE owing to the presence of intense hydrocarbon peaks.

Liquid chromatography made it possible to identify more analytes that would otherwise have been obscured by hydrocarbons. Liquid chromatography was also the most effective method of separation with respect to mass recovery, decolourisation and deodorisation. The disadvantages of liquid chromatography are large amounts of solvents required, poor retention of yellow colour-inducing impurities to silica and blockage of the column owing to the poor solubility of wax in the primary eluent (hexane) and perceived back pressure build-up. Solvent de-oiling was not very effective at removing colour and odour inducing impurities for wax A and B, however, significantly improved the colour and odour properties of wax C. UCE was effective at decolourising and deodorising waxes B and C, however, inclusion compounds could not be formed for wax A.

Silica adsorption removes polar compounds that are difficult to remove and is best used in combination with another refining method such as solvent de-oiling or hydrogenation. The yellow colour-inducing impurities are then readily removed by solvent de-oiling or hydrogenation. The major disadvantage to hydrogenation is the cost of catalysts and the hydrogen source. To improve the cost efficiency of the process, cheaper alternatives should be investigated such as nickel on alumina. The regeneration of nickel catalysts is also an area worth further investigating to improve the cost efficiency. The major advantage of hydrogenation is the lack of a requirement for a solvent, since the wax can easily be introduced into fixed-bed continuous processes as a melt. Solvent de-oiling does not require the use of catalysts or hydrogen, however, the high oil content of pyrolysis-derived wax accounts for a high loss of mass, since contaminants are not as easily separated from the oil. The high oil content could possibly be explained by the thermal degradation mechanism taking place; β-scission reactions that result in the formation of lower molecular weight alkanes and an alkenes must account for a large proportion of the crude wax.[17] Since β-scission reactions occur on the mid-chain section of polymers, lower molecular weight products are afforded. Not only does the mechanism taking place explain why the olefin content may be high, but also how low molecular weight products are formed and therefore, why the oil content of crude wax may be high.

The two developed refining processes: hydrogenation and solvent refining are both contrastable in their disadvantages and advantages. To determine the most effective treatment method, it is necessary to consider the cost effectiveness and the practicability of the processes used and what type of equipment, reagents and solvents are required. This research project has covered a wide range of analytical and treatment techniques and provides significant information for the further development of refining processes and analytical techniques. Some further ideas for further work are provided below and expand upon the already carried out methods in this project.

4.1. Further work and Recommendations

The scaling up and optimisation of a suitable wax refining process based on methods that have demonstrated effectiveness in removing colour and odour inducing impurities is of most importance and should be the primary goal for any further work being carried out. The developed process should include adsorption, solvent de-oiling and hydrogenation, or a combination of these processes. Furthermore, the development of green adsorbent materials derived from waste such as: the preparation of microcrystalline cellulose and the preparation/functionalisation of sand and glass could attract commercial interest owing to their desirable environmental credentials and low cost.[64–66] The developed adsorbent material would be used in adsorption processes for the refining of pyrolysis-derived wax.

4.1.1. Analysis

For further NMR characterisation, carbon-13 DEPT 45, 90 and 135 NMR in combination with quantitative carbon-13 experiments should be investigated as a method to speciate waxes based on their carbon environments. The aim of the DEPT experiment is to identify peaks corresponding to primary, secondary and tertiary carbon environments. The data from quantitative carbon-13 experiments may then be used to integrate the corresponding peaks and determine the carbon-13 percentages for each carbon environment. Variable temperature experiments may be required to improve the solubility of wax in the NMR solvent, which would enable higher concentrations of sample to be used to increase the sensitivity.

Further characterisation of aromatic compounds may also be made possible by carrying out a hydrogenation followed by urea clathrate extraction to enable a more effective extraction of straight chain compounds. This proposed procedure is based on the method developed by Novak *et al.* in which triglycerides are converted into fatty acid methyl esters by transesterification, followed by the removal of fatty acid methyl esters by urea clathrate extraction to enable detection of PAH by GC-MS.[31]

4.1.2. Adsorption Studies

The only adsorbent tested so far throughout the MSc project was silica. A more thorough adsorbent screening would be highly desirable. Clay/bleaching earth, bauxite and alumina are good examples of commonly used adsorbents in industry. Some examples of greener materials include microcrystalline cellulose, sand, waste glass and clay.[63–67] The adsorbent should have a high surface area and adsorption capacity therefore, analytical tools such as light scattering and BET may be useful for determining pore size distribution and particle size distribution.

The adsorption capacity is an important parameter, since it determines how much wax can be decolourised before the adsorbent bed is spent. The adsorption capacity can be determined by the point at which the adsorbent is spent. A simple way this could be indicated is by noting when the colour of the wax product starts to deteriorate and assessing how much wax can be processed per unit(mass) of adsorbent.

A suitable activation/regeneration procedure should be chosen and typically consists of heating at a high temperature (100 – 200 °C) for 6 hours and/or treating the adsorbent with an acid such as HCl.[63] Activation of adsorbents ensures that the material is free of impurities that may be present on the adsorbent surface, so that it can perform optimally. Adsorbents can typically be regenerated using the same methods used to prepare or activate them.

The functionalisation of surface groups would be interesting for improving the performance of an adsorbent, such as the preparation of cellulose oxalate by hydrolysis followed by esterification.[66] Furthermore, dendrimers can be grafted onto suitable sites to increase surface area and/or modify the functionality of the adsorbent.[68,69] Examples of solid supports incorporating dendrimers include sand and cellulose.[64,67] Dendrimers are highly branched polymers that can greatly increase the surface area and therefore, adsorption capacity. Dendrimers can be very costly so it’s important to take this into account and investigate using green materials and reagents for these processes to reduce cost, if this is to be considered in future studies.

Functionality, pore size distribution, surface area and elemental composition are important characteristics of adsorbents, therefore, it is worth considering suitable analytical procedures such as FTIR, BET, SEM and XRF. XPS may be useful for determining the surface elemental compositions of clay and glass, for example, since their composition may affect adsorption performance. For an example, see the analytical procedure used by Guo *et al*.[70]

5. Experimental Methods and Analytical Techniques

5.1. General Experimental Methods

Initial analysis was performed on crude waxes to determine their chemical properties: chemical functionality by FTIR and NMR, molecular weight distribution by GPC, heavy metals content by ICP and identification of volatiles by GC-MS. Waxes were separated by liquid chromatography, solvent de-oiling and urea clathrate extraction to separate impurities from waxes. Extracts and fractions containing impurities that were obtained by the separation methods were analysed by FTIR, NMR, GPC and GC-MS to determine chemical properties and identify contaminant components. Refined waxes were analysed by FTIR, NMR, GPC and ICP to compare their properties with those of crude waxes. Decolourisation and deodorisation processes were developed based on methods of separation and chemical treatment methods that are known to be effective: adsorption onto silica, solvent de-oiling, hydrogenation and oxidation. For the proposed processes, adsorption onto silica was combined with solvent de-oiling (see Figure *41*) and with hydrogenation (see Figure *47*) to investigate the most effective process at achieving the desired colour specification and maximising mass recovery.

5.2. Materials

Kerax Ltd provided wax A, B and C for the experimental procedures carried out in this research. GPC and GC-MS samples were prepared with HPLC grade chloroform that was purchased from Fisher Scientific UK Ltd. ICP multi element IV standard was purchased from Sigma Aldrich Ltd. 1,1,2,2-Tetrachloroethane-d2 for NMR analysis was purchased from Sigma Aldrich Ltd. Silica with pore sizes of 40 – 63 µm was purchased from VWR chemicals. Ultrapure grade nitric acid (70 % w/v) was purchased from sigma Aldrich. Urea and thiourea used for the extraction procedure were purchased from Fisher Scientific UK Ltd. Oxone® purchased from Fisher Scientific UK Ltd was used for oxidation reactions. Palladium on activated carbon support (with 20 wt. % loading) purchased from Sigma Aldrich Ltd was used for hydrogenation.

5.3. Methods of Separation

The separation of waxes into fractions using a range of techniques was carried out with the aim to obtain desirable colour and high mass recovery of wax. All samples and sample fractions obtained from separations were analysed by FTIR, NMR, GPC, ICP-AES and GC-MS.

5.3.1. Solubility Test

The solubility of the waxes in a range of solvents was tested by melting wax (1 g), adding some solvent (10 mL) and heating until the wax was fully dissolved. The solvents were: toluene, chloroform, hexane, DCM, ethyl acetate, tetrahydrofuran, acetone and methanol. The solutions were cooled to room temperature and the masses of white precipitates that formed were recorded. The precipitate formed from cooling wax B and C in ethyl acetate was heated under vacuum to evaporate the solvent and weighed.

5.3.2. Filtration of Wax A

Wax A had to be filtered before any separations were carried out, due to the presence of insoluble material independent of the temperature concentration or solvent used. Wax A (25 g) was dissolved in chloroform (300 mL) and then made into a slurry with celite. The slurry was then charged onto a sinter funnel packed with celite under vacuum. The insoluble residue was retained by the celite, the celite was rinsed with additional chloroform (300 mL) and the filtrate was evaporated under reduced pressure affording a soluble wax A which was stored for future experiments.

5.3.3. Acid-Base Extraction

Waxes were extracted with hydrochloric acid and sodium hydroxide to determine respectively basic and acidic contents. Toluene (100 mL) was added to wax (1 g) and filtered to remove any insoluble residue. The wax solution was extracted with 2 x 20 mL of 10 % hydrochloric acid solution in a separation funnel and an emulsion formed. The emulsion was gently swirled and left to settle and repeated if necessary. The aqueous layers were separated and collected in a conical flask. The wax solution (organic layer) was then extracted with 2 x 20 mL of 10 % sodium hydroxide solution in a separation funnel and an emulsion formed. As before, the emulsion was gently swirled and left to settle and repeated if necessary. The aqueous layers were separated and collected in a conical flask. The aqueous acid and base solutions were neutralised by adding a concentrated solution of the corresponding acid or base dropwise. The pH was determined using indicator paper. The neutralised hydrochloric acid solution was extracted with 2 x 20 mL of toluene to extract basic compounds. The neutralised sodium hydroxide solution was washed with 2 x 20 mL of toluene to extract acidic compounds. Both organic layers were dried with magnesium sulphate, vacuum filtered, and evaporated under reduced pressure. The residues obtained were weighed to determine the mass of acidic and basic components.

5.3.4. Silica Column Chromatography[12]

Silica column chromatography enabled the separation of wax samples into fractions based on their polarity by eluting through silica dry-packed into a sinter funnel with vacuum assistance. The experimental configuration for this experiment is shown below in Figure 48. For all experiments, a grade 2 sinter funnel was used with a 2.5 cm diameter packed with silica to a depth of 4 – 7 cm.

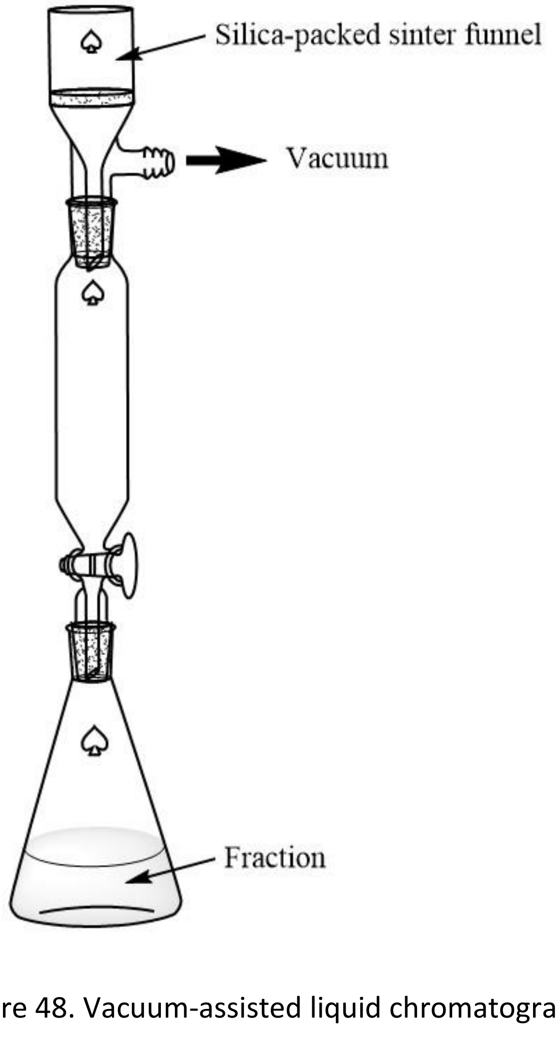

Figure 48. Vacuum-assisted liquid chromatography

Samples were prepared by dissolving wax (5 g) in hexane (250 mL). The sample solution was charged onto the column and eluted with hexane (100 mL) to elute the non-polar fraction. Medium polarity compounds were eluted with toluene (350 mL). High polarity compounds were eluted with 15% methanol/chloroform (200 mL). The three fractions were evaporated under reduced pressure affording three distinct fractions: non-polar, medium polarity and high polarity compounds.

5.3.5. Silica Column Regeneration and Elution Volume

The maximum volume of hexane to elute wax before the deterioration of colour was investigated. Masses of decolourised wax were recorded to demonstrate the mass of wax that can be processed per column. The column was re-used by flushing with a polar solvent and re-conditioned for the next run by flushing with decreasingly polar solvents. The experiment was tested using different solvent systems, as outlined below, to determine if the column can be regenerated and re-used.

For the first experiment, a known mass of wax B was dissolved in a known volume of hexane in a large conical flask. The sample was charged onto the column in 25 mL portions until the yellow colour started to appear in the fractions. The decolourised fractions were combined and evaporated under reduced pressure to determine the mass of recovered wax. To prepare the column for the next run, the column was flushed with hexane (50 mL) to elute any residual wax, toluene (100 mL) to remove medium polarity compounds and methanol (100 mL) to remove high polarity compounds. Immediately after, the column was charged again with toluene (100 mL) followed by of hexane (100 mL) to re-condition the column. The procedure was repeated using the same silica until the first fraction appeared yellow.

A repeat of the experiment was conducted using IPA as the polar solvent. A known mass of wax B was dissolved in a known volume of hexane in a large conical flask. The sample was charged onto the column in 25 mL portions until the yellow colour started to appear in the fractions. The decolourised fractions were combined and evaporated under reduced pressure to determine the mass of recovered wax. To prepare the column for the next run, the column was flushed with hexane (50 mL) to elute residual wax. 50 mL portions of 20:80 IPA/hexane were flushed through the column to remove contaminants; which was continued until the fractions turned colourless. The column was reconditioned by flushing with 100 mL of toluene followed by 100 mL of hexane and the procedure was repeated using the same silica until the first fraction appeared yellow.

A final repetition of the experiment was conducted without using IPA or methanol. Instead, a medium polarity solvent system was used to elute only the yellow coloured compounds. A known mass of wax B was dissolved in a known volume of hexane in a large conical flask. The sample was charged onto the column in 25 mL portions until the yellow colour started to appear in the fractions. The decolourised fractions were combined and evaporated under reduced pressure to determine the mass of recovered wax. To prepare the column for the next run, the column was flushed with hexane (50 mL) to elute residual wax. 50 mL portions of 20:80 ethyl acetate/hexane were flushed through the column until the fractions appeared colourless. The column was reconditioned by flushing with 200 mL of hexane and the procedure was repeated using the same silica until the first fraction appeared yellow.

5.3.6. Solvent de-oiling to Determine Oil Content[34]

Oil content was extracted by means of solvent de-oiling using ethyl acetate. Ethyl acetate (50 mL) was added to wax (5 g) and heated until dissolved. The solution was cooled to room temperature and a precipitate formed. The suspension was immersed in an acetone/dry ice bath maintained at -32 °C for 15 minutes. The wax cake was washed with 4 x 25 mL of ethyl acetate at -32 °C and the filtrate was evaporated under reduced pressure, affording a brown oil. The wax cake was heated under vacuum to remove residual ethyl acetate and then accurately weighed.

5.3.7. Investigation of Urea and Thiourea Clathrate Extraction[40]

Waxes were separated by extracting urea clathrates and decomposing them. Iso-paraffins were separated in the same manner using thiourea. Wax (5 g) was dissolved in toluene (25 mL) in a conical flask. A saturated solution of urea in methanol was made up by dissolving urea (5 g) in methanol (10 mL). The saturated urea solution was added to the flask and the mixture was stirred at 65 °C for 15 minutes. Immediately after, the mixture was stirred at room temperature for 30 minutes. Finally, the mixture was immersed in a salt/ice bath and stirred for another 15 minutes. The white crystals were vacuum filtered and washed with 3 x 20 mL of hexane. The filtrate (filtrate 1) was filtered for a second time to recover additional white crystals and transferred into a separate round bottomed flask to perform the extraction of iso-paraffins with thiourea. The white crystals were decomposed by adding to 100 mL of distilled water and heated the suspension at 80 °C until the crystals disappeared and a waxy organic layer was formed. Then, toluene (20 mL) was added to the water to dissolve the organic content. The organic layer was separated and the aqueous layer was extracted with a further 3 x 20 mL of toluene. The combined organic layers were washed with 2 x 100 mL of distilled water to remove any residual urea. The aqueous layers were discarded as waste and the organic phase was dried with magnesium sulphate and vacuum filtered. Toluene was evaporated under reduced pressure affording the wax. The next step was to extract iso-paraffins with thiourea. A saturated solution of thiourea (5 g) in methanol (10 mL) was made up. Filtrate 1 was concentrated under reduced pressure to a volume of 30 mL. The saturated thiourea solution was then added to filtrate 1 in a round bottomed flask and the mixture was stirred at 65 °C for 15 minutes. Immediately after, the mixture was stirred at room temperature for 30 minutes. Finally, the mixture was immersed in a salt/ice bath and stirred for another 15 minutes. The white crystals were vacuum filtered and washed with 3 x 20 mL of hexane. The filtrate (filtrate 2) was filtered for a second time to recover white crystals and then evaporated under reduced pressure to and weighed to determine the oil content. The white crystals were decomposed by adding to 100 mL of distilled water and heated the suspension at 80 °C until the crystals disappeared. Then, toluene (20 mL) was added to the water to dissolve the organic content, the organic layer was separated and the aqueous layer was extracted with a further 3 x 20 mL of toluene. The combined organic layers were washed with 2 x 100 mL of distilled water to remove any residual urea. The aqueous layers were discarded as waste and the organic phase was dried with magnesium sulphate and vacuum filtered. Toluene was removed under reduced pressure affording the organic extract.

5.4. Characterisation

5.4.1. Gel Permeation Chromatography

Samples were weighed out to a few milligrams and diluted with the corresponding amount of HPLC grade chloroform in small glass vials to give a concentration of 1-2 mg mL^{-1}. For samples obtained by silica column chromatography, 1 mL of the prepared sample solutions (as described in section 1.3.1) was filtered into a HPLC sample vial. Polystyrene molecular weight calibration standards were prepared in the same manner and all samples and standards were left overnight in glass sample vials to dissolve. After dissolution, the samples were taken up in a syringe and filtered through membrane filter tips into HPLC sample vials. GPC analysis was performed using two Phenomenex Phenogel^{TM} 50 Å and 100 Å fixed bed columns in tandem to improve the resolution. The 50 Å pore sizes enables the analysis of molecular weights in the range of 100 – 3,000 Da and the 100 Å pore size covers a molecular weight range of 1,000 – 15,000 Da. Molecular weights are based on polystyrene standards.

5.4.2. Inductively Coupled Plasma Atomic Emission Spectroscopy (ICP-AES)

The analysis was performed on an Agillent 5100 ICP-OES spectrometer. An initial screening experiment was conducted to determine the presence of heavy metals. Each wax (100 mg) was weighed into a sampling vial and digested in concentrated ultrapure nitric acid solution (70 % w/v, 5 mL) with stirring using the CEM Discover SP-D microwave reactor. The parameters were configured on the interface (time, temperature, venting). The heating time was set to 25 minutes at 135 °C for the first experiment, which was increased to 45 minutes for each experiment thereafter. Pressure was vented at 200 psi to prevent excessive build-up of NO_2 gas. After digestion, the acid-sample solutions were left to vent before diluting them to 3.5 % w/v by pipetting acid-sample solution (0.5 mL) into a 15 mL centrifuge tube and making up to the 10 mL mark with ultrapure water.

The parameters from the last experiment were optimised further to reduce the digestion time. Waxes A, B and C (150 mg) were weighed out into a Pyrex® microwave reaction vessel. Concentrated ultrapure nitric acid (70 % w/v, 5 mL) was added to the reaction vessel and the samples were digested for 15 minutes at 200 °C. Pressure was vented at 200 psi to prevent excessive build-up of NO_2 gas. Once digested, the samples were diluted to 50 mL in a volumetric flask using ultrapure water. 5 mL of sample solution was measured into a 15 mL centrifuge tube. A stock solution of nitric acid (3.5 % w/v) was made up by measuring out 25 mL of 70 % nitric acid solution in measuring cylinder and transferring to a 500 mL volumetric flask. A stock solution of internal standard was made up by diluting 1 mL of yttrium solution with 50 mL of ultrapure water. Calibration standards were made up by pipetting the corresponding amount into 15 mL centrifuge tubes (shown in table 22). 1 mL of internal standard stock solution was pipetted into each centrifuge tube containing sample or calibration standard. Each sample and calibration standard were made up to 10 mL with nitric acid stock solution. Two blanks were prepared by pipetting 1 mL of internal standard stock solution into a centrifuge tube and making up to 10 mL with nitric acid stock solution.

Table 31. Preparation of ICP Calibration Standards

Calibration standard	Volume added to flask (µL)	Dilution volume
Multi element iv	2	10
Multi element iv	5	10
Multi element iv	10	10
Multi element iv	20	10
Multi element iv	40	10
Titanium std.	2	10
Titanium std.	5	10
Titanium std.	10	10
Titanium std.	20	10
Titanium std.	40	10

5.4.3. Nuclear Magnetic Resonance Spectroscopy

^{1}H NMR experiments were carried out on a Bruker AVANCE III 400 spectrometer. Samples were prepared by dissolving a known mass of wax in a measured volume of deuterated solvent. Deuterated chloroform was selected as a suitable solvent owing to its improved ability to dissolve the waxes over other solvents.

Correlation tables provided by Williams and Fleming and experimental data from Myers et al. were used to assist in the assignment of peaks.[26,30] The integral ratio of CH and CH_2 peaks was calculated to determine the degree of branching. The degree of unsaturation was determined by calculating the number of allyl groups per -CH_2 group. The relaxation delay (D1) was set to 5 times the longest T_1 to reduce error. This was determined to be 30 seconds by inversion recovery. COSY experiments were carried out to determine short-range proton couplings which assist in identifying overlapping allyl signals in the 1.5 – 3.0 ppm region.

5.4.4. Infrared Spectroscopy

No sample preparation was necessary for infrared spectroscopy. After running a background, solid samples were gently smeared onto the crystal and the clamp was screwed down. For liquid samples, one drop was pipetted onto the crystal. The infrared spectrum was obtained on an Agilent Cary 630 ATR spectrometer. Correlations provided by Williams and Fleming were used to assign peaks.[26]

5.4.5. Gas Chromatography-Mass Spectrometry

All GC-MS experiments were carried out on a Shimadzu GCMS-TQ8040 instrument. Headspace GC was used to characterise volatile components of crude wax that may be responsible for odour. This involved injecting the gas contained in the headspace of a sample vial containing wax after a period of heating and agitation. Wax samples (500 mg) were weighed into a headspace vial and placed onto the autosampler tray in which the samples were agitated at 80 °C for 15 minutes. Analysis was performed using a Restek Rxi-5Sil MS (30 m x 0.25 mm x 0.25 µm – 5 m integrated guard) column in spilt mode. The initial oven temperature was 40.0 °C and was ramped at 20.0 °C per minute to reach a final temperature of 280 °C with a hold time of 5 minutes. Helium was used as a carrier gas and the split ratio was set to 100. This was changed to 10 for waxes B and C for the re-run. The ion source temperature on the mass spectrometer was set to 250 °C. Peaks were manually integrated and their mass fragment data was matched with the NIST library to identify compounds.

Liquid injection was used to inject the samples dissolved in chloroform to characterise volatiles and semi-volatiles. Samples were prepared in HPLC grade chloroform at concentrations between 1 – 2 mg mL^{-1}. Analysis was performed on a Restek Rxi-5Sil MS (30 m x 0.25 mm x 0.25 µm - 5m integrated guard) column in split mode with a split ratio of 1. The injection volume was 1 µL and the inlet temperature was 250 °C. The initial oven temperature was 40.0 °C with a hold time of 2 minutes and ramped at 15 °C min^{-1} to reach a final temperature of 330 °C with a hold time of 10 minutes and a total run time of 31.3 minutes. The ion source on the mass spectrometer was set to 250 °C. Peaks on the chromatogram were integrated automatically and compounds were identified by matching their mass fragment patterns and retention indices with those in the NIST library.

5.4.6. UV-vis Spectroscopy

10 mg of medium polarity fraction obtained from liquid chromatography (section 3.1.2) was weighed into a sample vial and dissolved in 3 mL of chloroform. 0.1 mL of the solution was diluted to 5 mL of chloroform in a volumetric flask to prepare calibration standard 1. Calibration standard 1 was diluted by a factor of 2, 5, 10 and 20 to prepare calibration standards 2, 3, 4 and 5 respectively. Samples were transferred to a glass cuvette and analysed in the range of 200 – 800 nm wavelength. 262 nm was the wavelength chosen for calibration.

To measure the absorbance of colour-inducing contaminants in refined waxes, 10 mg of refined wax was dissolved in 10 mL of chloroform. Samples were transferred to a glass cuvette and analysed in the range of 190 – 500 nm.

5.5. Decolourisation and Deodorisation Processes

A scalable decolourisation and deodorisation process has been developed using physical and chemical methods. The physical methods were used to separate compounds based on their polarity and solubility. The aim of oxidative treatment was to convert impurities into more easily removable compounds that can be removed by liquid-liquid extraction or adsorption. Hydrogenation was used to convert impurities into saturates to improve the colour and mass recovery of wax after a pre-treatment step of adsorption. Process schemes were drawn using Microsoft Visio.

5.5.1. Oxidation

Wax samples (1 g) were weighed into round bottomed flasks and dissolved in cyclohexane (50 mL). Oxone®, in the form of granules (5 g) was added to the flask and refluxed at 80 °C for 90 minutes with vigorous stirring. After 90 minutes, the Oxone® was separated by filtration and the organic solution was washed with 2 x 100 mL of brine in a separation funnel to remove oxidised impurities and residual Oxone®. Brine was selected as the wash solvent to reduce the likelihood of forming an emulsion to enable a more efficient separation. The organic layer was dried with magnesium sulphate and vacuum filtered. The solvent was removed under reduced pressure and the sample weighed to determine the mass recovery of wax. The experiment was repeated 9 times to determine repeatability. The experiment was repeated a further 9 times using toluene as a solvent to determine if changing the solvent had any effect on the effectiveness of decolourisation.

The experiment was repeated without the use of a solvent. 10 % hydrogen peroxide solution (10 mL) was added to molten wax (5 g) stirring at 80 °C. After leaving overnight, hexane (20 mL) was added to enable the separation of wax in a separation funnel. The wax/hexane was transferred to a separation funnel and washed with 3 x 10 mL of brine to remove any residual peroxide. The organic layer was dried with magnesium sulphate and vacuum filtered. The solvent was removed under reduced pressure and the samples were weighed to determine the mass recovery.

A simple test was carried out by dissolving 1 g of wax after oxidation in toluene and filtering the solution through a silica plug. The solution was evaporated under reduced pressure to sequester the wax so that any decrease in colour intensity could be observed.

5.5.2. Solvent De-Oiling of Wax Pre-Treated by Silica Adsorption

A pre-treatment step of adsorption was used to remove polar compounds, followed by solvent de-oiling carried out to remove yellow/orange impurities. Wax (10 g) was heated to 80 °C in a round bottomed flask with a stirrer bar and silica gel (5 g) was added slowly with stirring to prevent clumping. After 15 minutes the wax was extracted by washing the silica with 3 x 10 mL of hexane while hot and decanting the supernatant into a conical flask. The three extracts were combined and acetone (30 mL) was added to the conical flask to precipitate the wax. The suspension was vacuum filtered and the wax cake was washed with 3 x 10 mL of neat acetone to remove contaminants. The filtrate was cooled in a salt-ice bath to precipitate residual wax and vacuum filtered. The residual wax was re-combined with the wax cake and transferred into to a pre-weighed 50 mL round bottomed flask. Residual solvent was removed by heating the wax cake under vacuum and then weighed. The filtrate was evaporated under reduced pressure and weighed to determine oil content. Polar contaminants were desorbed from the silica by heating in 15:85 methanol/chloroform. The filtrate was vacuum distilled and waxy residue was weighed.

5.5.3. Catalytic Hydrogenation of Wax Pre-Treated by Silica Adsorption

Hydrogen gas was sourced from an electrolytic hydrogen generator. Wax (5 g) was weighed out into a conical flask and dissolved in toluene (100 mL). The solution was filtered through a silica plug. The silica was washed with 4 x 25 mL of toluene and the filtrate was collected in a

250 mL round bottomed flask and then concentrated under reduced pressure to approximately 30 mL. The solution was transferred to a 100 mL round bottomed flask and palladium on carbon (0.5 g) was added. The flask was sealed with a rubber septum and purged by bubbling the reaction mixture with hydrogen gas. The reaction mixture was left stirring overnight at 70 °C under an atmosphere of hydrogen. The contents of the flask were vacuum filtered twice to remove the catalyst and the solvent was removed under reduced pressure. Residual solvent was removed by heating the flask in an oil bath at 80 °C under vacuum. The flask was weighed on an accurate balance to determine mass recovery of wax.

6. References

1 C. Rosevelt, M. Los Huertos, C. Garza and H. M. Nevins, *Mar. Pollut. Bull.*, 2013, **71**, 299–306.

2 S. Budsaereechai, A. J. Hunt and Y. Ngernyen, *RSC Adv.*, 2019, **9**, 5844–5857.

3 R. Thahir, A. Altway, S. R. Juliastuti and Susianto, *Energy Reports*, 2019, **5**, 70–77.

4 G. Elordi, M. Arabiourrutia, J. Bilbao and M. Olazar, *Energy and Fuels*, 2018, **32**, 3751–3759.

5 R. Aguado, M. Olazar, M. J. San José, B. Gaisán and J. Bilbao, *Energy and Fuels*, 2002, **16**, 1429–1437.

6 E. Hájeková and M. Bajus, *J. Anal. Appl. Pyrolysis*, 2005, **74**, 270–281.

7 M. Arabiourrutia, G. Elordi, G. Lopez, E. Borsella, J. Bilbao and M. Olazar, *J. Anal. Appl. Pyrolysis*, 2012, **94**, 230–237.

8 D. Loudon, D. Bezuidenhout, G. Meyer, I. Behrmann, H.-J. Scheidat and H. Feitkenhauer, *US pat., US0166909A1*, 2015.

9 M. T. Zaky and N. H. Mohamed, *J. Taiwan Inst. Chem. Eng.*, 2010, **41**, 360–366.

10 V. McDaniel, *US Pat., US3108943*, 1963.

11 M. D. Ackerson, S.-H. Arabshahi and R. E. Babcock, *US pat., US5474668*, 1995.

12 P. T. Williams and E. A. Williams, *J. Anal. Appl. Pyrolysis*, 1999, **51**, 107–126.

13 G. Yan, X. Jing, H. Wen and S. Xiang, *Energy and Fuels*, 2015, **29**, 2289–2298.

14 I. Çit, A. Sinağ, T. Yumak, S. Uçar, Z. Misirlioğlu and M. Canel, *Polym. Bull.*, 2010, **64**, 817–834.

15 U. Hujuri, A. K. Ghoshal and S. Gumma, *Waste Manag.*, 2010, **30**, 814–820.

16 S. Jose, S. Thomas, P. K. Biju, P. Koshy and J. Karger-Kocsis, *Polym. Degrad. Stab.*, 2008, **93**, 1176–1187.

17 S. E. Levine and L. J. Broadbelt, *Polym. Degrad. Stab.*, 2009, **94**, 810–822.

18 M. Predel and W. Kaminsky, *Polym. Degrad. Stab.*, 2000, **70**, 373–385.

19 S. Qian, T. Igarashi and K. H. Nitta, *Polym. Bull.*, 2011, **67**, 1661–1670.

20 T. Pilusa, M. Shukla and E. Muzenda, *Int. Conf. Chem. Min. Metall. Eng.*, 2013, 265–268.

21 G. Lopez, M. Artetxe, M. Amutio, J. Bilbao and M. Olazar, *Renew. Sustain. Energy Rev.*, 2017, 73, 346–368.

22 P. Das and P. Tiwari, *Waste Manag.*, 2018, **79**, 615–624.

23 A. Ochoa, I. Barbarias, M. Artetxe, A. G. Gayubo, M. Olazar, J. Bilbao and P. Castaño, *Appl. Catal. B Environ.*, 2017, **209**, 554–565.

24 Y. Zheng, J. Bai, J. Xu, X. Li and Y. Zhang, *Waste Manag.*, 2018, **72**, 87–98.

25 E. J. Sommer, *US pat., US6610981B2*, 2003.

26 D. H. Williams, *Spectroscopic methods in organic chemistry*, McGraw-Hill, London ; New York, 5th ed., 1995.

27 P. Das and P. Tiwari, *Resour. Conserv. Recycl.*, 2018, **128**, 69–77.

28 D. Biermann and W. Schmidt, *J. Am. Chem. Soc.*, 1980, **102**, 3163–3173.

29 C. Vasile, M. A. Brebu, T. Karayildirim, J. Yanik and H. Darie, *Fuel*, 2007, **86**, 477–485.

30 M. E. Myers, J. Stollsteimer and A. M. Wims, *Anal. Chem.*, 1975, **47**, 2010–2015.

31 Z. Nyiri, M. Novák, Z. Bodai, N. Petrovics and Z. Eke, *Talanta*, 2017, **174**, 214–220.

32 M. Korvela, M. Andersson and J. Pettersson, *J. Anal. At. Spectrom.*, 2018, **33**, 1770–1776.

33 H. Sakurai, J. Noro, A. Kawase, M. Fujinami and K. Oguma, *Anal. Sci.*, 2006, **22**, 225–228.

34 R. A. Nadkarni, *Guide to ASTM test methods for the analysis of petroleum products and lubricants*, ASTM International, 2007.

35 L. Maas, R. Geiman and C. Adams, *US pat., US4701254*, 1987.

36 A. Kinsel, *US pat., US2160874,* 1939.

37 R. M. Baily, H. F. Hitchcox and N. J. Cranford, *US pat., US2733188*, 1956.

38 V. M. Bhatnagar, *J. Struct. Chem.*, 1968, 8, 513–529.

39 G. Dellow, *US pat., US3328313*, 1967.

40 A. A. Lappas, D. Patiaka, D. Ikonomou and I. A. Vasalos, *Ind. Eng. Chem. Res.*, 1997, **36**, 3110–3115.

41 T. Yamazaki, T. Tanabe and T. Sugahara, *ACS Omega*, 2018, **3**, 13154–13159.

42 M. Novák, C. Kirchkeszner, D. Palya, Z. Bodai, Z. Nyiri, N. Magyar, J. Kovács, T. Rikker and Z. Eke, *Int. J. Environ. Anal. Chem.*, 2015, **95**, 1471–1488.

43 E. Snyder, *US pat., US4169843*, 1979.

44 S. E. Denmark, Z. Wu, C. M. Crudden and H. Matsuhashi, *J. Org. Chem.*, 1997, **62**, 8288–8289.

45 B. Yu, A. H. Liu, L. N. He, B. Li, Z. F. Diao and Y. N. Li, *Green Chem.*, 2012, **14**, 957–962.

46 P. J. Kropp, G. W. Breton, J. D. Fields, J. C. Tung and B. R. Loomis, *J. Am. Chem. Soc.*, 2000, **122**, 4280–4285.

47 F. Silva, A. Baker, J. Stansall, W. Michalska, M. S. Yusubov, M. Graz, R. Saunders, G. J. S. Evans and T. Wirth, *European J. Org. Chem.*, 2018, **2018**, 2134–2137.

48 E. Provost, V. Chevallier, M. Bouroukba, D. Petitjean and M. Dirand, *J. Chem. Eng. Data*, 1998, **43**, 745–749.

49 J. N. Hahladakis, C. A. Velis, R. Weber, E. Iacovidou and P. Purnell, *J. Hazard. Mater.*, 2018, 344, 179–199.

50 P. B. Tchounwou, C. G. Yedjou, A. K. Patlolla and D. J. Sutton, *Exp suppl.*, 2012, **101**, 133–164.

51 G. Leonardos, D. Kendall and N. Barnard, *J. Air Pollut. Control Assoc.*, 1969, **19**, 91–95.

52 Á. Stumpf, K. Tolvaj and M. Juhász, in *Journal of Chromatography A*, 1998, vol. 819, pp. 67–74.

53 W. Ren, R. M. Spearrin, D. F. Davidson and R. K. Hanson, in *8th US National Combustion Meeting 2013*, 2013, vol. 1, pp. 81–91.

54 E. W. Tegelaar, J. W. De Leeuw and P. J. Holloway, *J. Anal. Appl. Pyrolysis*, 1989, **15**, 289–295.

55 M. N. Siddiqui and H. H. Redhwi, *Fuel Process. Technol.*, 2009, **90**, 545–552.

56 E. V. Antonakou and D. S. Achilias, *Waste and Biomass Valorization*, 2013, 4, 9–21.

57 S. Kumar and K. M. Agrawal, *Pet. Sci. Technol.*, 2014, **32**, 261–266.

58 T. Yamazaki, T. Tanabe and T. Sugahara, *ACS Omega*, 2018, **3**, 13154–13159.

59 J. F. Clare, *Accredit. Qual. Assur.*, 2005, **10**, 283–288.

60 J. P. Candy and P. Fouilloux, *J. Catal.*, 1975, **38**, 110–119.

61 B. Jager, R. C. Kelfkens and A. P. Steynberg, *Stud. Surf. Sci. Catal.*, 1994, **81**, 419–425.

62 R. Rauch, A. Kiennemann and A. Sauciuc, *The Role of Catalysis for the Sustainable Production of Bio-fuels and Bio-chemicals*, Elsevier, 2013.

63 Momina, M. Shahadat and S. Isamil, *RSC Adv.*, 2018, 8, 24571–24587.

64 V. Khatibikamal, A. Torabian, H. Ahmad panahi and M. Baghdadi, *J. Hazard. Mater.*, 2019, 357–364.

65 N. R. M, G. Aa and A. Am, *J. Ind. Env. Chem.*, 2018, **2**, 7–18.

66 D. Li, J. Henschen and M. Ek, *Green Chem.*, 2017, **19**, 5564–5567.

67 M. S. Islam, L. Chen, J. Sisler and K. C. Tam, *J. Mater. Chem. B*, 2018, 6, 864–883.

68 B. Zhang, F. Li, Y. Wang, C. Wu, M. Zhang and Y. Zhao, *US Pat., US2018/0215636A1*, US pat., China, 2018.

69 Z. Lyu, L. Ding, A. Y. T. Huang, C. L. Kao and L. Peng, *Mater. Today Chem.*, 2019, 13, 34–48.

70 D. Guo, N. Muhammad, C. Lou, D. Shou and Y. Zhu, *New J. Chem.*, 2019, **43**, 121–129.

Characterisation and Process Development Studies on Waxes Derived from Plastic Pyrolysis

By

JOSHUA NICHOLAS ROBINSON

JANUARY 2020

Appendices

Contents

Appendix A: Sample Masses and Mass Recoveries

Appendix B: GPC and GC-MS Chromatograms

Appendix C: GC-MS and ICP Raw and Processed Data Tables

Appendix A: Sample Masses and Mass Recoveries

1. Insoluble Residue

Wax	Mass of Filter Paper (g)	Filter Paper + insoluble Residue (g)	Insoluble Residue (g)
A	0.159	0.528	0.369
B	0.163	0.165	0.002
C	0.160	0.164	0.004

2. Acid-Base Extraction
   2.1. Wax Recovery

Wax	Starting Material (g)	Mass Recovery (g)
A Recovered Wax	1.089	0.615
B Base Extracted	1.078	0.011
C Recovered Wax	1.032	0.803

   2.2. Extracts

Wax	Starting Material (g)	Mass Recovery (g)
A Basic Components	1.089	0.004
A Acidic Components	1.089	0.001
B Basic Components	1.078	0.008
B Acidic Components	1.078	0.011
C Basic Components	1.032	0.005
C Acidic Components	1.032	0.000

3. Filtration of Wax A for Solvent Extraction and Urea Clathrate Experiments

Wax A was filtered through celite prior to solvent extraction and urea clathrate experiments. The mass of wax recovered after filtration is given below.

Wax	Starting Mass (g)	Mass Recovery (g)
A	26.764	17.293

4. Liquid Chromatography

Wax	Fraction	Starting Material (g)	Mass Recovery (g)
A	Non Polar	5.828	3.81
A	Medium Polarity	5.828	1.13
A	High Polarity	5.828	0.019
B	Non Polar	5.085	4.622
B	Medium Polarity	5.085	0.151
B	High Polarity	5.085	0.065
C	Non Polar	5.102	4.856
C	Medium Polarity	5.102	0.364
C	High Polarity	5.102	0.083

5. Solvent Extraction

Wax	Extract	Starting Material (g)	Mass Recovery (g)
A	Wax	4.880	3.273
A	Oil	4.880	0.898
B	Wax	4.996	2.620
B	Oil	4.996	1.884
C	Wax	5.095	1.744
C	Oil	5.095	2.945

6. Urea Clathrate Formation

Wax	Extract	Starting Material (g)	Mass Recovery (g)
B	Wax Extract	5.044	2.386
B	Clathrate Oil	5.044	2.197
B	Thiourea Extract	5.044	0.001
C	Wax Extract	5.036	1.267
C	Clathrate Oil	5.036	0.015
C	Thiourea Extract	5.036	2.872

7. Hydrogenation

7.1. Hydrogenation of Oil Extract Using Palladium on Carbon Catalyst

Wax	Starting Material (g)	Mass Recovery (g)
B	2.617	2.120

7.2. Hydrogenation of Crude Wax C Using Palladium on Carbon Catalyst

Wax	Starting Material (g)	Mass Recovery (g)
C	5.045	4.515

7.3. Hydrogenation of Pre-treated Waxes Using Palladium on Carbon Catalyst

Wax	Starting Material (g)	Mass Recovery (g)
B	5.069	4.073
C	4.920	3.799

7.4. Hydrogenation of Pre-treated Waxes Using Raney Nickel Catalyst

Wax	Starting Material (g)	Mass Recovery (g)
A	5.777	3.727
B	4.920	4.119
C	4.936	4.232

8. Oxidation Using Oxone®

Sample	Solvent	Starting Material (g)	Mass Recovery
B1	Cyclohexane	1.0558	0.6157
B2	Cyclohexane	1.0285	0.4516
B3	Cyclohexane	0.9916	0.7231
B4	Cyclohexane	1.0204	0.7997
B5	Cyclohexane	0.9638	0.7113
B6	Cyclohexane	1.0700	0.8383
B7	Cyclohexane	0.9654	0.7892
B8	Cyclohexane	1.0715	0.9552

B9	Cyclohexane	0.9290	1.0075
C1	Cyclohexane	1.0625	0.9456
C2	Cyclohexane	1.1132	0.8654
C3	Cyclohexane	1.0247	0.8402
C4	Cyclohexane	1.0050	0.7958
C5	Cyclohexane	1.0002	0.8328
C6	Cyclohexane	1.0428	1.0211
C7	Cyclohexane	1.0067	0.7892
C8	Cyclohexane	1.0087	0.8713
C9	Cyclohexane	0.9962	1.0723

Sample	Solvent	Starting Material (g)	Mass Recovery
B1	Toluene	1.0172	0.7563
B2	Toluene	1.0508	0.7365
B3	Toluene	1.0372	0.8258
B4	Toluene	1.0490	0.7921
B5	Toluene	1.0167	0.7955
B6	Toluene	1.0100	0.7905
B7	Toluene	1.0357	0.7900
B8	Toluene	0.9648	0.8286
C1	Toluene	1.0480	0.9098
C2	Toluene	0.9971	0.8319
C3	Toluene	1.0575	0.6794
C4	Toluene	1.0548	0.9614
C5	Toluene	1.0425	0.8773
C6	Toluene	1.0446	0.9956
C7	Toluene	1.0186	0.3827
C8	Toluene	1.0178	0.8606
C9	Toluene	0.9884	0.8047

9. Combined method: Adsorption and Solvent De-oiling

Wax	Fraction	Starting Material (g)	Mass Recovery (g)
B	Wax	10.036	2.342
B	Oil	10.036	2.617
B	Residue	10.036	2.650

Appendix B: GPC and GC-MS Chromatograms

1. GPC Chromatograms

The same column and solvent were used for all chromatograms, as below.

Column: Phenomenex Phenogel™ 50 Å and 100 Å in tandem.

Solvent: Chloroform from Fisher Scientific (HPLC grade).

1.1. Crude

1.1.1. Wax A

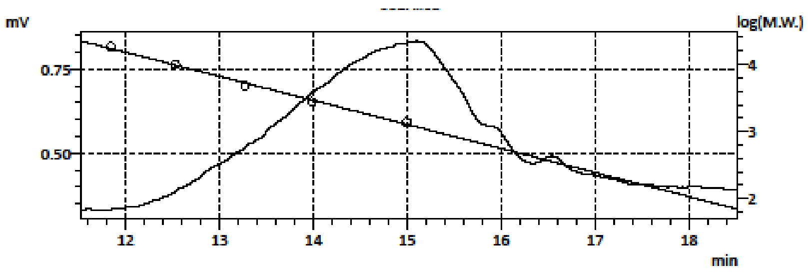

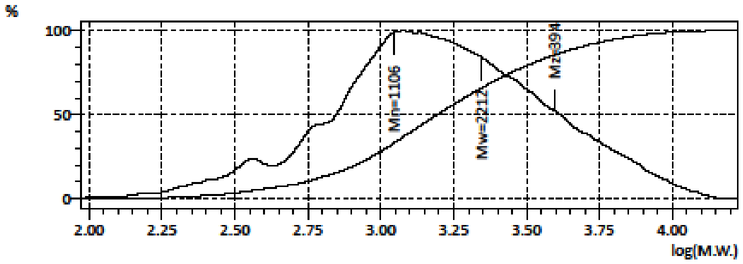

1.1.2. Wax B

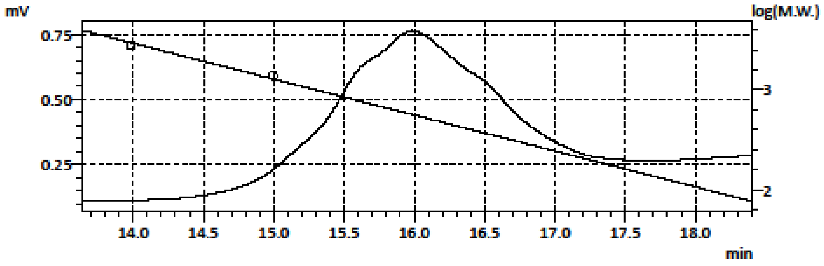

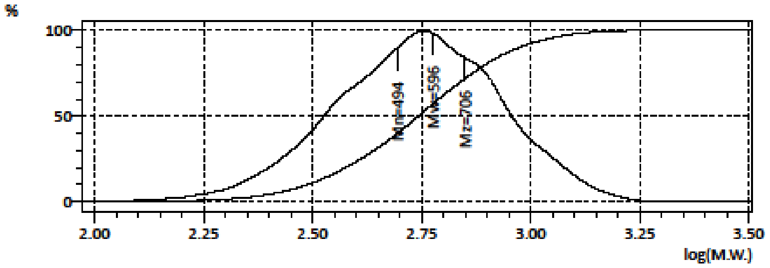

1.1.3. Wax C

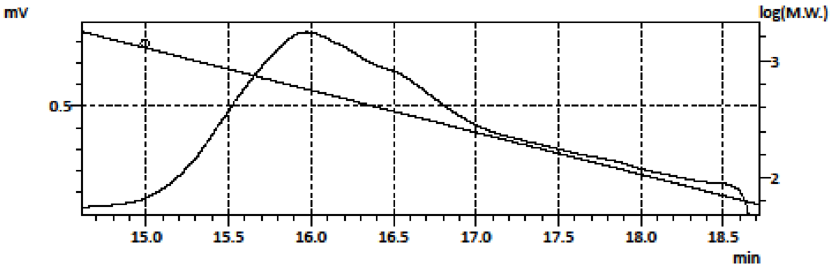

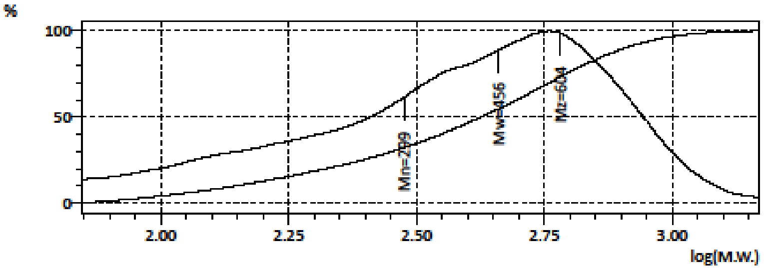

1.2. Liquid Chromatography

1.2.1. Wax A non-polar fraction

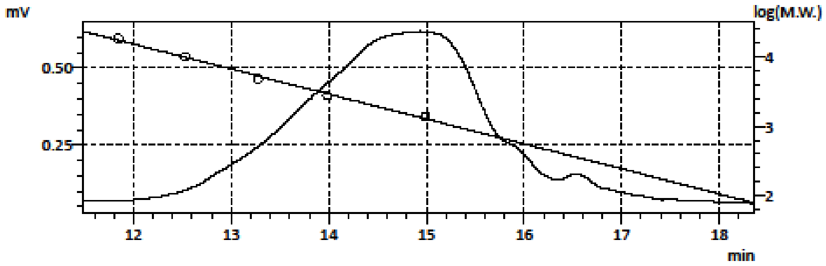

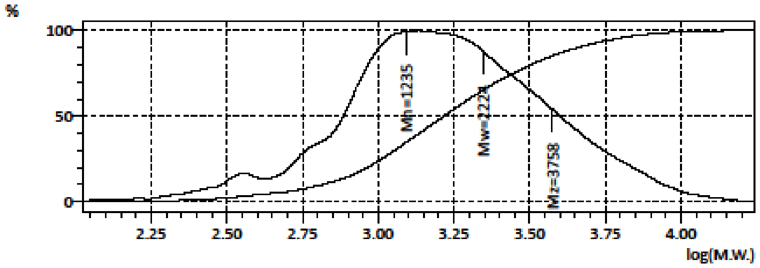

1.2.2. Wax A medium polarity fraction

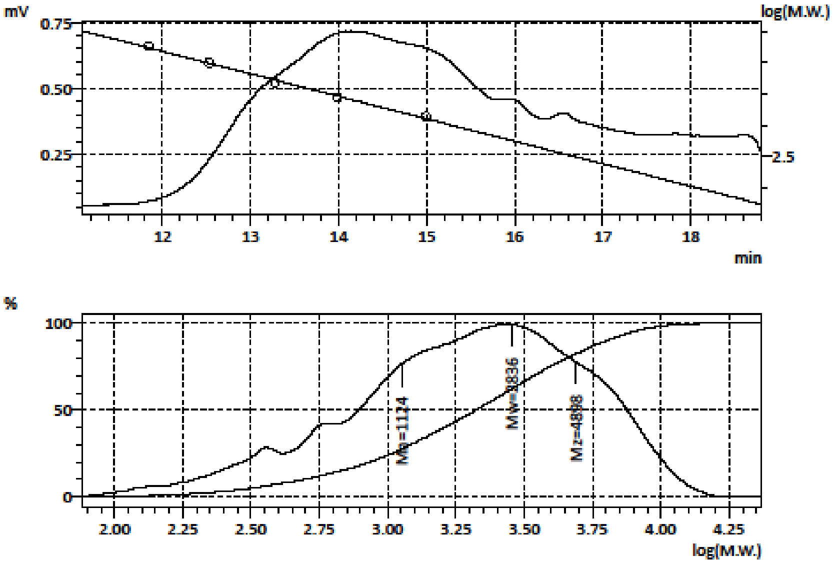

1.2.3. Wax A high polarity fraction

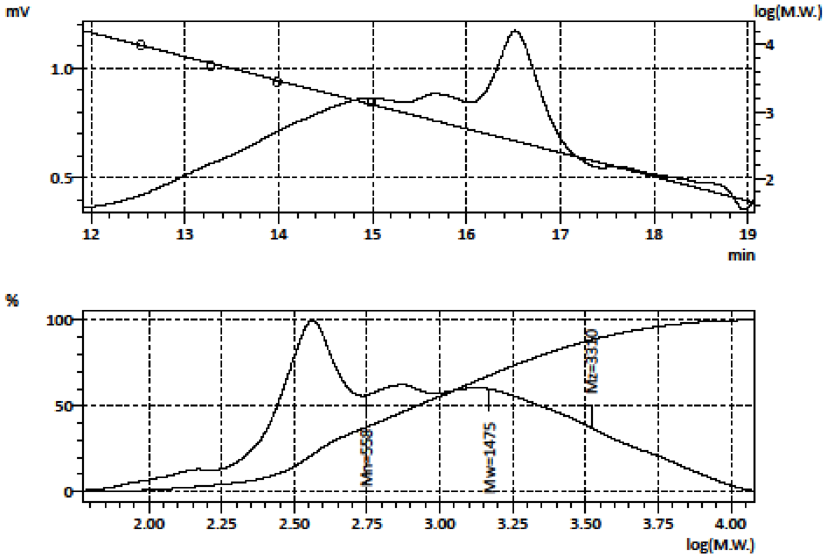

1.2.4. Wax B non-polar fraction

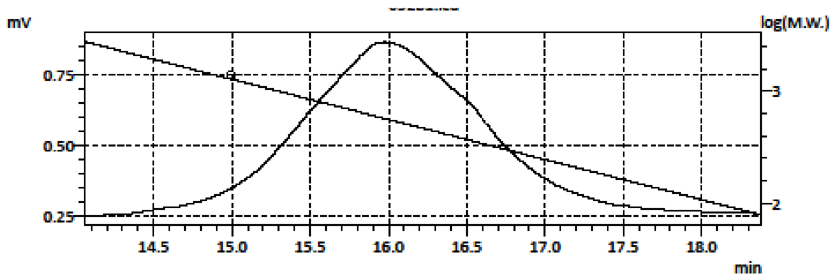

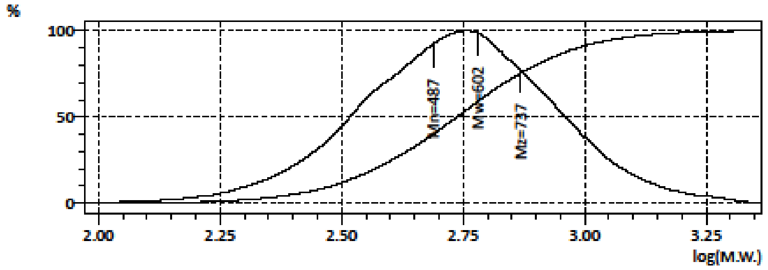

1.2.5. Wax B medium polarity fraction

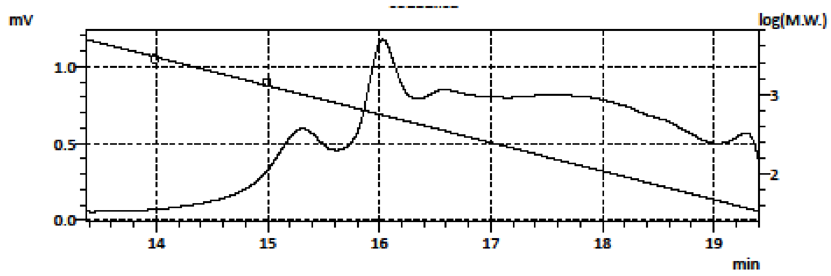

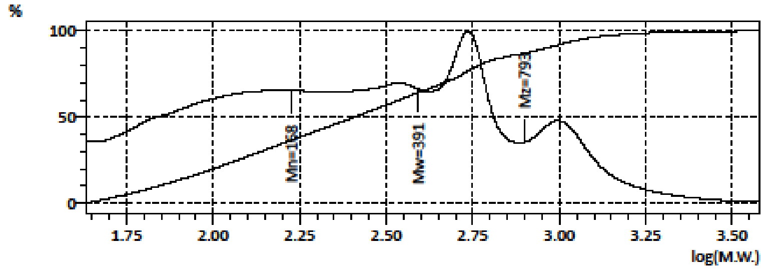

1.2.6. Wax B high polarity fraction

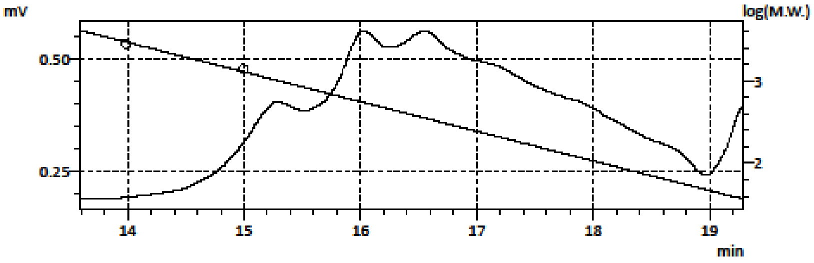

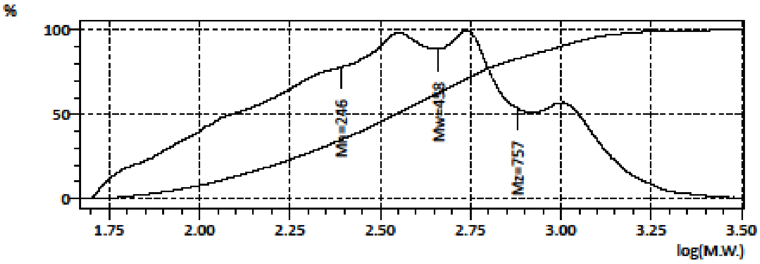

1.2.7. Wax C non-polar fraction

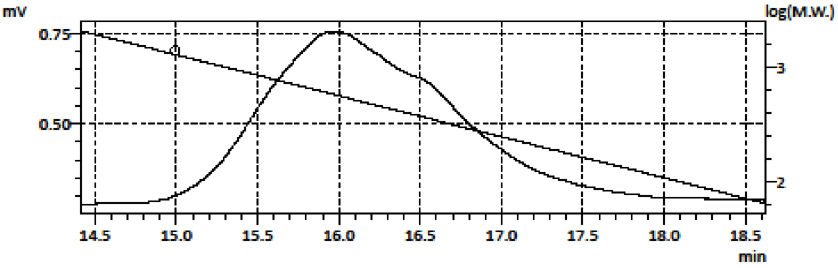

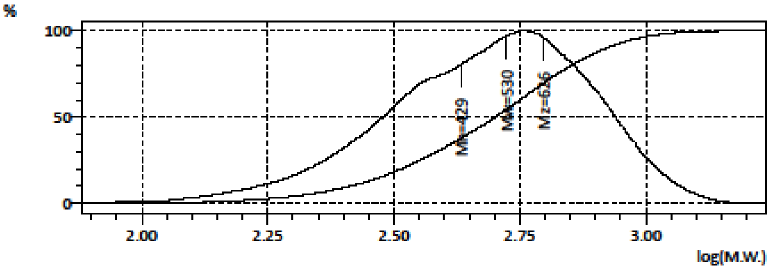

1.2.8. Wax C medium polarity fraction

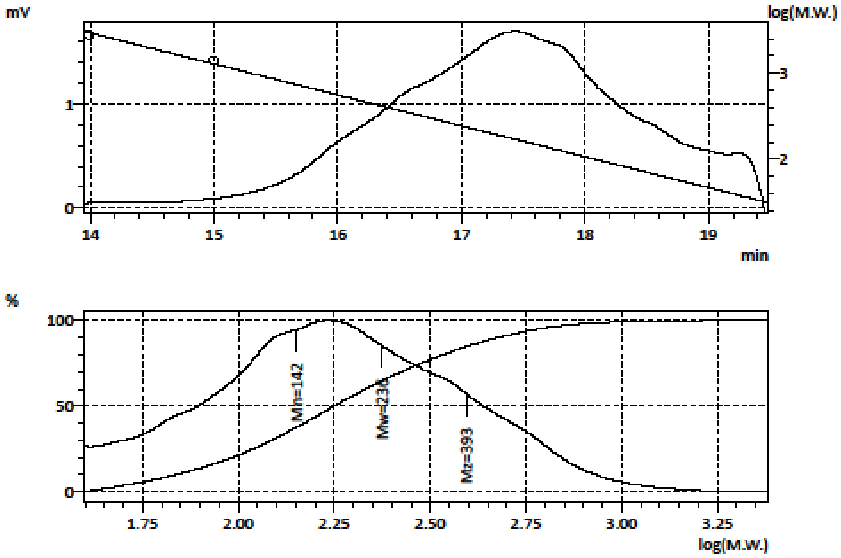

1.2.9. Wax C high polarity fraction

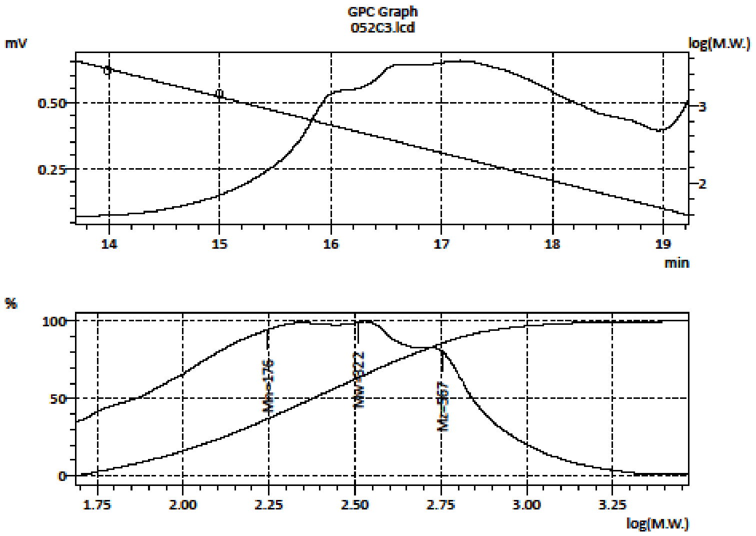

1.3. Solvent Extraction

1.3.1. De-oiled wax A

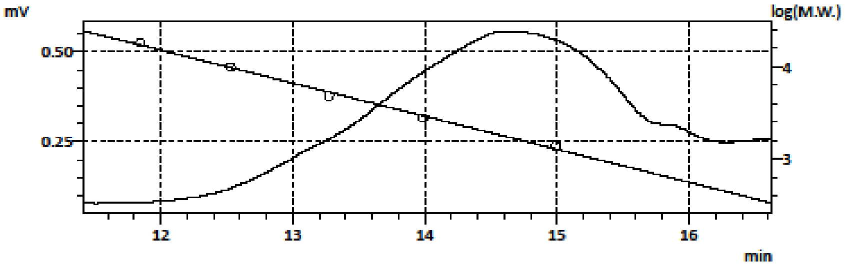

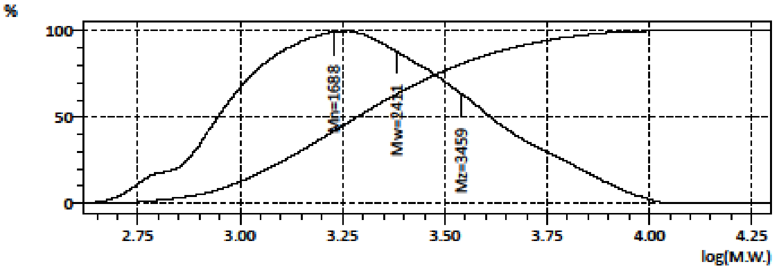

1.3.2. Wax A oil extract

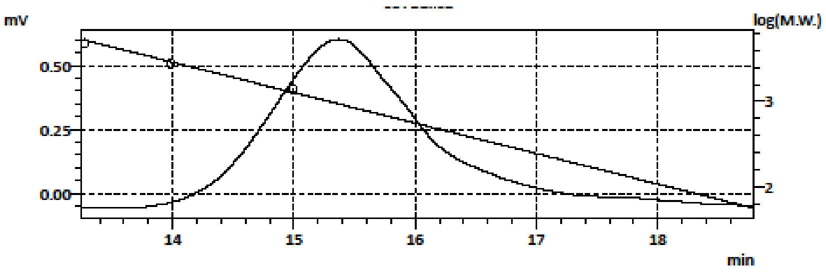

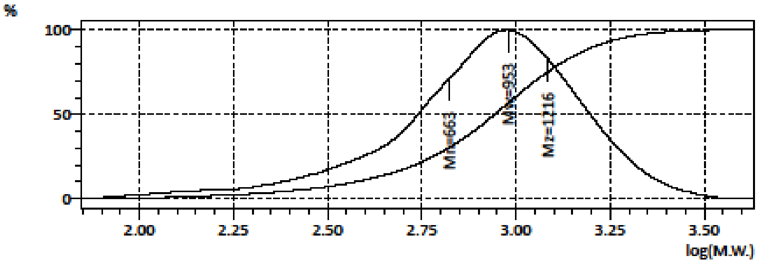

1.3.3. De-oiled wax B

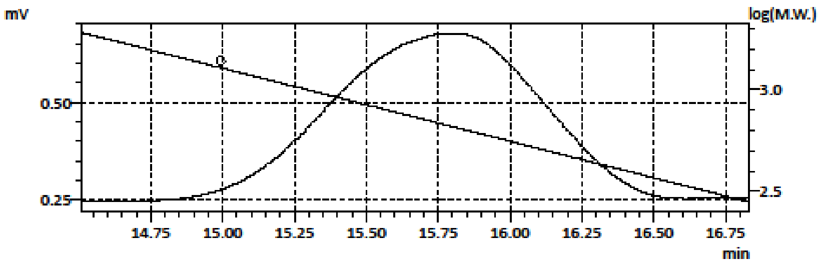

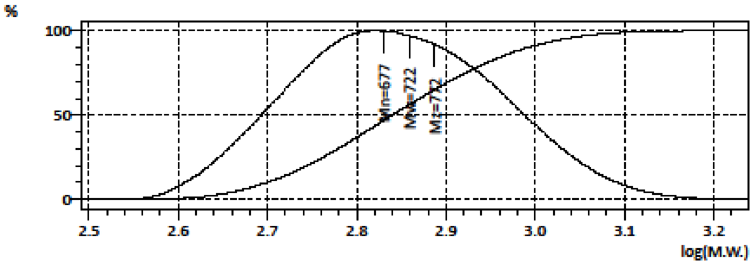

1.3.4. Wax B oil extract

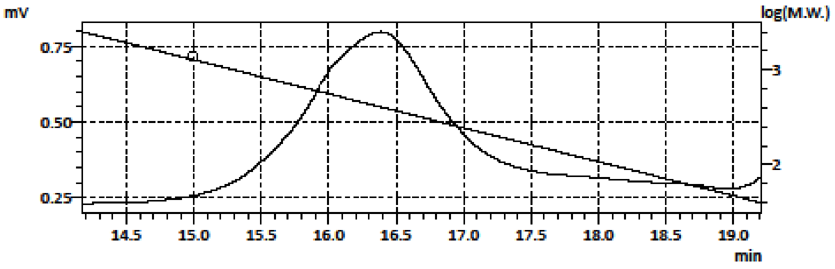

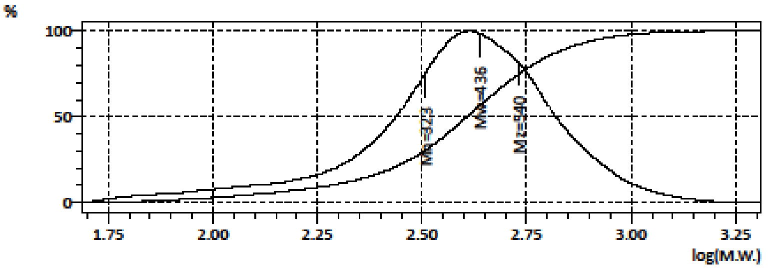

1.3.5.De-oiled wax C

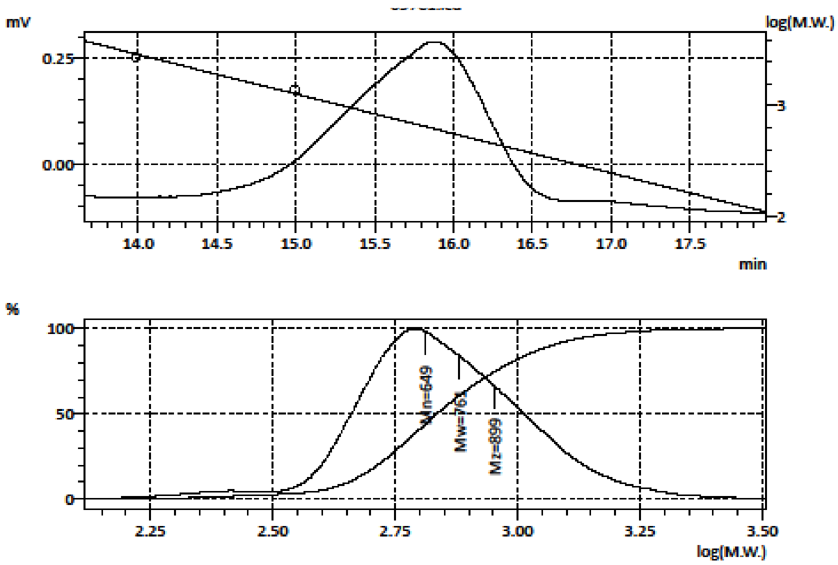

1.3.6.Wax C oil extract

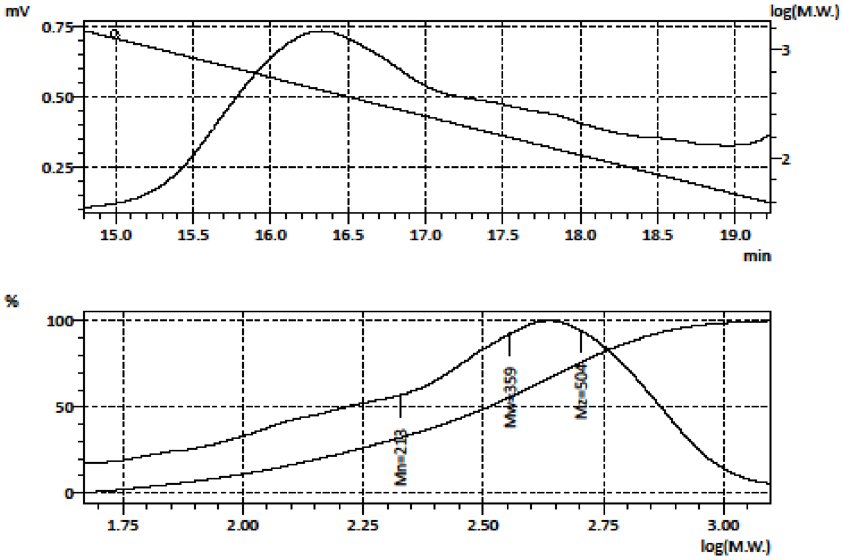

1.4. Urea Clathrate Formation

1.4.1. Clathrate wax, wax B

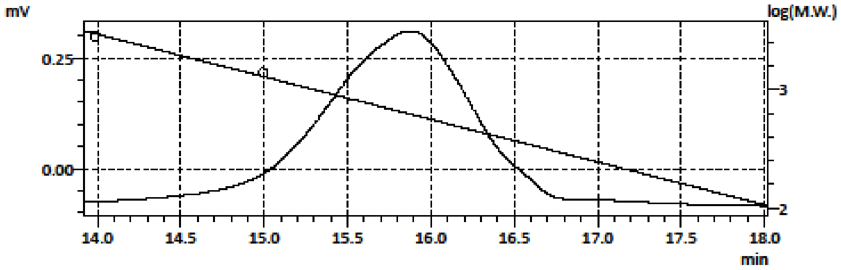

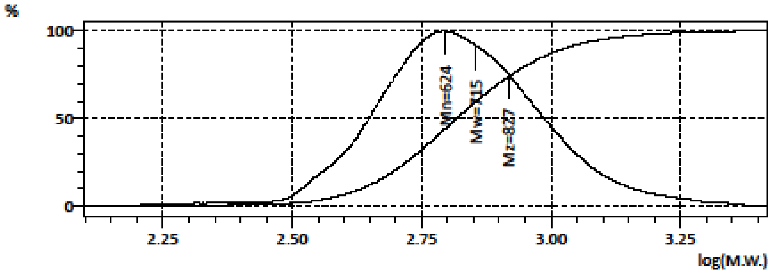

1.4.2. Clathrate oil, wax B

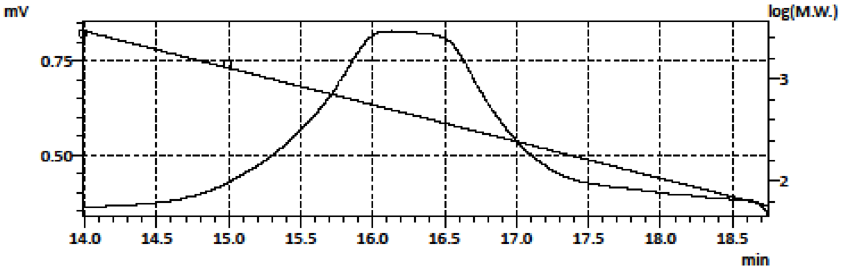

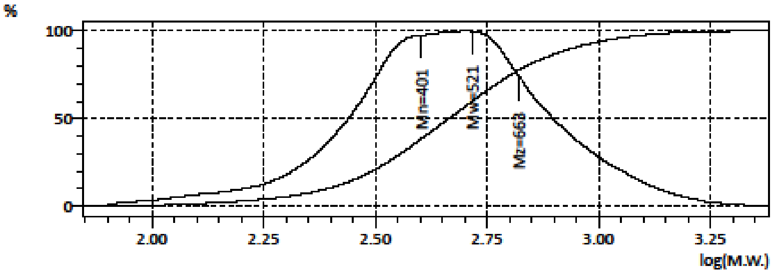

1.4.3.Clathrate wax, wax C

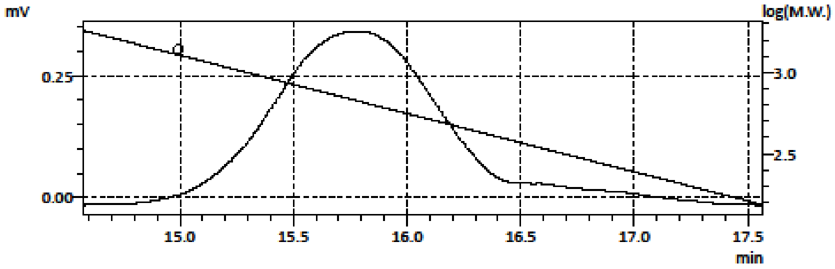

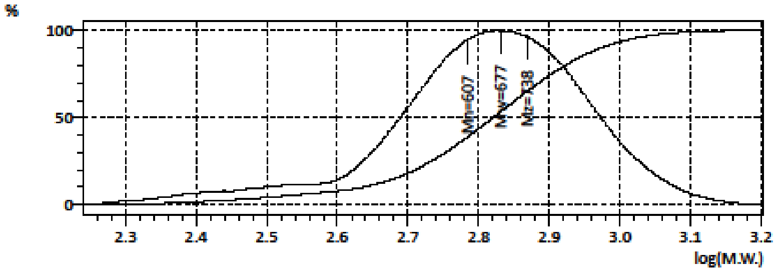

1.4.4.Clathrate oil, wax C

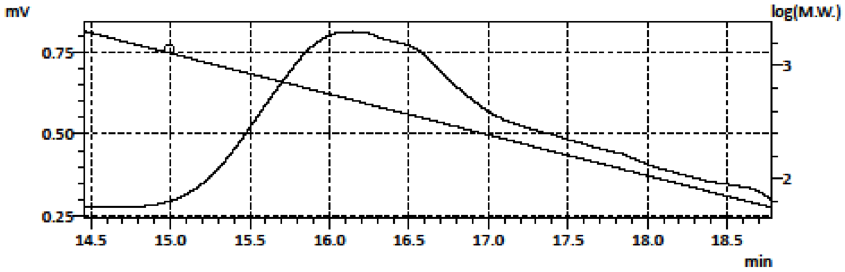

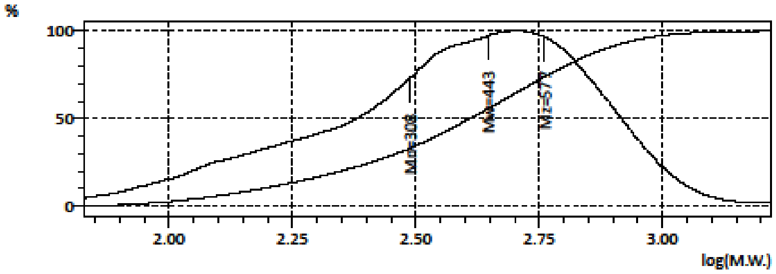

2. GCMS Chromatograms

2.1. Headspace GC-MS Analysis of Crude Wax

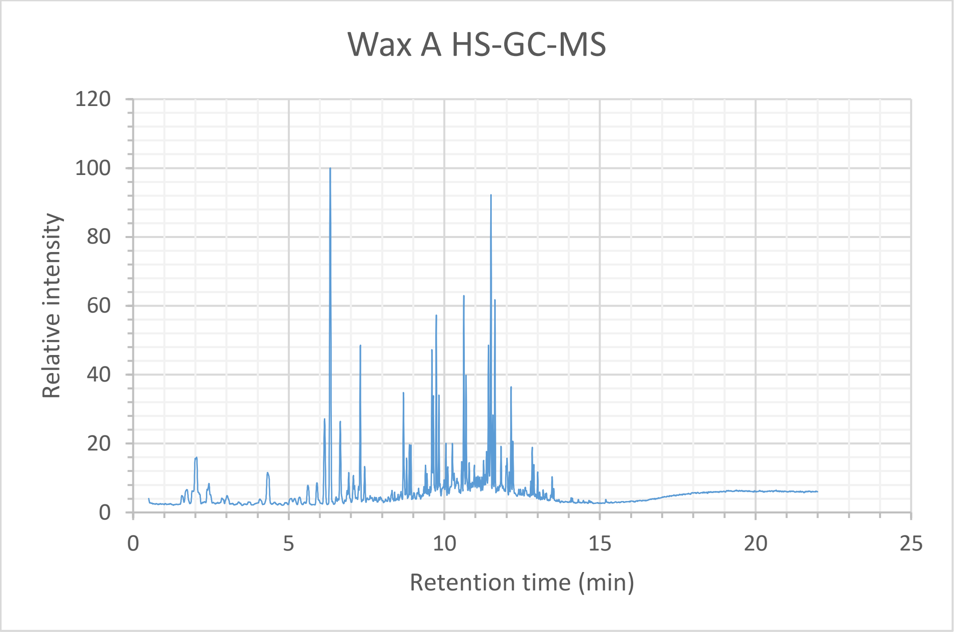

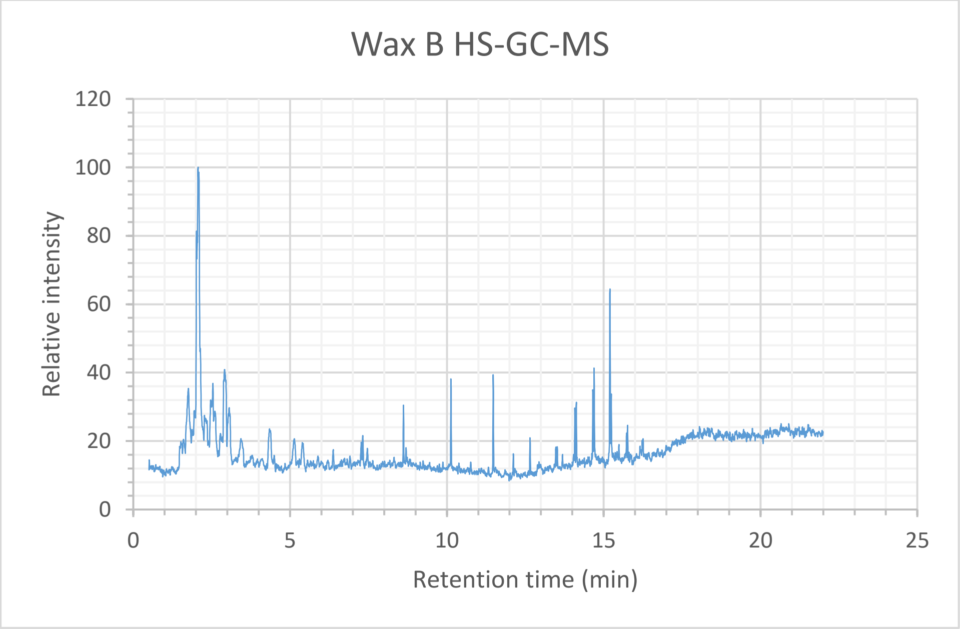

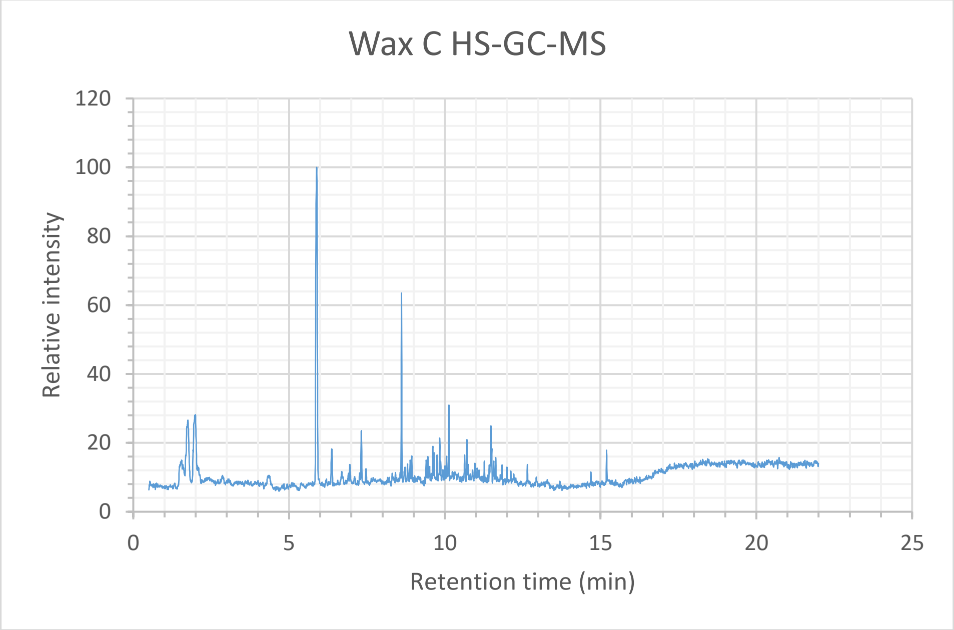

2.2. GC-MS Analysis of Fractions and Extracts Containing Impurities

2.2.1. Chloroform Blank

The data provided below represents what was detected by GC-MS in the blank containing neat chloroform.

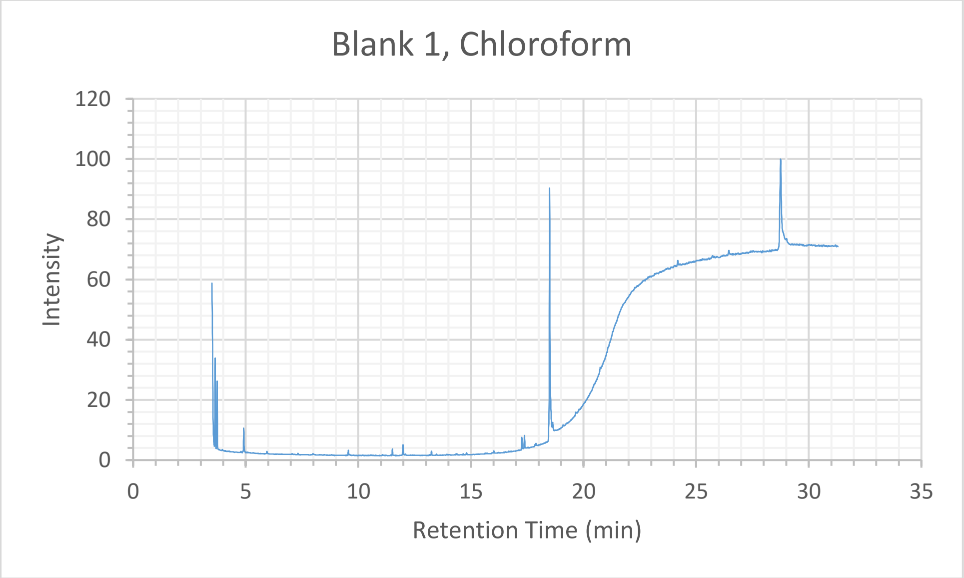

2.2.2. Liquid Chromatography Fractions

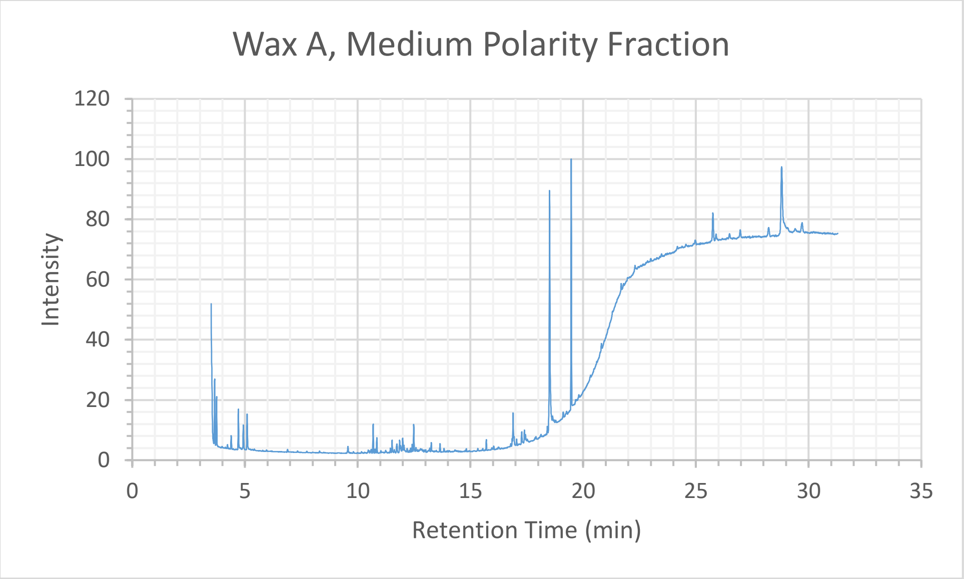

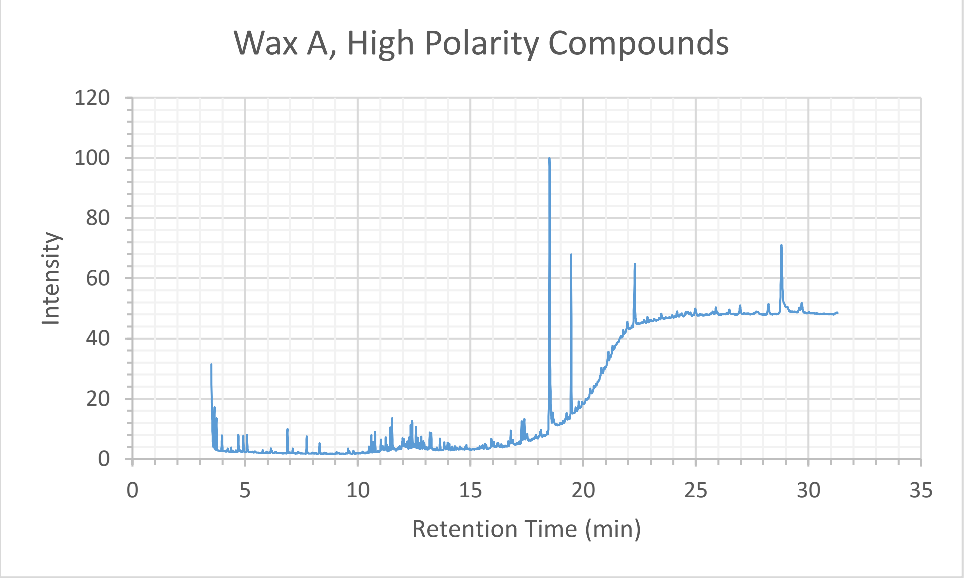

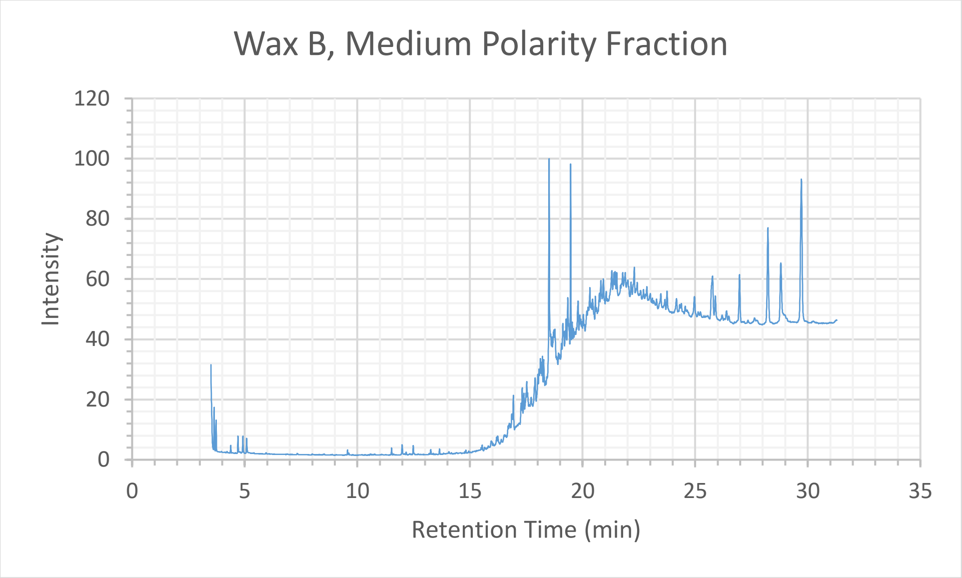
Wax B, Medium Polarity Fraction
Intensity
120
100
80
60
40
20
0
0
5
10
15
20
25
30
35
Retention Time (min)

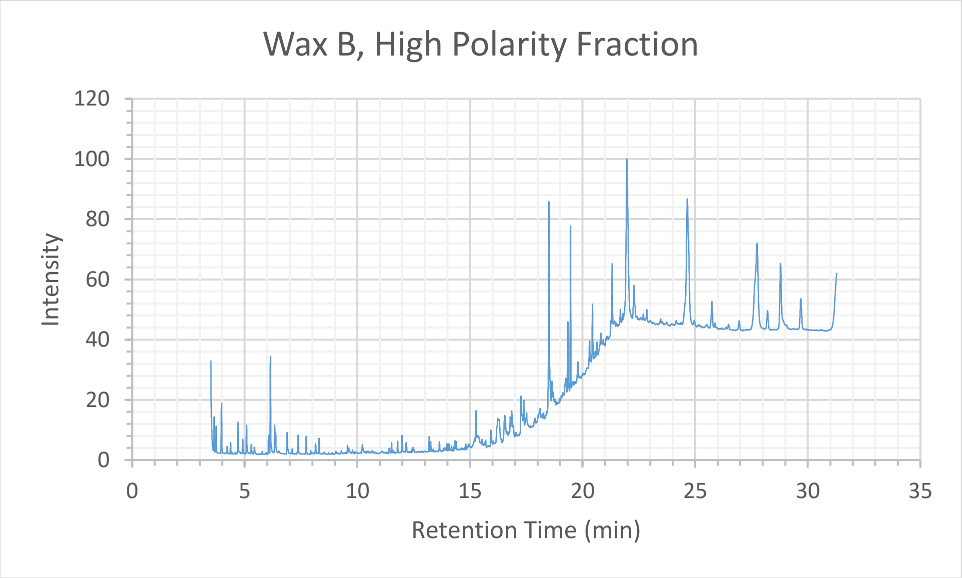
Wax B, High Polarity Fraction
Intensity
120
100
80
60
40
20
0
0
5
10
15
20
25
30
35
Retention Time (min)

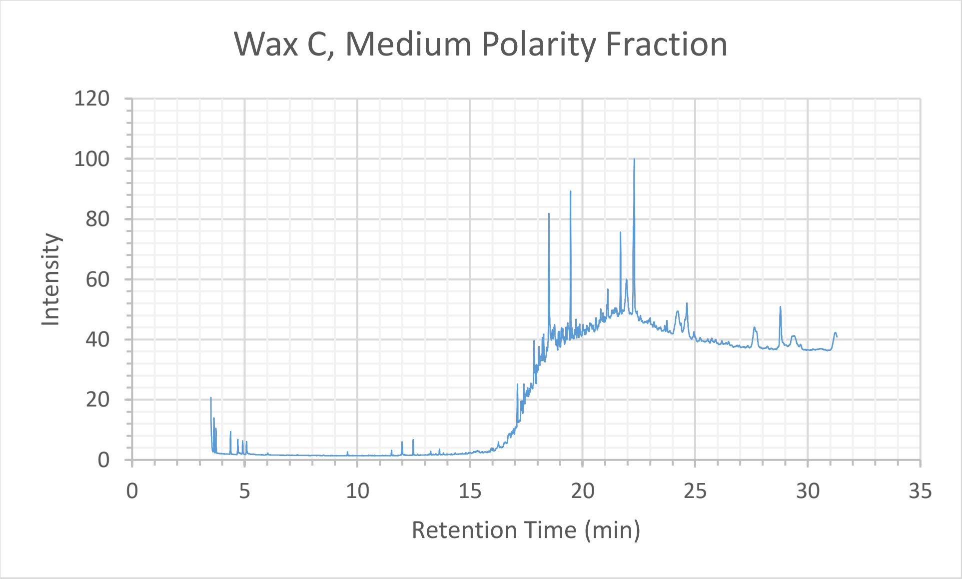
Wax C, Medium Polarity Fraction
Intensity
120
100
80
60
40
20
0
0
5
10
15
20
25
30
35
Retention Time (min)

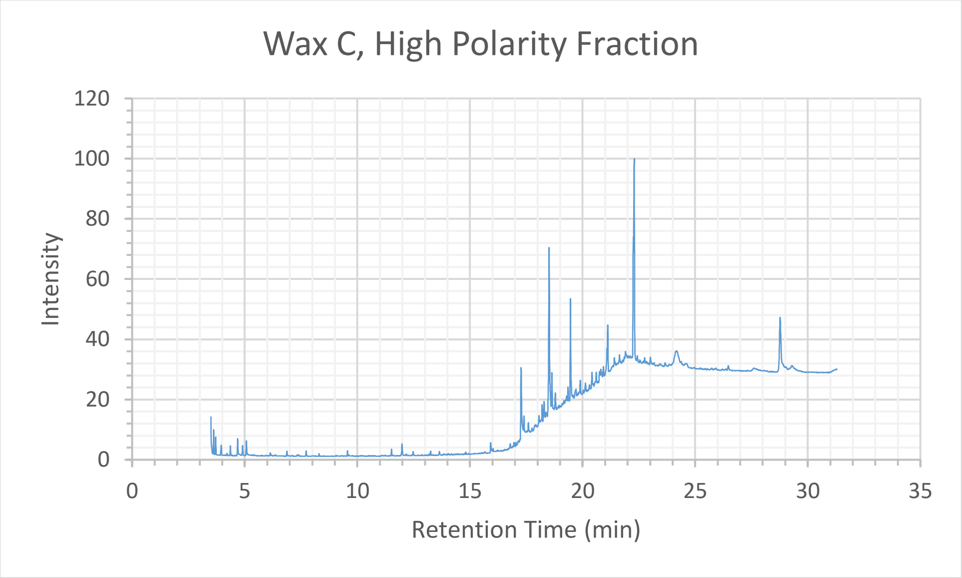

2.2.3. Solvent Extraction

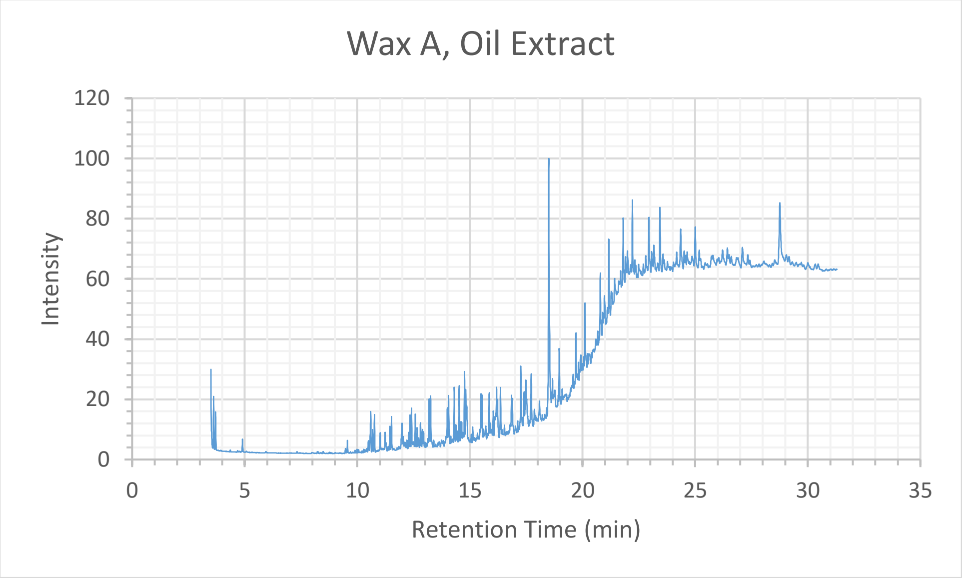

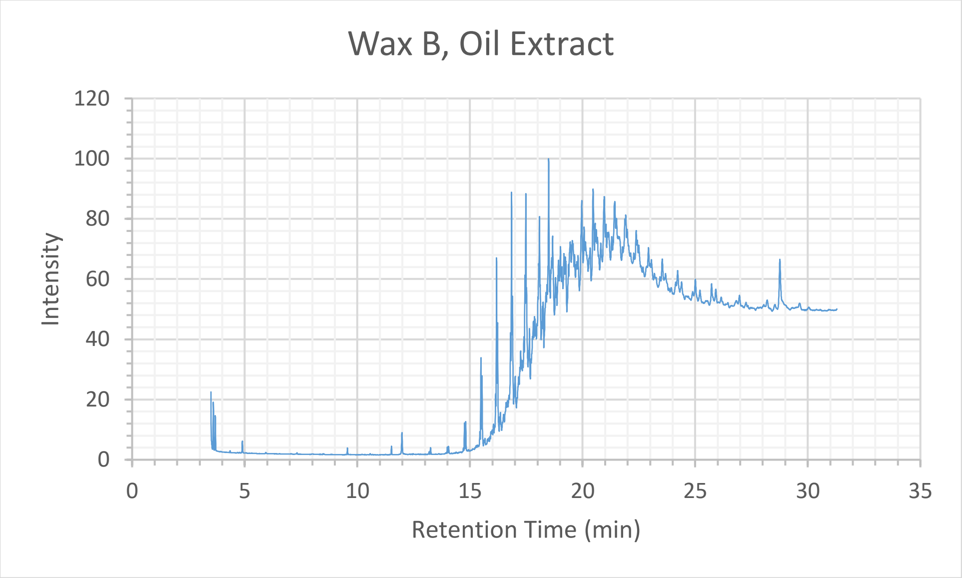
Wax B, Oil Extract
Intensity
Retention Time (min)
0
20
40
60
80
100
120
0
5
10
15
20
25
30
35

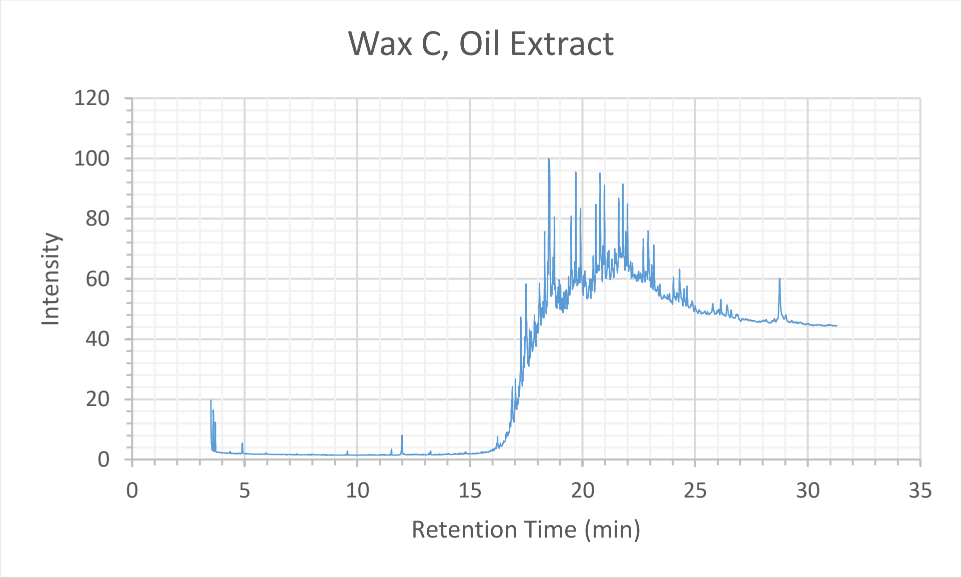
Wax C, Oil Extract
Intensity
Retention Time (min)
0
20
40
60
80
100
120
0
5
10
15
20
25
30
35

2.2.4. Urea Clathrate Formation

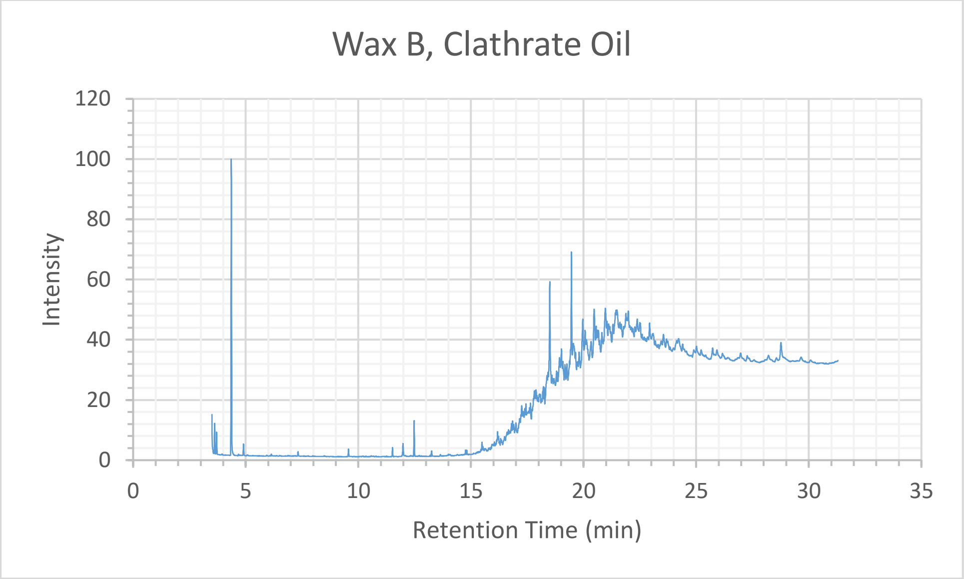

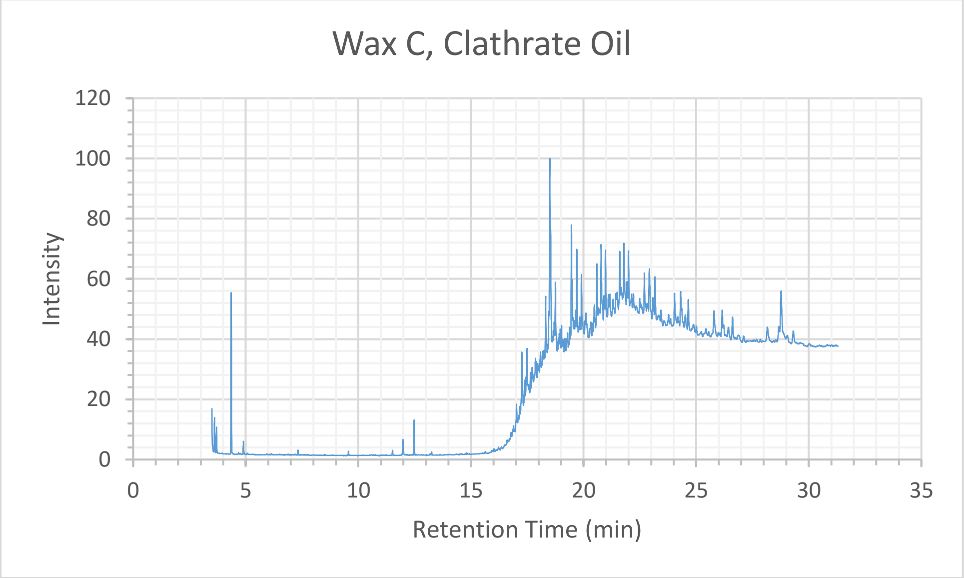

Appendix C: GC-MS and ICP Raw and Processed Data Tables

1. Headspace GC-MS
    1.1. Crude wax A

Peak	SI	Name	Mol.Weight	Mol.Form	Retention Index
1	94	2-Methyl-1-pentene	84	C_6H_{12}	585
2	96	4-Methylheptane	114	C_8H_{18}	752
3	92	Trans-1,1,3,4-Tetramethylcyclopentane	126	C_9H_{18}	856
4	98	2,4-Dimethyl-1-heptene	126	C_9H_{18}	819
5	97	1,3,5-Trimethylcyclohexane	126	C_9H_{18}	903
6	90	(2E,4E)-6,6-Dimethyl-2,4-heptadiene	124	C_9H_{16}	847
9	95	1-Butyl-2-ethylcyclobutane	140	$C_{10}H_{20}$	999
10	95	n-Decane	142	$C_{10}H_{22}$	1015
11	94	3,3,5-Trimethylheptane	142	$C_{10}H_{22}$	867
12	94	3,3,5-Trimethylheptane	142	$C_{10}H_{22}$	867
17	96	1-Undecene	154	$C_{11}H_{22}$	1105
18	96	n-Undecane	156	$C_{11}H_{24}$	1115
22	93	Z-8-Dodecen-1-ol	184	$C_{12}H_{24}O$	1465
23	94	1-Tetradecene	196	$C_{14}H_{28}$	1403
24	95	n-Dodecane	170	$C_{12}H_{26}$	1214
28	90	1-Hexadecyne	222	$C_{16}H_{30}$	1609
29	95	1-Tetradecene	196	$C_{14}H_{28}$	1403
36	92	1,13-Tetradecadiene	194	$C_{14}H_{26}$	1393
37	95	1-Tetradecanol	214	$C_{14}H_{30}O$	1656
38	95	n-Tetradecane	198	$C_{14}H_{30}$	1413
39	91	cis-9-Octadecen-1-ol	268	$C_{18}H_{36}O$	2061
40	95	1-Pentadecanol	228	$C_{15}H_{32}O$	1755
41	95	n-Heptadecane	240	$C_{17}H_{36}$	1711
43	93	1-Hexadecanol	242	$C_{16}H_{34}O$	1854

1.2. Crude Wax B

Peak	SI	Name	Mol.Weight	Mol.Form	Retention Index
6	92	2-Methyl-1-pentene	84	C_6H_{12}	585
8	93	1-Hexene	84	C_6H_{12}	608
15	91	1,2-Dimethylcyclopentane	98	C_7H_{14}	722
16	91	1,2-Dimethylcyclopentane	98	C_7H_{14}	722
18	94	Toluene	92	C_7H_8	794
19	90	1,3,5,7-Cyclooctatetraene	104	C_8H_8	888
20	91	1-Nonene	126	C_9H_{18}	906
27	91	n-Heptadecane	240	$C_{17}H_{36}$	1711
28	92	1-Nonadecene	266	$C_{19}H_{38}$	1900
29	95	n-Heptadecane	240	$C_{17}H_{36}$	1711
30	94	1-Nonadecene	266	$C_{19}H_{38}$	1900
31	95	n-Heptadecane	240	$C_{17}H_{36}$	1711
33	93	n-Heneicosane	296	$C_{21}H_{44}$	2109

1.3. Crude Wax C

Peak	SI	Name	Mol.Weight	Mol.Form	Retention Index
6	95	2,4-Dimethyl-1-heptene	126	C_9H_{18}	819
20	92	n-Undecane	156	$C_{11}H_{24}$	1115
27	94	n-Dodecane	170	$C_{12}H_{26}$	1214

2. GC-MS Analysis of Fractions and Extracts Containing Impurities

2.1. Chloroform Blank

Peak	SI	Name	Mol.Weight	Mol.Form	Retention Index
1	97	Dibromomethane	172	CH_2Br_2	0
2	97	Bromodichloromethane	162	$CHBrCl_2$	0
3	93	2-Hexanol	102	$C_6H_{14}O$	780

4	96	Pentadecane	212	$C_{15}H_{32}$	1512
5	96	Tetradecane	198	$C_{14}H_{30}$	1413
6	95	Dimethyl phthalate	194	$C_{10}H_{10}O_4$	1440
7	95	Heneicosane	296	$C_{21}H_{44}$	2109
8	91	9-Octadecenamide	281	$C_{18}H_{35}NO$	2228
9	92	Octadecanamide	283	$C_{18}H_{37}NO$	2220
10	92	9-Octadecenamide	281	$C_{18}H_{35}NO$	2228
11	92	Octadecanamide	283	$C_{18}H_{37}NO$	2220

2.2. Liquid Chromatography

2.2.1.Wax A Medium Polarity Fraction

Peak	SI	Name	Mol.Weight	Mol.Form	Retention Index
1	97	Dibromomethane	172	CH_2Br_2	0
2	97	Bromodichloromethane	162	$CHBrCl_2$	0
4	97	Toluene	92	C_7H_8	794
6	93	2-Hexanol	102	$C_6H_{14}O$	780
8	94	Benzaldehyde	106	C_7H_6O	982
9	95	Dodecane	170	$C_{12}H_{26}$	1214
10	94	Pentamethylbenzene	148	$C_{11}H_{16}$	1246
12	95	1-Methylnaphthalene	142	$C_{11}H_{10}$	1345
14	97	1-Methylnaphthalene	142	$C_{11}H_{10}$	1345
16	90	1-Tetradecene	196	$C_{14}H_{28}$	1403
17	96	Tetradecane	198	$C_{14}H_{30}$	1413
19	96	2,6-Dimethylnaphthalene	156	$C_{12}H_{12}$	1458
20	96	1,3-Dimethylnaphthalene	156	$C_{12}H_{12}$	1458
21	95	2,6-Dimethylnaphthalene	156	$C_{12}H_{12}$	1458
22	95	Dimethyl phthalate	194	$C_{10}H_{10}O_4$	1440
24	92	1,3-Dimethylnaphthalene	156	$C_{12}H_{12}$	1458
26	95	n-Pentadecanol	228	$C_{15}H_{32}O$	1755
28	94	2,4-Di-tert-butylphenol	206	$C_{14}H_{22}O$	1555
31	95	n-Heneicosane	296	$C_{21}H_{44}$	2109
34	95	Heneicosane	296	$C_{21}H_{44}$	2109
35	94	n-Hexadecanoic acid methyl ester	270	$C_{17}H_{34}O_2$	1878
38	90	(9Z,12Z)-9,12-Octadecadien-1-ol	266	$C_{18}H_{34}O$	2069
39	93	9-Octadecenoic acid, methyl ester, (E)-	296	$C_{19}H_{36}O_2$	2085
41	92	Methyl stearate	298	$C_{19}H_{38}O_2$	2077
42	91	9-Octadecenamide, (Z)-	281	$C_{18}H_{35}NO$	2228
43	92	Hexadecanamide	255	$C_{16}H_{33}NO$	2021

47	91	9-Octadecenamide, (Z)-	281	$C_{18}H_{35}NO$	2228
51	95	Phthalic acid, di(2-propylpentyl) ester	390	$C_{24}H_{38}O4$	2704
69	90	Tetrapentacontane	758	$C_{54}H_{110}$	5389
72	90	Hexacontane	842	$C_{60}H_{122}$	5985

2.2.2.Wax A High Polarity Fraction

Peak	SI	Name	Mol.Weight	Mol.Form	Retention Index
1	97	Dibromomethane	172	CH_2Br_2	0
2	97	Bromodichloromethane	162	$CHBrCl_2$	0
3	96	2-Pentanol, 2-methyl-	102	$C_6H_{14}O$	709
5	96	Toluene	92	C_7H_8	794
10	93	2-Hexanol, (R)-	102	$C_6H_{14}O$	780
15	96	Benzaldehyde	106	C_7H_6O	982
16	95	Ethane, pentachloro-	200	C_2HCl_5	953
17	95	Benzyl alcohol	108	C_7H_8O	1036
18	96	Ethane, hexachloro-	234	C_2Cl_6	995
19	95	Tetradecane	198	$C_{14}H_{30}$	1413
21	93	Phenol, 3-(1-methylethyl)-	136	$C_9H_{12}O$	1149
22	93	1-Tetradecene	196	$C_{14}H_{28}$	1403
26	90	1-Heptanol, 2,4-diethyl-	172	$C_{11}H_{24}O$	1229
27	90	Ethanol, 2-(2-butoxyethoxy)-, acetate	204	$C_{10}H_{20}O_4$	1334
31	90	1,13-Tetradecadiene	194	$C_{14}H_{26}$	1393
32	96	1-Pentadecene	210	$C_{15}H_{30}$	1502
33	95	Tetradecane	198	$C_{14}H_{30}$	1413
37	93	Dimethyl phthalate	194	$C_{10}H_{10}O_4$	1440
40	90	Dodecane, 4,6-dimethyl-	198	$C_{14}H_{30}$	1285
42	96	1-Tetradecanol	214	$C_{14}H_{30}O$	1656
43	95	Heneicosane	296	$C_{21}H_{44}$	2109
56	96	Heneicosane	296	$C_{21}H_{44}$	2109
57	91	Benzenesulfonamide, 2-methyl-	171	$C_7H_9NO_2S$	1557
60	92	1-Tetradecanol	214	$C_{14}H_{30}O$	1656
62	91	Heneicosane	296	$C_{21}H_{44}$	2109
63	90	Ethanol, 2-(dodecyloxy)-	230	$C_{14}H_{30}O_2$	1731
68	91	Nonadecyl trifluoroacetate	380	$C_{21}H_{39}F_3O_2$	2110
69	94	Heneicosane	296	$C_{21}H_{44}$	2109
70	92	n-Pentadecanol	228	$C_{15}H_{32}O$	1755
75	91	l-(+)-Ascorbic acid 2,6-dihexadecanoate	652	$C_{38}H_{68}O_8$	4765
76	91	Tetradecanamide	227	$C_{14}H2_9NO$	1822
78	92	Heneicosane	296	$C_{21}H_{44}$	2109
83	93	1-Heptacosanol	396	$C_{27}H_{56}O$	2948
84	91	Heneicosane	296	$C_{21}H_{44}$	2109
87	90	9-Octadecenamide, (Z)-	281	$C_{18}H_{35}NO$	2228
88	94	1,2-Ethanediol, dibenzoate	270	$C_{16}H_{14}O_4$	2099
89	92	Hexadecanamide	255	$C_{16}H_{33}NO$	2021
91	90	Heneicosane	296	$C_{21}H_{44}$	2109
96	91	1-Heptacosanol	396	$C_{27}H_{56}O$	2948
100	90	9-Octadecenamide, (Z)-	281	$C_{18}H_{35}NO$	2228

108	91	Dotriacontane	450	$C_{32}H_{66}$	3202
109	96	Phthalic acid, di(2-propylpentyl) ester	390	$C_{24}H_{38}O_4$	2704
114	92	Tetrapentacontane	758	$C_{54}H_{110}$	5389
125	91	Tetrapentacontane	758	$C_{54}H_{110}$	5389
128	91	Tetrapentacontane	758	$C_{54}H_{110}$	5389
135	91	Hexacontane	842	$C_{60}H_{122}$	5985
137	90	Hexacontane	842	$C_{60}H_{122}$	5985
143	91	Tetrapentacontane	758	$C_{54}H_{110}$	5389
146	91	Hexacontane	842	$C_{60}H_{122}$	5985
147	91	Hexacontane	842	$C_{60}H_{122}$	5985
150	91	Hexacontane	842	$C_{60}H_{122}$	5985

2.2.3.Wax B Medium Polarity Fraction

Peak	SI	Name	Mol.Weight	Mol.Form	Retention Index
1	96	Methane, dibromo-	172	CH_2Br_2	0
2	97	Methane, bromodichloro-	162	$CHBrCl_2$	0
4	97	Toluene	92	C_7H_8	794
6	93	2-Hexanol, (R)-	102	$C_6H_{14}O$	780
8	96	Tetradecane $$ n-Tetradecane $$	198	$C_{14}H_{30}$	1413
10	97	Tetradecane	198	$C_{14}H_{30}$	1413
11	95	Dimethyl phthalate	194	$C_{10}H_{10}O_4$	1440
13	95	Phenol, 2,4-bis(1,1-dimethylethyl)-	206	$C_{14}H_{22}O$	1555
14	95	Heptadecane	240	$C_{17}H_{36}$	1711
17	96	Heneicosane	296	$C_{21}H_{44}$	2109
42	94	Fluoranthene	202	$C_{16}H_{10}$	1802
55	92	Pyrene, 1-methyl-	216	$C_{17}H_{12}$	2097
56	92	Pyrene, 1-methyl-	216	$C_{17}H_{12}$	2097
59	91	9-Octadecenamide, (Z)-	281	$C_{18}H_{35}NO$	2228
75	96	Phthalic acid, di(2-propylpentyl) ester	390	$C_{24}H_{38}O_4$	2704
101	90	Tetrapentacontane	758	$C_{54}H_{110}$	5389
103	94	Perylene	252	$C_{20}H_{12}$	2353
104	90	Benzo[k]fluoranthene	252	$C_{20}H_{12}$	2353
117	90	Tetrapentacontane	758	$C_{54}H_{110}$	5389
121	93	Indeno[1,2,3-cd]pyrene	276	$C_{22}H_{12}$	2677
125	92	Indeno[1,2,3-cd]pyrene	276	$C_{22}H_{12}$	2677
127	90	Hexacontane	842	$C_{60}H_{122}$	5985
136	91	Tetrapentacontane	758	$C_{54}H_{110}$	5389
140	91	Tetrapentacontane	758	$C_{54}H_{110}$	5389
142	91	Hexacontane	842	$C_{60}H_{122}$	5985
146	92	Hexacontane	842	$C_{60}H_{122}$	5985

2.2.4.Wax B High Polarity Fraction

Peak	SI	Name	Mol.Weight	Mol.Form	Retention Index
1	97	Methane, dibromo-	172	CH_2Br_2	0
2	96	Methane, bromodichloro-	162	$CHBrCl_2$	0
3	96	2-Pentanol, 2-methyl-	102	$C_6H_{14}O$	709
4	95	3-Pentanol, 3-methyl-	102	$C_6H_{14}O$	709
5	97	Toluene	92	C_7H_8	794
10	92	2-Hexanol, (R)-	102	$C_6H_{14}O$	780
11	90	2-Pentanone, 4-hydroxy-	102	$C_5H_{10}O_2$	817
13	93	2-Pentanone, 4-hydroxy-4-methyl-	116	$C_6H_{12}O_2$	845
18	97	Hexylene glycol	118	$C_6H_{14}O_2$	872
22	97	Benzaldehyde	106	C_7H_6O	982
24	94	Ethane, pentachloro-	200	C_2HCl_5	953
25	90	6-Methylheptane-1,6-diol	146	$C_8H_{18}O_2$	1151
26	94	Benzyl alcohol	108	C_7H_8O	1036
29	96	Ethane, hexachloro-	234	C_2Cl_6	995
30	95	Nonanal	142	$C_9H_{18}O$	1104
31	90	Propane, 1,1,2,3,3-pentachloro-	214	$C_3H_3Cl_5$	1151
36	93	Ethanol, 2-phenoxy-	138	$C_8H_{10}O_2$	1212
44	94	Tetradecane	198	$C_{14}H_{30}$	1413
45	93	Dodecanal	184	$C_{12}H_{24}O$	1402
46	93	Nonanoic acid, 9-oxo-, methyl ester	186	$C_{10}H_{18}O_3$	1371
50	92	Phenol, 2,4-bis(1,1-dimethylethyl)-	206	$C_{14}H_{22}O$	1555
51	91	Heptadecanal	254	$C_{17}H_{34}O$	1899
53	92	Propanoic acid, 2-methyl-, 1-(1,1-dimethylethyl)-2-methyl-1,3-propanediyl ester	286	$C_{16}H_{30}O_4$	1605
54	96	Heneicosane	296	$C_{21}H_{44}$	2109
55	95	Tetradecanal	212	$C_{14}H_{28}O$	1601
58	92	1-Tetradecanol	214	$C_{14}H_{30}O$	1656
64	91	2,6-Diisopropylnaphthalene	212	$C_{16}H_{2}0$	1727
68	94	Heneicosane	296	$C_{21}H_{44}$	2109
69	92	Hexadecanal	240	$C_{16}H_{32}O$	1800
71	95	Phthalic acid, hex-3-yl isobutyl ester	306	$C_{18}H_{26}O_4$	2107
78	90	Tetradecanamide	227	$C_{14}H_{29}NO$	1822
79	90	Nonadecyl pentafluoropropionate	430	$C_{22}H_{39}F_5O_2$	2071
80	90	Heneicosane	296	$C_{21}H_{44}$	2109
81	91	Pentadecanal-	226	$C_{15}H_{30}O$	1701
84	94	n-Nonadecanol-1	284	$C_{19}H_{40}O$	2153
85	90	1-Heptacosanol	396	$C_{27}H_{56}O$	2948
91	91	Hexadecanamide	255	$C_{16}H_{33}NO$	2021
93	90	Eicosyl trifluoroacetate	394	$C_{22}H_{41}F_3O_2$	2210
107	90	9-Octadecenamide, (Z)-	281	$C_{18}H_{35}NO$	2228

119	96	Phthalic acid, di(2-propylpentyl) ester	390	$C_{24}H_{38}O_4$	2704
130	90	Tetrapentacontane, 1,54-dibromo-	914	$C_{54}H_{108}Br_2$	5981
144	92	1-Heptacosanol	396	$C_{27}H_{56}O$	2948
150	92	Tetrapentacontane	758	$C_{54}H_{110}$	5389
163	90	Hexacontane	842	$C_{60}H_{122}$	5985
172	90	Hexacontane	842	$C_{60}H_{122}$	5985
175	90	Tetrapentacontane	758	$C_{54}H_{110}$	5389
176	91	Hexacontane	842	$C_{60}H_{122}$	5985
179	91	Hexacontane	842	$C_{60}H_{122}$	5985

2.2.5.Wax C Medium Polarity Fraction

Peak	SI	Name	Mol.Weight	Mol.Form	Retention Index
1	96	Methane, dibromo-	172	CH_2Br_2	0
2	97	Methane, bromodichloro-	162	$CHBrCl_2$	0
3	97	Toluene	92	C_7H_8	794
5	92	2-Hexanol, (R)-	102	$C_6H_{14}O$	780
7	93	Cyclohexanone	98	$C_6H_{10}O$	891
8	95	Tetradecane	198	$C_{14}H_{30}$	1413
9	95	Tetradecane	198	$C_{14}H_{30}$	1413
10	95	Dimethyl phthalate	194	$C_{10}H_{10}O_4$	1440
11	94	Phenol, 2,4-bis(1,1-dimethylethyl)-	206	$C_{14}H_{22}O$	1555
12	94	Heneicosane	296	$C_{21}H_{44}$	2109
15	90	Heneicosane	296	$C_{21}H_{44}$	2109
20	90	9,10-Bis(bromomethyl)anthracene	362	$C_{16}H_{12}Br_2$	2601
29	92	4H-Benz[de]anthracene, 5,6-dihydro-	218	$C_{17}H_{14}$	2026
33	95	Fluoranthene	202	$C_{16}H_{10}$	1802
47	92	Pyrene, 1-methyl-	216	$C_{17}H_{12}$	2097
48	92	Pyrene, 1-methyl-	216	$C_{17}H_{12}$	2097
50	90	9-Octadecenamide, (Z)-	281	$C_{18}H_{35}NO$	2228
55	90	Pyrene, 1,3-dimethyl-	230	$C_{18}H_{14}$	2210
56	90	Pyrene, 1,3-dimethyl-	230	$C_{18}H_{14}$	2210
64	96	Phthalic acid, di(2-propylpentyl) ester	390	$C_{24}H_{38}O_4$	2704
95	93	Perylene	252	$C_{20}H_{12}$	2353
98	95	Benzene, 1,3,5-triphenyl-	306	$C_{24}H_{18}$	2741
115	93	Indeno[1,2,3-cd]pyrene	276	$C_{22}H_{12}$	2677
119	91	Hexacontane	842	$C_{60}H_{122}$	5985
130	91	Hexacontane	842	$C_{60}H_{122}$	5985
134	91	Hexacontane	842	$C_{60}H_{122}$	5985

2.2.6.Wax C High Polarity Fraction

Peak	SI	Name	Mol.Weight	Mol.Form	Retention Index
1	96	Methane, dibromo-	172	CH_2Br_2	0
2	97	Methane, bromodichloro-	162	$CHBrC_{l2}$	0
3	97	Toluene	92	C_7H_8	794
5	92	2-Hexanol, (R)-	102	$C_6H_{14}O$	780
7	93	Cyclohexanone	98	$C_6H_{10}O$	891
8	95	Tetradecane	198	$C_{14}H_{30}$	1413
9	95	Tetradecane	198	$C_{14}H_{30}$	1413
10	95	Dimethyl phthalate	194	$C_{10}H_{10}O_4$	1440
11	94	Phenol, 2,4-bis(1,1-dimethylethyl)-	206	$C_{14}H_{22}O$	1555
12	94	Heneicosane	296	$C_{21}H_{44}$	2109
15	90	Heneicosane	296	$C_{21}H_{44}$	2109
20	90	9,10-Bis(bromomethyl)anthracene	362	$C_{16}H_{12}Br_2$	2601
29	92	4H-Benz[de]anthracene, 5,6-dihydro-	218	$C_{17}H_{14}$	2026
33	95	Fluoranthene	202	$C_{16}H_{10}$	1802
47	92	Pyrene, 1-methyl-	216	$C_{17}H_{12}$	2097
48	92	Pyrene, 1-methyl-	216	$C_{17}H_{12}$	2097
50	90	9-Octadecenamide, (Z)-	281	$C_{18}H_{35}NO$	2228
55	90	Pyrene, 1,3-dimethyl-	230	$C_{18}H_{14}$	2210
56	90	Pyrene, 1,3-dimethyl-	230	$C_{18}H_{14}$	2210
64	96	Phthalic acid, di(2-propylpentyl) ester	390	$C_{24}H_{38}O_4$	2704
95	93	Perylene	252	$C_{20}H_{12}$	2353
98	95	Benzene, 1,3,5-triphenyl-	306	$C_{24}H_{18}$	2741
115	93	Indeno[1,2,3-cd]pyrene	276	$C_{22}H_{12}$	2677
119	91	Hexacontane	842	$C_{60}H_{122}$	5985
130	91	Hexacontane	842	$C_{60}H_{122}$	5985
134	91	Hexacontane	842	$C_{60}H_{122}$	5985

2.3. Solvent Extraction

2.3.1. Wax A Oil Extract

Peak	SI	Name	Mol.Weight	Mol.Form	Retention Index
4	95	1-Dodecanol	186	$C_{12}H_{26}O$	1457
4	95	1-Dodecene	168	$C_{12}H_{24}$	1204
4	95	1-Undecanol	172	$C_{11}H_{24}O$	1357
5	96	Tridecane	184	$C_{13}H_{28}$	1313
5	96	Dodecane	170	$C_{12}H_{26}$	1214
5	96	Dodecane	170	$C_{12}H_{26}$	1214
6	90	Dodecane, 4,6-dimethyl-	198	$C_{14}H_{30}$	1285
7	92	Dodecane, 4,6-dimethyl-	198	$C_{14}H_{30}$	1285
7	91	Decane, 3,3,6-trimethyl-	184	$C_{13}H_{28}$	1165
7	91	Decane, 2,8,8-trimethyl-	184	$C_{13}H_{28}$	1165
8	91	Dodecane, 4,6-dimethyl-	198	$C_{14}H_{30}$	1285
8	91	Decane, 3,3,6-trimethyl-	184	$C_{13}H_{28}$	1165
10	96	1-Tetradecene $$ n-Tetradec-1-ene	196	$C_{14}H_{28}$	1403
10	96	1-Tridecene	182	$C_{13}H_{26}$	1304
10	96	3-Hexadecene, (Z)-	224	$C_{16}H_{32}$	1620
17	96	1-Pentadecene	210	$C_{15}H_{30}$	1502
17	96	1-Tetradecene	196	$C_{14}H_{28}$	1403
17	95	3-Octadecene, (E)-	252	$C_{18}H_{36}$	1818
18	97	Tetradecane	198	$C_{14}H_{30}$	1413
18	97	Tetradecane	198	$C_{14}H_{30}$	1413
18	96	Pentadecane	212	$C_{15}H_{32}$	1512
19	93	Dimethyl phthalate	194	$C_{10}H_{10}O_4$	1440
19	92	Dimethyl phthalate	194	$C_{10}H_{10}O_4$	1440

19	91	Dimethyl phthalate	194	$C_{10}H_{10}O_4$	1440
20	91	Dodecane, 4,6-dimethyl-	198	$C_{14}H_{30}$	1285
20	90	Heneicosane	296	$C_{21}H_{44}$	2109
22	91	Dodecane, 4,6-dimethyl-	198	$C_{14}H_{30}$	1285
22	90	Decane, 2,8,8-trimethyl-	184	$C_{13}H_{28}$	1165
23	90	1-Decanol, 2-hexyl-	242	$C_{16}H_{34}O$	1790
24	96	1-Tetradecanol	214	$C_{14}H_{30}O$	1656
24	96	1-Heptadecene	238	$C_{17}H_{34}$	1701
24	96	1-Pentadecene	210	$C_{15}H_{30}$	1502
25	96	Heneicosane	296	$C_{21}H_{44}$	2109
25	96	Heptadecane	240	$C_{17}H_{36}$	1711
25	95	Nonadecane	268	$C_{19}H_{40}$	1910
29	90	1-Dodecanol, 2-hexyl-	270	$C_{18}H_{38}O$	1989
29	90	1-Decanol, 2-hexyl-	242	$C_{16}H_{34}O$	1790
29	90	Octacosyl trifluoroacetate	506	$C_{30}H_{57}F_3O_2$	3005
35	93	9-Octadecen-1-ol, (Z)-	268	$C_{18}H_{36}O$	2061
35	92	1,19-Eicosadiene	278	$C_{20}H_{38}$	1989
35	91	(R)-(-)-(Z)-14-Methyl-8-hexadecen-1-ol	254	$C_{17}H_{34}O$	1898
36	92	1-Hexadecanol	242	$C_{16}H_{34}O$	1854
36	92	1-Hexadecanol	242	$C_{16}H_{34}O$	1854
36	92	n-Heptadecanol-1	256	$C_{17}H_{36}O$	1954
37	96	Heneicosane	296	$C_{21}H_{44}$	2109
37	95	Heptadecane	240	$C_{17}H_{36}$	1711
37	95	Heptadecane	240	$C_{17}H_{36}$	1711
47	95	n-Pentadecanol	228	$C_{15}H_{32}O$	1755
47	94	1-Tetradecanol	214	$C_{14}H_{30}O$	1656
47	94	n-Heptadecanol-1	256	$C_{17}H_{36}O$	1954
48	96	Heneicosane	296	$C_{21}H_{44}$	2109
48	96	Heptadecane	240	$C_{17}H_{36}$	1711

48	95	Eicosane	282	$C_{20}H_{42}$	2009
58	94	Nonadecyl pentafluoropropionate	430	$C_{22}H_{39}F_5O_2$	2071
58	94	Eicosyl trifluoroacetate	394	$C_{22}H_{41}F_3O_2$	2210
58	94	Heneicosyl trifluoroacetate	408	$C_{23}H_{43}F_3O_2$	2309
59	94	Heneicosane	296	$C_{21}H_{44}$	2109
59	94	Octadecane	254	$C_{18}H_{38}$	1810
59	94	Heneicosane	296	$C_{21}H_{44}$	2109
63	90	1-Decanol, 2-hexyl-	242	$C_{16}H_{34}O$	1790
69	91	9-Octadecen-1-ol, (Z)-	268	$C_{18}H_{36}O$	2061
69	91	9-Octadecen-1-ol, (Z)-	268	$C_{18}H_{36}O$	2061
69	91	1,19-Eicosadiene	278	$C_{20}H_{38}$	1989
70	94	1-Nonadecene	266	$C_{19}H_{38}$	1900
70	94	n-Pentadecanol	228	$C_{15}H_{32}O$	1755
70	94	n-Nonadecanol-1	284	$C_{19}H_{40}O$	2153
71	94	Heneicosane	296	$C_{21}H_{44}$	2109
71	94	Eicosane	282	$C_{20}H_{42}$	2009
71	93	Heneicosane	296	$C_{21}H_{44}$	2109
82	94	1-Nonadecene	266	$C_{19}H_{38}$	1900
82	94	Behenic alcohol	326	$C_{22}H_{46}O$	2451
82	93	1-Heptacosanol	396	$C_{27}H_{56}O$	2948
83	92	Heneicosane	296	$C_{21}H_{44}$	2109
83	92	Heneicosane	296	$C_{21}H_{44}$	2109
83	92	Octadecane	254	$C_{18}H_{38}$	1810
90	91	(Z)-14-Tricosenyl formate	366	$C_{24}H_{46}O_2$	2679
90	90	9-Octadecen-1-ol, (Z)-	268	$C_{18}H_{36}O$	2061
90	90	Oleyl alcohol, trifluoroacetate	364	$C_{20}H_{35}F_3O_2$	2019
91	94	1-Heptacosanol	396	$C_{27}H_{56}O$	2948
91	94	Behenic alcohol	326	$C_{22}H_{46}O$	2451
91	94	9-Tricosene, (Z)-	322	$C_{23}H_{46}$	2315

108	93	Nonadecyl heptafluorobutyrate	480	$C_{23}H_{39}F_7O_2$	2032
108	93	Nonadecyl pentafluoropropionate	430	$C_{22}H_{39}F_5O_2$	2071
108	93	Docosyl heptafluorobutyrate	522	$C_{26}H_{45}F_7O_2$	2330

2.3.2.Wax B Oil Extract

Peak	SI	Name	Mol.Weight	Mol.Form	Retention Index
3	93	2-Hexanol, (R)-	102	$C_6H_{14}O$	780
4	96	Pentadecane	212	$C_{15}H_{32}$	1512
5	97	Tetradecane	198	$C_{14}H_{30}$	1413
6	96	Dimethyl phthalate	194	$C_{10}H_{10}O_4$	1440
7	96	Heneicosane	296	$C_{21}H_{44}$	2109
8	96	1-Nonadecene	266	$C_{19}H_{38}$	1900
9	96	Heneicosane	296	$C_{21}H_{44}$	2109
10	94	9-Octadecen-1-ol, (Z)-	268	$C_{18}H_{36}O$	2061
11	96	1-Nonadecene	266	$C_{19}H_{38}$	1900
12	97	Heneicosane	296	$C_{21}H_{44}$	2109
14	94	1,19-Eicosadiene	278	$C_{20}H_{38}$	1989
15	96	1-Nonadecene	266	$C_{19}H_{38}$	1900
16	95	Heneicosane	296	$C_{21}H_{44}$	2109
17	90	Oleyl alcohol, trifluoroacetate	364	$C_{20}H_{35}F_3O_2$	2019
18	95	Nonadecyl trifluoroacetate	380	$C_{21}H_{39}F_3O_2$	2110
21	90	9-Tricosene, (Z)-	322	$C_{23}H_{46}$	2315
24	90	17-Pentatriacontene	490	$C_{35}H_{70}$	3508
25	90	Cyclohexane, nonadecyl-	350	$C_{25}H_{50}$	2570
26	94	9-Octadecen-1-ol, (Z)-	268	$C_{18}H_{36}O$	2061
27	94	1-Nonadecene	266	$C_{19}H_{38}$	1900
28	92	Heneicosane	296	$C_{21}H_{44}$	2109

29	90	Octacosanol	410	$C_{28}H_{58}O$	3047
30	93	Eicosyl heptafluorobutyrate	494	$C_{24}H_{41}F_7O_2$	2131
36	93	(Z)-14-Tricosenyl formate	366	$C_{24}H_{46}O_2$	2679
37	91	1-Nonadecene	266	$C_{19}H_{38}$	1900
38	91	Triacontane	422	$C_{30}H_{62}$	3003
39	94	1-Heptacosanol	396	$C_{27}H_{56}O$	2948
47	93	1,16-Hexadecanediol	258	$C_{16}H_{34}O_2$	2097
51	90	1-Eicosene	280	$C_{20}H_{40}$	1999
59	90	(Z)-14-Tricosenyl formate	366	$C_{24}H_{46}O_2$	2679
101	91	Hexacontane	842	$C_{60}H_{122}$	5985
102	90	Hexacontane	842	$C_{60}H_{122}$	5985
106	90	Hexacontane	842	$C_{60}H_{122}$	5985
123	90	Hexacontane	842	$C_{60}H_{122}$	5985
129	90	Hexacontane	842	$C_{60}H_{122}$	5985
135	90	Hexacontane	842	$C_{60}H_{122}$	5985
136	90	Hexacontane	842	$C_{60}H_{122}$	5985
141	90	Hexacontane	842	$C_{60}H_{122}$	5985
149	90	Hexacontane	842	$C_{60}H_{122}$	5985

2.3.3.Wax C Oil Extract

Peak	SI	Name	Mol.Weight	Mol.Form	Retention Index
1	96	Methane, dibromo-	172	CH_2Br_2	0
2	97	Methane, bromodichloro-	162	$CHBrCl_2$	0
3	93	2-Hexanol, (R)-	102	$C_6H_{14}O$	780
4	96	Tridecane	184	$C_{13}H_{28}$	1313
5	97	Tetradecane	198	$C_{14}H_{30}$	1413
6	96	Dimethyl phthalate	194	$C_{10}H_{10}O_4$	1440
7	96	Nonadecane	268	$C_{19}H_{40}$	1910

8	95	1-Nonadecene	266	$C_{19}H_{38}$	1900
9	96	Heneicosane	296	$C_{21}H_{44}$	2109
11	90	n-Tetracosanol-1	354	$C_{24}H_{50}O$	2650
14	92	Eicosane	282	$C_{20}H_{42}$	2009
17	94	1-Heptacosanol	396	$C_{27}H_{56}O$	2948
18	93	Eicosane	282	$C_{20}H_{42}$	2009
96	90	1,1':3',1''-Terphenyl, 5'-phenyl-	306	$C_{24}H_{18}$	2741

2.4. Urea Clathrate Formation

2.4.1.Wax B Clathrate Oil

Peak	SI	Name	Mol.Weight	Mol.Form	Retention Index
1	96	Methane, dibromo-	172	CH_2Br_2	0
2	97	Methane, bromodichloro-	162	$CHBrCl_2$	0
3	97	Toluene	92	C_7H_8	794
5	92	2-Hexanol, (R)-	102	$C_6H_{14}O$	780
7	94	Cyclohexanone	98	$C_6H_{10}O$	891
8	96	Dodecane	170	$C_{12}H_{26}$	1214
9	96	Tetradecane	198	$C_{14}H_{30}$	1413
10	96	Dimethyl phthalate	194	$C_{10}H_{10}O_4$	1440
11	95	Phenol, 2,4-bis(1,1-dimethylethyl)-	206	$C_{14}H_{22}O$	1555
12	95	Heneicosane	296	$C_{21}H_{44}$	2109
14	92	Heneicosane	296	$C_{21}H_{44}$	2109
18	92	Naphthalene, 2-phenyl-	204	$C_{16}H_{12}$	1918
27	91	4H-Benz[de]anthracene, 5,6-dihydro-	218	$C_{17}H_{14}$	2026
31	94	Fluoranthene	202	$C_{16}H_{10}$	1802
38	90	Retene	234	$C_{18}H_{18}$	2144
45	92	Pyrene, 1-methyl-	216	$C_{17}H_{12}$	2097
46	92	Pyrene, 1-methyl-	216	$C_{17}H_{12}$	2097
48	90	9-Octadecenamide, (Z)-	281	$C_{18}H_{35}NO$	2228

54	90	Pyrene, 1,3-dimethyl-	230	$C_{18}H_{14}$	2210
62	96	Phthalic acid, di(2-propylpentyl) ester	390	$C2_{4}H_{38}O_{4}$	2704
92	93	Perylene	252	$C_{20}H_{12}$	2353
95	95	Benzene, 1,3,5-triphenyl-	306	$C_{24}H_{18}$	2741
117	93	Anthanthrene	276	$C_{22}H_{12}$	2859

2.4.2.Wax C Clathrate Oil

Peak	SI	Name	Mol.Weight	Mol.Form	Retention Index
1	97	Methane, dibromo-	172	CH_2Br_2	0
2	97	Methane, bromodichloro-	162	$CHBrCl_2$	0
3	98	Toluene	92	C_7H_8	794
4	93	2-Hexanol, (R)-	102	$C_6H_{14}O$	780
5	95	Undecane	156	$C_{11}H_{24}$	1115
6	96	Dodecane	170	$C_{12}H_{26}$	1214
7	97	Tetradecane	198	$C_{14}H_{30}$	1413
8	96	Dimethyl phthalate	194	$C_{10}H_{10}O_4$	1440
9	95	Phenol, 2,4-bis(1,1-dimethylethyl)-	206	$C_{14}H_{22}O$	1555
10	96	Heneicosane	296	$C_{21}H_{44}$	2109
11	92	Tetradecanamide	227	$C_{14}H_{29}NO$	1822
19	90	Nonadecyl pentafluoropropionate	430	$C_{22}H_{39}F_5O_2$	2071
66	94	Phthalic acid, di(2-propylpentyl) ester	390	$C_{24}H_{38}O_4$	2704

3. ICP

3.1. Raw (Exported) Data

Experiment naming system

The number refers to the experiment and the letter corresponds to which wax it is e.g. 052A refers to wax A purified by liquid chromatography. Only waxes were analysed by ICP, extracts and fractions were not.

Crude wax: 001
Liquid Chromatography: 052
Urea clathrate extraction: 054
Solvent extraction: 057

Label	Element, wavelength (nm)	Measured concentration (ppb)	Calculated concentration (ppm)	Concentration SD
001A	Al 396.152	97.67	62.5	0.21
001A	Ba 455.403	59.93	38.3	0.27
001A	Ca 396.847	1348.7	862.9	15.06
001A	Cd 214.439	2.67	1.7	0.14
001A	Cr 267.716	4.41	2.8	0.11
001A	Cr 283.563	3.23	2.1	0.23
001A	Fe 238.204	97.78	62.6	0.11
001A	K 766.491	238.82	152.8	3.66
001A	Li 460.289	9.49	6.1	3.99
001A	Li 670.783	0.23	0.1	0.09
001A	Mg 279.553	323.93	207.2	0.04
001A	Mn 257.610	6.57	4.2	0.2
001A	Ni 231.604	1.57	1.0	0.48
001A	Pb 220.353	7.62	4.9	0.68
001A	Sr 407.771	2.09	1.3	0.03
001A	Ti 334.941	127.07	81.3	0.28
001A	Ti 336.122	124.7	79.8	0.31
001A	Y 224.303	1	0.6	0.01

001A	Y 371.029	0.99	0.6	0.01
001A	Y 488.368	1	0.6	0.01
001A	Zn 213.857	56.75	36.3	0.74
001B	Al 396.152	57.14	38.9	0.34
001B	Ba 455.403	1.76	1.2	0.03
001B	Ca 396.847	174.07	118.5	0.08
001B	Cd 214.439	-0.25	0	0.05
001B	Cr 267.716	-0.09	0	0.06
001B	Cr 283.563	-1.11	0	0.11
001B	Fe 238.204	51.59	35.1	0.13
001B	K 766.491	109.29	74.4	3.69
001B	Li 460.289	3.92	2.7	1.69
001B	Li 670.783	-0.1	0	0.08
001B	Mg 279.553	56.37	38.4	0.04
001B	Mn 257.610	3.9	2.7	0.16
001B	Ni 231.604	-0.93	0	1.08
001B	Pb 220.353	1.23	0.8	2.55
001B	Sr 407.771	-0.61	0	0.01
001B	Ti 334.941	-8.4	0	0.12
001B	Ti 336.122	-7.76	0	0.07
001B	Y 224.303	1	0.7	0.01
001B	Y 371.029	0.98	0.7	0.01
001B	Y 488.368	0.99	0.7	0.01
001B	Zn 213.857	34.4	23.4	0.11
001C	Al 396.152	69.55	44.4	0.15
001C	Ba 455.403	49.65	31.7	0.12
001C	Ca 396.847	1073.04	685.2	2.85
001C	Cd 214.439	-0.14	0	0.07
001C	Cr 267.716	-1.57	0	0.2
001C	Cr 283.563	-2.59	0	0.1

001C	Fe 238.204	65.12	41.6	0.17
001C	K 766.491	334.73	213.7	3.17
001C	Li 460.289	6.08	3.9	6.9
001C	Li 670.783	0.06	0.0	0.03
001C	Mg 279.553	391.34	249.9	0.58
001C	Mn 257.610	6.42	4.1	0.16
001C	Ni 231.604	-0.6	0	1.21
001C	Pb 220.353	2.17	1.4	2.26
001C	Sr 407.771	3.33	2.1	0.01
001C	Ti 334.941	-8.01	0	0.03
001C	Ti 336.122	-7.29	0	0.02
001C	Y 224.303	1	0.6	0.01
001C	Y 371.029	0.98	0.6	0.01
001C	Y 488.368	1	0.6	0.01
001C	Zn 213.857	54.02	34.5	0.28
040B	Al 396.152	70.72	44.6	0.38
040B	Ba 455.403	4.54	2.9	0.07
040B	Ca 396.847	156.6	98.7	1
040B	Cd 214.439	-0.07	0	0.05
040B	Cr 267.716	-1.07	0	0.13
040B	Cr 283.563	-2.2	0	0.14
040B	Fe 238.204	40.2	25.3	0.39
040B	K 766.491	73.41	46.3	2.97
040B	Li 460.289	15.32	9.7	5.44
040B	Li 670.783	0.13	0.1	0.04
040B	Mg 279.553	64.79	40.8	0.02
040B	Mn 257.610	3.43	2.2	0.22
040B	Ni 231.604	-0.69	0	0.68
040B	Pb 220.353	2.43	1.5	0.22
040B	Sr 407.771	-0.68	0	0

040B	Ti 334.941	-8.92	0	0.01
040B	Ti 336.122	-7.37	0	0.02
040B	Y 224.303	1.01	0.6	0.01
040B	Y 371.029	0.98	0.6	0.01
040B	Y 488.368	1.01	0.6	0.01
040B	Zn 213.857	25.16	15.9	0.32
040C	Al 396.152	81.64	51.1	0.2
040C	Ba 455.403	39.35	24.6	0.05
040C	Ca 396.847	663.8	415.4	3.94
040C	Cd 214.439	-0.1	0	0.07
040C	Cr 267.716	-1.48	0	0.07
040C	Cr 283.563	-3.65	0	0.15
040C	Fe 238.204	43.57	27.3	0.26
040C	K 766.491	247.6	154.9	1.08
040C	Li 460.289	11.7	7.3	10.14
040C	Li 670.783	-0.12	0	0.03
040C	Mg 279.553	257.23	161.0	0.27
040C	Mn 257.610	3.69	2.3	0.07
040C	Ni 231.604	-0.36	0	0.73
040C	Pb 220.353	-0.37	0	0.6
040C	Sr 407.771	1.4	0.9	0.01
040C	Ti 334.941	-9	0	0.04
040C	Ti 336.122	-7.54	0	0.01
040C	Y 224.303	1.01	0.6	0.01
040C	Y 371.029	0.98	0.6	0.01
040C	Y 488.368	1.01	0.6	0.01
040C	Zn 213.857	48.81	30.5	0.2
052A1	Al 396.152	69.53	45.9	0.04
052A1	Ba 455.403	6.06	4.0	0.09
052A1	Ca 396.847	124.21	82.0	1.7

052A1	Cd 214.439	-0.24	0	0.04
052A1	Cr 267.716	-1.2	0	0.1
052A1	Cr 283.563	-3.7	0	0.17
052A1	Fe 238.204	56.84	37.5	0.22
052A1	K 766.491	89.05	58.8	4.31
052A1	Li 460.289	11.59	7.7	1.57
052A1	Li 670.783	-0.47	0	0.08
052A1	Mg 279.553	83.44	55.1	0.17
052A1	Mn 257.610	1.5	1.0	0.06
052A1	Ni 231.604	-1.68	0	0.41
052A1	Pb 220.353	3.31	2.2	2.36
052A1	Sr 407.771	-0.85	0	0.01
052A1	Ti 334.941	-8.89	0	0.01
052A1	Ti 336.122	-7.48	0	0.08
052A1	Y 224.303	1.09	0.7	0.02
052A1	Y 371.029	1.06	0.7	0.02
052A1	Y 488.368	1.09	0.7	0.02
052A1	Zn 213.857	50.96	33.6	2.43
052B1	Al 396.152	51.84	34.2	0.21
052B1	Ba 455.403	1.3	0.9	0.01
052B1	Ca 396.847	70.43	46.5	0.12
052B1	Cd 214.439	-0.22	0	0.04
052B1	Cr 267.716	-1.37	0	0.04
052B1	Cr 283.563	-2.91	0	0.12
052B1	Fe 238.204	33.39	22.0	0.17
052B1	K 766.491	75.15	49.6	3.42
052B1	Li 460.289	6.62	4.4	3.81
052B1	Li 670.783	0.23	0.2	0.05
052B1	Mg 279.553	20.24	13.4	0.02
052B1	Mn 257.610	4.03	2.7	0.2

052B1	Ni 231.604	-0.51	0	0.53
052B1	Pb 220.353	0.8	0.5	1.34
052B1	Sr 407.771	-0.95	0	0
052B1	Ti 334.941	-9.04	0	0.01
052B1	Ti 336.122	-8.21	0	0.04
052B1	Y 224.303	0.99	0.7	0.01
052B1	Y 371.029	0.95	0.6	0.01
052B1	Y 488.368	0.99	0.7	0.01
052B1	Zn 213.857	9.98	6.6	0.1
052C1	Al 396.152	90.24	61.0	0.35
052C1	Ba 455.403	4.1	2.8	0.03
052C1	Ca 396.847	267.27	180.7	0.7
052C1	Cd 214.439	-0.07	0	0.11
052C1	Cr 267.716	-1	0	0.14
052C1	Cr 283.563	-2.47	0	0.12
052C1	Fe 238.204	72.74	49.2	0.28
052C1	K 766.491	115.67	78.2	3.22
052C1	Li 460.289	12.63	8.5	1.74
052C1	Li 670.783	2.7	1.8	0.06
052C1	Mg 279.553	73.64	49.8	0.08
052C1	Mn 257.610	4.3	2.9	0.04
052C1	Ni 231.604	-0.58	0	0.61
052C1	Pb 220.353	3.7	2.5	2.49
052C1	Sr 407.771	-0.11	0	0
052C1	Ti 334.941	-8.81	0	0.02
052C1	Ti 336.122	-8.16	0	0.04
052C1	Y 224.303	0.99	0.7	0.01
052C1	Y 371.029	0.95	0.6	0.01
052C1	Y 488.368	0.99	0.7	0.01
052C1	Zn 213.857	102.07	69.0	0.28

054B1	Al 396.152	78.95	54.5	0.22
054B1	Ba 455.403	2.89	2.0	0.03
054B1	Ca 396.847	160.64	110.9	0.93
054B1	Cd 214.439	-0.19	0	0.11
054B1	Cr 267.716	-1.23	0	0.07
054B1	Cr 283.563	-2.79	0	0.16
054B1	Fe 238.204	43.35	29.9	0.2
054B1	K 766.491	129.31	89.2	4.14
054B1	Li 460.289	11.74	8.1	3.43
054B1	Li 670.783	2.39	1.6	0.09
054B1	Mg 279.553	36.18	25.0	0.16
054B1	Mn 257.610	2.81	1.9	0.4
054B1	Ni 231.604	-1.51	0	0.17
054B1	Pb 220.353	1.31	0.9	1.03
054B1	Sr 407.771	-0.8	0	0
054B1	Ti 334.941	-9	0	0.06
054B1	Ti 336.122	-8.31	0	0.04
054B1	Y 224.303	0.99	0.7	0.01
054B1	Y 371.029	0.95	0.7	0.01
054B1	Y 488.368	0.99	0.7	0.01
054B1	Zn 213.857	31.59	21.8	0.05
054C1	Al 396.152	47.74	31.4	0.23
054C1	Ba 455.403	5.27	3.5	0.03
054C1	Ca 396.847	144.85	95.4	0.47
054C1	Cd 214.439	-0.14	0	0.06
054C1	Cr 267.716	-1.35	0	0.11
054C1	Cr 283.563	-2.88	0	0.06
054C1	Fe 238.204	42.54	28.0	0.13
054C1	K 766.491	89.34	58.8	3.11
054C1	Li 460.289	7.99	5.3	2.73

054C1	Li 670.783	-0.23	0	0.05
054C1	Mg 279.553	72.12	47.5	0.14
054C1	Mn 257.610	6.24	4.1	0.28
054C1	Ni 231.604	-0.89	0	0.76
054C1	Pb 220.353	1.32	0.9	0.83
054C1	Sr 407.771	-0.74	0	0.01
054C1	Ti 334.941	-9.3	0	0.05
054C1	Ti 336.122	-7.76	0	0.06
054C1	Y 224.303	1	0.7	0.01
054C1	Y 371.029	0.95	0.6	0.01
054C1	Y 488.368	1	0.7	0.01
054C1	Zn 213.857	33.96	22.4	0.35
057A1	Al 396.152	94.5	62.5	0.82
057A1	Ba 455.403	40.7	26.9	0.24
057A1	Ca 396.847	668.3	442.3	3.22
057A1	Cd 214.439	-0.02	0	0.07
057A1	Cr 267.716	-1.25	0	0.09
057A1	Cr 283.563	-3.2	0	0.17
057A1	Fe 238.204	56.95	37.7	0.25
057A1	K 766.491	217.36	143.9	2.74
057A1	Li 460.289	7.76	5.1	2.65
057A1	Li 670.783	-0.29	0	0.05
057A1	Mg 279.553	272.65	180.4	0.22
057A1	Mn 257.610	4.03	2.7	0.06
057A1	Ni 231.604	4.81	3.2	0.34
057A1	Pb 220.353	1.12	0.7	0.73
057A1	Sr 407.771	1.29	0.9	0.01
057A1	Ti 334.941	-8.92	0	0.01
057A1	Ti 336.122	-7.64	0	0.02
057A1	Y 224.303	1.05	0.7	0.01

057A1	Y 371.029	1.01	0.7	0.01
057A1	Y 488.368	1.06	0.7	0.01
057A1	Zn 213.857	243.56	161.2	1.17
057B1	Al 396.152	53.23	35.1	0.23
057B1	Ba 455.403	5.14	3.4	0.05
057B1	Ca 396.847	116.39	76.8	0.49
057B1	Cd 214.439	-0.17	0	0.11
057B1	Cr 267.716	-1.39	0	0.16
057B1	Cr 283.563	-3.19	0	0.06
057B1	Fe 238.204	27.85	18.4	0.01
057B1	K 766.491	86.48	57.0	3.12
057B1	Li 460.289	9.99	6.6	2.59
057B1	Li 670.783	0	0	0.05
057B1	Mg 279.553	36.33	24.0	0.01
057B1	Mn 257.610	1.38	0.9	0.14
057B1	Ni 231.604	2.59	1.7	0.93
057B1	Pb 220.353	0.82	0.5	2.51
057B1	Sr 407.771	-0.82	0	0.01
057B1	Ti 334.941	-9.1	0	0.03
057B1	Ti 336.122	-7.98	0	0.08
057B1	Y 224.303	0.99	0.7	0.01
057B1	Y 371.029	0.94	0.6	0.01
057B1	Y 488.368	0.99	0.7	0.01
057B1	Zn 213.857	20.79	13.7	0.03
057C1	Al 396.152	51.2	32.3	0.12
057C1	Ba 455.403	11.1	7.0	0.06
057C1	Ca 396.847	102.69	64.8	1.36
057C1	Cd 214.439	-0.07	0	0.07
057C1	Cr 267.716	0.21	0.1	0.22
057C1	Cr 283.563	-1.59	0	0.08

057C1	Fe 238.204	57.88	36.5	0.16
057C1	K 766.491	356.23	224.9	2
057C1	Li 460.289	10.92	6.9	7.79
057C1	Li 670.783	-0.1	0	0.05
057C1	Mg 279.553	127.7	80.6	0.03
057C1	Mn 257.610	1.14	0.7	0.16
057C1	Ni 231.604	23.39	14.8	1.07
057C1	Pb 220.353	0.29	0.2	0.69
057C1	Sr 407.771	-0.94	0	0
057C1	Ti 334.941	-8.27	0	0.02
057C1	Ti 336.122	-7.22	0	0.03
057C1	Y 224.303	0.99	0.6	0.01
057C1	Y 371.029	0.94	0.6	0.01
057C1	Y 488.368	0.99	0.6	0.01
057C1	Zn 213.857	466.64	294.6	7.89

3.2. Processed Data

3.2.1.Liquid Chromatogrphy

3.2.1.1. Wax A

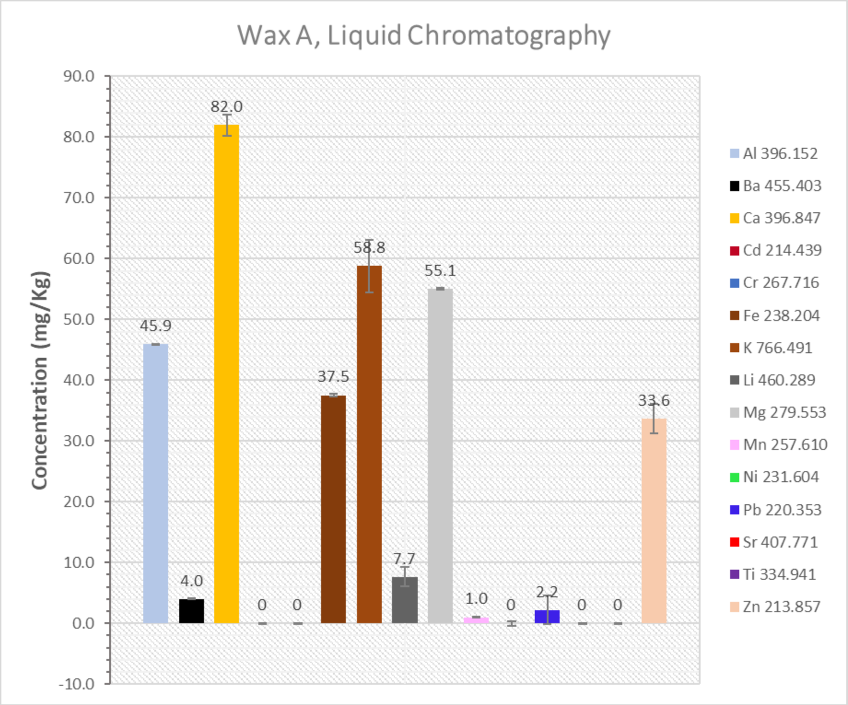

3.2.1.2. Wax B

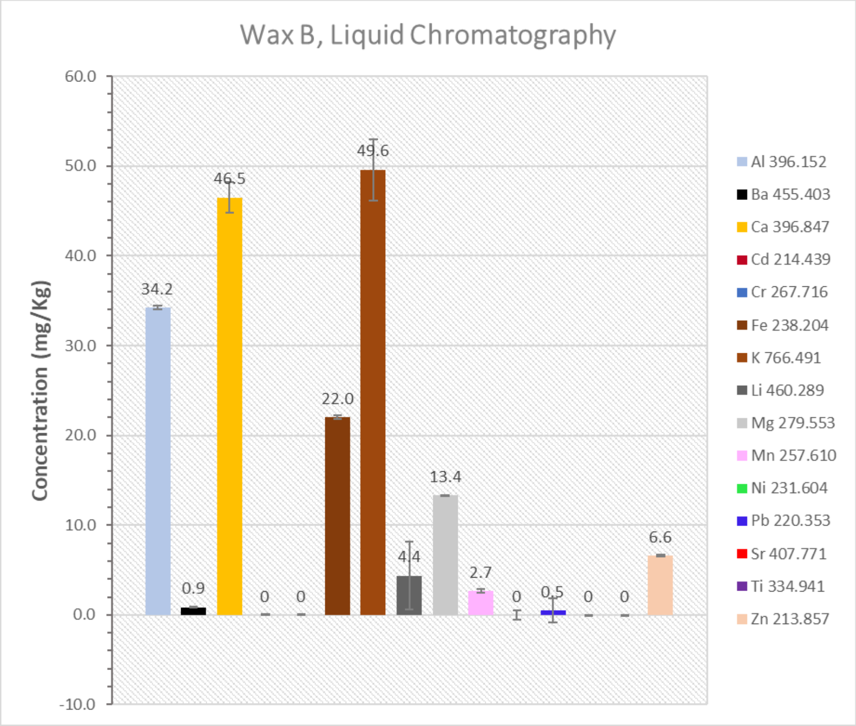

Wax B, Liquid Chromatography
Concentration (mg/Kg)
60.0
50.0
40.0
30.0
20.0
10.0
0.0
-10.0
34.2
0.9
46.5
0
0
22.0
49.6
4.4
13.4
2.7
0
0.5
0
0
6.6
Al 396.152
Ba 455.403
Ca 396.847
Cd 214.439
Cr 267.716
Fe 238.204
K 766.491
Li 460.289
Mg 279.553
Mn 257.610
Ni 231.604
Pb 220.353
Sr 407.771
Ti 334.941
Zn 213.857

3.2.1.3. Wax C

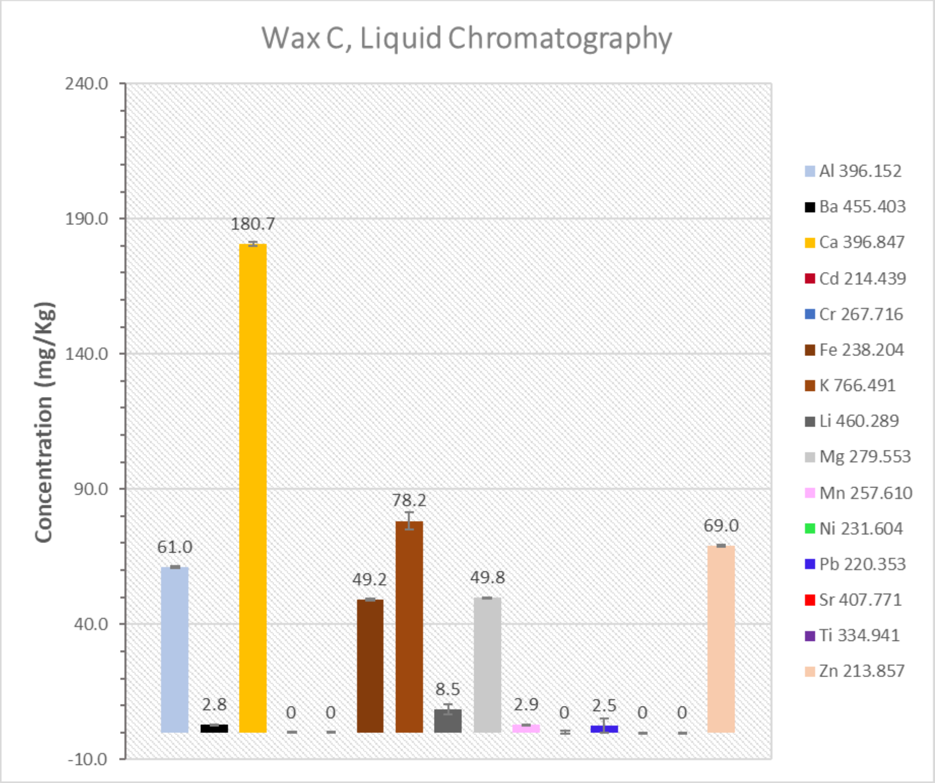

3.2.2.Solvent Extraction

3.2.2.1. Wax A

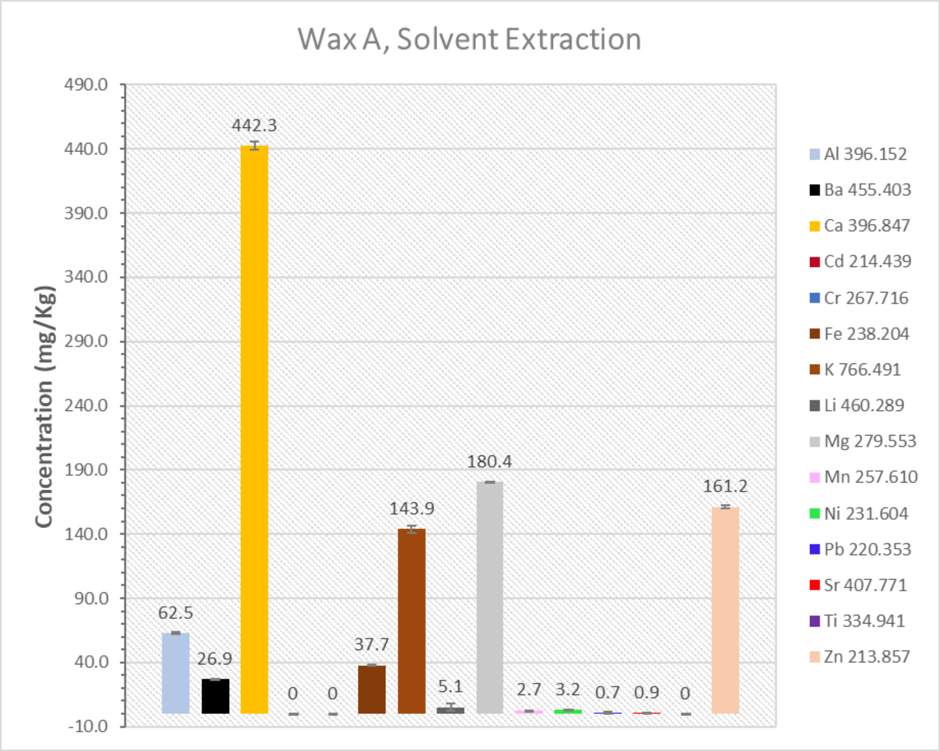

3.2.2.2. Wax B

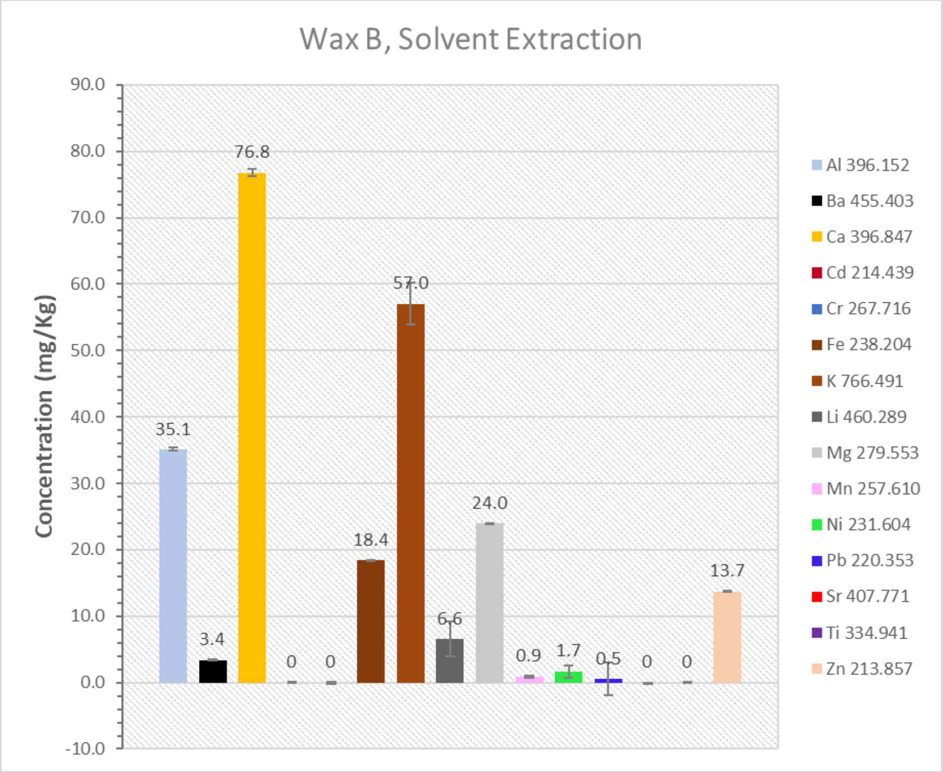

3.2.2.3. Wax C

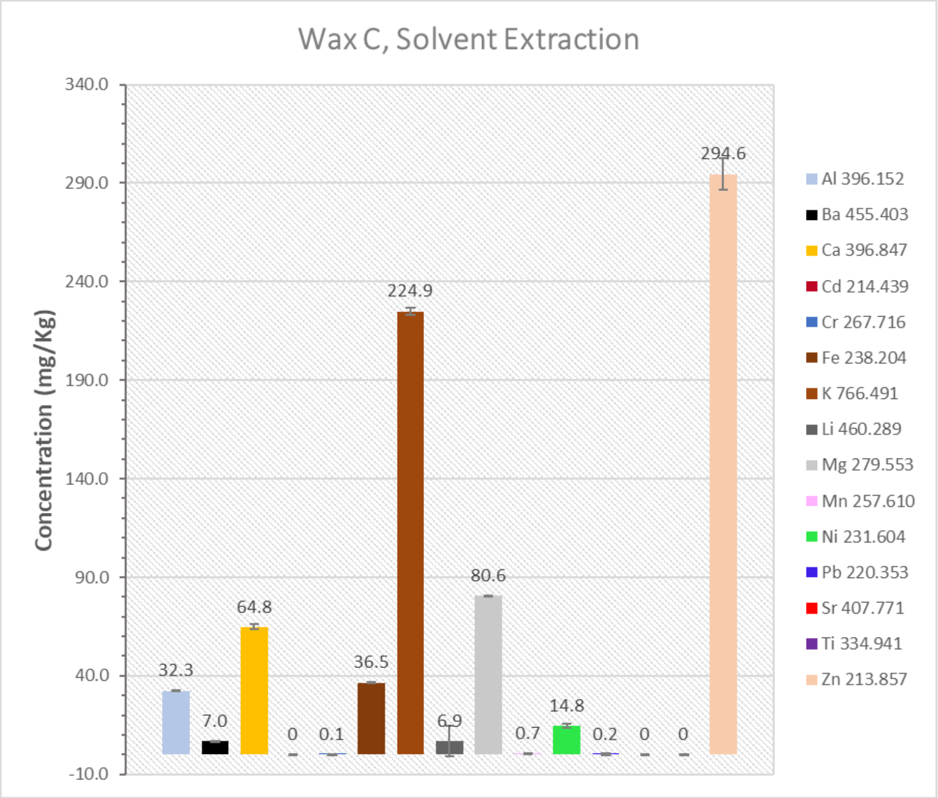

3.2.3. Urea Clathrate Extraction

3.2.3.1. Wax B

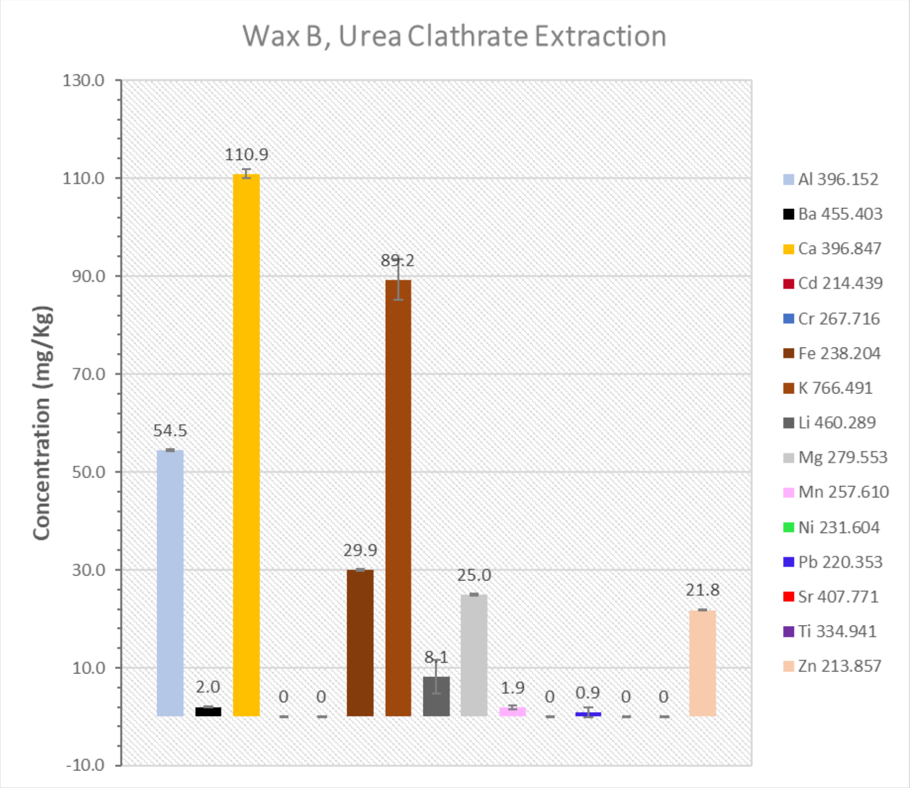

3.2.3.2. Wax C